HAPTIC COMMUNICATION FOR REMOTE MOBILE AND MANIPULATOR ROBOT OPERATIONS IN HAZARDOUS ENVIRONMENTS

Michael COUNSELL

Research Institute for Advanced Engineering,
School of Acoustics and Electronic Engineering,
University of Salford, Salford, UK

Contents

List of Figures

List of Tables

ACKNOWLEDGEMENTS

ABSTRACT

Nuclear decommissioning involves the use of remotely deployed mobile vehicles and manipulators controlled via teleoperation systems. Manipulators are used for tooling and sorting tasks, and mobile vehicles are used to locate a manipulator near to the area that it is to be operated upon and also to carry a camera into a remote area for monitoring and assessment purposes.

Teleoperations in hazardous environments are often hampered by a lack of visual information. Direct line of sight is often only available through small, thick windows, which often become discoloured and less transparent over time. Ideal camera locations are generally not possible, which can lead to areas of the cell not being visible, or at least difficult to see. Damage to the mobile, manipulator, tool or environment can be very expensive and dangerous.

Despite the advances in the recent years of autonomous systems, the nuclear industry prefers generally to ensure that there is a human in the loop. This is due to the safety critical nature of the industry. Haptic interfaces provide a means of allowing an operator to control aspects of a task that would be difficult or impossible to control with impoverished visual feedback alone. Manipulator end-effector force control and mobile vehicle collision avoidance are examples of such tasks.

Haptic communication has been integrated with both a Schilling Titan II manipulator teleoperation system and Cybermotion K2A mobile vehicle teleoperation system. The manipulator research was carried out using a real manipulator whereas the mobile research was carried out in simulation. Novel haptic communication generation algorithms have been developed. Experiments have been conducted using both the mobile and the manipulator to assess the performance gains offered by haptic communication.

The results of the mobile vehicle experiments show that haptic feedback offered performance improvements in systems where the operator is solely responsible for control of the vehicle. However in systems where the operator is assisted by semi autonomous behaviour that can perform obstacle avoidance, the advantages of haptic feedback were more subtle.

The results from the manipulator experiments served to support the results from the mobile vehicle experiments since they also show that haptic feedback does not always improve operator performance. Instead, performance gains rely heavily on the nature of the task, other system feedback channels and operator assistance features. The tasks performed with the manipulator were peg insertion, grinding and drilling.

Chapter 1

Introduction

Nuclear plant decommissioning involves the extensive use of remotely deployed mobile vehicles and robot manipulators controlled via teleoperation systems. The primary purpose of these devices is to allow a person to work without being exposed to the dangers of being within a hazardous environment. These teleoperation systems allow a person to use their cognitive reasoning and problem solving skills whilst being in a safe environment. Common teleoperation manipulator tasks are as follows:

- waste sorting,

- grinding,

- drilling,

- shearing (cutting through objects with a large scissors-like tool),

- swabbing (sampling dust and dirt from within a cell) and

- plasma arc cutting.

Mobile vehicles are sometimes used to locate a manipulator near to the area that it is to be operated upon. They can also be used to carry a camera into a remote area for monitoring and assessment purposes.

In general, most teleoperation systems that are in use within the nuclear industry rely on joystick and key interfaces to control the device. Cameras and small windows commonly provide visual feedback, audio feedback is also sometimes present. Modern systems, where there is a large separation between the cell and the operator rarely provide the operator with any form of force/haptic feedback. The word "haptic" originates from the Greek word "haptikos" which

means "able to touch or grasp" (Oxford-Dictionary, 1999). Hence, in this context, haptic feedback is used to describe a system that is capable of providing the user with a synthesized sense of touch.

Teleoperations in hazardous environments are often hampered by a lack of visual information. Direct line of sight is often only available through small, thick windows, which often become discoloured and less transparent over time. Ideal camera locations are generally not possible, which can lead to areas of the cell not being visible, or at least difficult to see. Also, visual feedback is often of limited use for some tasks since it does not naturally provide the operator with information regarding the forces and torques that are being generated due to environmental contact. If an operator attempted to use a manipulator to move a firmly fixed object, then vision alone would not allow the operator to know how much force the manipulator was applying to the object and in what direction. Situations such as this are clearly dangerous. Relaxing the gripper is not a safe option since it could cause the manipulator to "whiplash", which in a confined environment could cause damage to surrounding objects. Damage to the mobile, manipulator, tool or environment can be very expensive and dangerous within a hazardous environment such as a nuclear plant. Experienced manipulator operators often learn to determine approximate end point forces by using a cognitive model of the system and environmental visual cues such as:

- environmental object flexure,

- manipulator flexure,

- amount of sparks given off during grinding,

- sound of the tool (if available),

- manipulator dynamics.

Despite these visual cues mistakes are still possible. This is due mainly to extremes in motivational state caused by emotional and environmental factors such as:

- monotony and boredom

- noise (distractions)

- fatigue

- diurnal variations (time of day effects)

2

- stress

- non intuitive teleoperation system

- lack of data feedback to the operator

- misleading data feedback (this differs from lack of feedback since it is possible for a system to provide many feedback channels, however in a misleading format.)

The first five points from the above list are general factors that influence human performance, regardless of the specific task (Hockey, 1984). The latter three points create operator uncertainty in a teleoperation system. Since it is accepted that uncertainty increases reaction time (Fitts & Posner, 1973), performance is consequently decreased. Obviously, operator uncertainty also has a large influence on the number of errors made. According to the Yerkes-Dobson Law (Yerkes & Dodson, 1908), both low and high levels of stimulus or arousal can lead to poor performance. The law sates that the function of performance against arousal can be plotted as an inverted U, where optimal performance is towards the centre of the arousal range of the graph. Addition of haptic feedback to a system could act to increase operator arousal, which could either increase or decrease performance depending on the level of arousal. What this means, of course, is that addition of haptic feedback could provide missing and useful information to an operator and thus increase performance, alternatively it could cause sensory overload due to too much stimulus and thus cause a reduction in performance.

There is clearly a requirement for force control in manipulator teleoperation systems, however this does not necessarily have to be provided by a human in the control loop. Force control could be realised by either computer control, or by providing the operator with the means of performing the control (human in the loop). Despite the continuing advancements in autonomous systems, the nuclear industry generally prefers to ensure that there is a human in the loop. This is due to the safety critical nature of the industry. Haptic interfaces provide a means of allowing the operator to control the manipulator forces. Whereas regular joysticks only allow the operator to accurately control the manipulator motion. Semi-autonomous behaviour can be supported by haptic interfaces since they allow a bi-directional flow of data between the operator and the teleoperation system. The operator can use the haptic interface as a command input device and the teleoperation system can feedback information regarding its operation and the status of the task.

Other researchers have shown that haptic/force feedback can improve operator performance when using non-industrial teleoperation systems, often to control electric manipulators (Howe & Kontarinis, 1992)(Massimino & Sheriden, 1994)(Howe, 1992)(Hannaford *et al.*, 1991). Few have focused on industrial specification manipulators and realistic tasks (Lawrence *et al.*, 1995)(Wilhelmsen, 1997). Also, force feedback has been the major focus of most research, rather than the wider issue of haptic communication. The difference being that true force feedback systems present the operator with a scaled representation of the true end-effector force, often through a six (or higher) degrees of freedom (d.o.f.) interface (Daniel *et al.*, 1993)(Daniel & McAree, 1998), whereas haptic communication systems present the user with a haptic sensation that may convey pseudo end-effector forces and torques. Performance improvements have been shown in terms of safety, less time to completion and also less damage to a manipulator due to over-stressing. Despite this, there have been cases where haptic feedback has retarded overall system performance. Draper et al (Draper *et al.*, 1999) used a Fitts tapping test to evaluate the performance of their Autonomous/Teleoperated Operations Manipulator, both with their feedback system engaged and disengaged. The Fitts tapping test is often used to evaluate the performance of teleoperation systems. The test predominantly involves Cartesian motion in one degree of freedom between two targets or tapping regions. The mean time to move between the two targets is used as a measure of performance. Fitts law states that the mean time to move between the two targets is a function of the distance between the two targets and the width or tolerance of the target. The equation for mean time is as follows.

$$MT = a + b \log_2(2A/W) \qquad (1.1)$$

Where MT is the mean time, a and b are system constants and A and W are the distance between the targets and target width respectively. Draper et al found that force reflection increased the mean time for task completion for their system. Unfortunately, completion time was the only measure of performance, hence the effect of haptic feedback on accuracy and force control was not published.

By its nature, haptic communication is not limited to presenting manipulator end-effector forces and torques. Haptic communication provides a low bandwidth communication channel that can be used to present the operator with information on a wide range of task factors such as:

- Collision proximity

- Alarm status

- Software status

- Manipulator singularities etc

- Behaviour of semi-autonomous element of mobile robot, i.e. collision avoidance

Mobile robot operations within hazardous environments are hampered in the same manner as manipulator operations. Cameras, which are fitted to the vehicle offer constant quality views regardless of the location of the mobile in the environment. However there are usually large blind spots. These blind spots can cause problems when the vehicles are being operated in confined environments. As with the manipulators, any damage to the robot or environment can be very costly.

In general collision avoidance/control is arguably the most important use of haptic feedback within teleoperation system. If the operator is required to perform all of the collision avoidance, then the surrounding environment of the mobile vehicle needs to be known. This data can be conveyed through the haptic interface. Alternatively, if the mobile robot contains a semi-autonomous control element, then it is desirable to feed back the behaviour of the vehicle to the operator so that it can be decided if and when this semi-autonomous behaviour should be over-ridden.

Chapter 2 of this document presents an extensive literature review that covers haptic feedback from the technology's roots within the nuclear industry through to modern emerging uses such as medical training and computer aided design.

Chapter 3 of this document details the system that has been developed in order to study the effect of adding haptic communication to a mobile vehicle teleoperation system. Experiments were conducted using varying modes of vehicle control both with and without haptic feedback. Chapter 3 also presents the statistical analysis of the results of the experiments and also the conclusions that are drawn.

Chapter 4 and chapter 5 respectively cover the development of a high quality 3 d.o.f. haptic interface and its integration with the UK Robotics ATC manipulator control system. Chapter 5 also covers the development of novel task based haptic communication algorithms. Chapter 6 then builds upon chapters 4 and 5 by detailing the research that was carried out using the 3 d.o.f. haptic interface to control a Schilling Titan II hydraulic manipulator. Operators used the manipulator and haptic interface to perform peg insertion, grinding and drilling tasks with varying levels of haptic and visual feedback. The results from the experiments are presented along with the conclusions that are drawn.

Chapter 2

Literature Review

2.1 Introduction

The word "haptic" refers to the sense of touching or exploring an environment primarily with one's hands. The concept of a haptic interface is not new. Over the past fifty years, many different devices have been built for both research and commercial use. Areas that have benefited from the use of haptic interfaces are:

- Robot teleoperation systems

- Entertainment

- Medical research

- Medical surgery

- Training systems

- Limb rehabilitation

- Molecular manipulation

- CAD/CAM

- Automotive research, design and development

- Desktop computer interface

- PC Interface for the people with disabilities

- Representation of mathematical data

- Virtual Reality

Some of the very first haptic interfaces that were developed were used to control remote manipulators in hazardous areas such as nuclear environments (Goertz, 1952)(Goertz, 1954)(Goertz *et al.*, 1961)(Goertz, 1964)(Flatau, 1965)(Flatau *et al.*, 1972)(Flatau, 1977)(Vertut *et al.*, 1976)(Hill, 1977). The kinematics of these early haptic devices was often very similar or identical to the manipulator kinematics. Very early systems used a direct mechanical link to provide the force feedback, whereas relatively more recent systems used electrical coupling using servo systems. The direct mechanical link of the early systems was generally a tape/cable drive system, which meant that the master and slave had to be relatively close together to keep the feedback link relatively short (Hamel & Feldman, 1984)(Vertut, 1964).

2.2   Haptic interface design

Over the years, non-commercial haptic interfaces have been produced for many different purposes. Different fields of research have produced many different designs. The haptic interfaces that have been developed vary from single degree of freedom devices (Colgate & Brown, 1994)(Brown, 1995)(Colgate & Schenkel, 1994)(Jones & Hunter, 1990) through to a 22 degrees of freedom force reflecting exoskeleton developed for use in underwater telerobotic applications (Jacobsen *et al.*, 1989).

Differing design configurations of haptic devices have been found to be suitable to different applications. Two degrees of freedom devices have been used in the control of mobile vehicles (Barnes & Counsell, 1998), biomechanical research (Adelstein, 1989) and also studies into force bandwidth issues (Howe & Kontarinis, 1992). Adelstein (Adelstein, 1989), used a two degrees of freedom device to study human arm tremor, but noted that the device could be used in a broad range of applications.

For general use, three degrees of freedom devices have become popular, probably because of the ease of mapping between the three degrees of freedom and the three Cartesian coordinates of space, x, y and z. There are also several widely accepted, relatively simple mechanical designs for producing three d.o.f. devices. These are discussed at length in chapter 4. Applications include manipulator teleoperation systems (Counsell & Barnes, 1999), design issue studies (Ellis *et al.*, 1996), stability studies (Taylor & Milella, 1997) and open surgery simulation (Burdea, 1997).

Six (and greater) degrees of freedom devices have been developed for use in the teleoperation of manipulators (Daniel *et al.*, 1993)(Wilhelmsen, 1997)(Hannaford

et al., 1991)(Maekawa & Hollerbach, 1998)(Nahvi *et al.*, 1998). Here the operator is presented with a manipulandum that has the capability of presenting the operator with all three torque's (roll, pitch and yaw) and three forces (x, y and z) acting on a slave manipulator end effector. Systems such as these are termed as force reflecting systems since an operator feels a scaled version of the actual forces and torques that are present at the manipulator end effector.

While the majority of haptic interfaces that have been produced have been desktop or floor mounted and joystick-like in design there are several distinct and notable exceptions (Bergamasco & Prisco, 1997)(Burdea *et al.*, 1992)(Howe & Kontarinis, 1992). Burdea et al developed a four degrees of freedom force feedback glove, where the thumb and three primary fingers are each attached to a pneumatic actuator. This is a body grounded system, which means that the haptic interface is supported by the user, rather than a desktop or floor. The device, named the Rutgers Master (RMI), is designed to be used in virtual reality research. Virtual environments have been created to allow the safe training of operators/students in areas such as airport luggage checking and medical surgical training, where errors made in real life situations would be very costly in comparison to the development of the training system. A medical training simulation system has been developed that allows medical students to experience the sensation of a tumour/cyst that is hidden beneath the surface of the skin (Dinsmore *et al.*, 1997). The student sits in front of a Silicon Graphics machine whilst wearing the RMI device. This system allows student training and diagnosis performance evaluation without the need of a real life human patient.

Bergamasco and Prisco (Bergamasco & Prisco, 1997) developed a 7 d.o.f anthropomorphic haptic interface for the upper limb. Both system feasibility and usefulness of anthropomorphic haptic interfaces were studied. Key features such as highly intuitive operation, universal applicability and large workspace are cited. CAD and VR are suggested as the typical application areas of the device.

The computational difficulty of modeling virtual environments for both visual and haptic display has been highlighted by Ruspini et al (Ruspini & Khatib, 1998)(Ruspini *et al.*, 1997b)(Ruspini *et al.*, 1997a). It is well accepted that the modeling and display of static virtual environments often requires a considerable amount of processing power. Therefore when a haptic display is added to a visual display system, the amount of processing power that is required can be very high. Ruspini et al approached this problem by splitting the processing between two computers. The low level servo control of the haptic interface (a Phantom in this case) is controlled by one machine, while the high level environmental model and

graphics generation is performed by a second machine. The two computers are connected via TCP/IP over an Ethernet connection.

2.3   Entertainment industry haptic interfaces

In recent years, the entertainment/games industry has been one of the primary users of commercial haptic technologies. Haptic interfaces are used to improve the realism of both arcade games and more recently home computer games through the introduction of relatively inexpensive products such as the Microsoft SideWinder Force Feedback Pro Joystick (Microsoft SideWinder Force Feedback Pro, 2002). Key features of this type of device are:

- One or two degrees of freedom

- Inexpensive, value for money (approximately. £100)

- Device configurations are mainly joystick or steering wheel type in design

- The haptic sensations are usually generated by using built-in microprocessors

Even more simple haptic interfaces have been used to good effect on some game consoles. Rather than joysticks, the game console controllers are hand held units that rumble/vibrate in response to certain gaming situations such as hitting an opponent, crashing a car or firing a gun.

2.4   CAD and virtual prototyping applications

Virtual Reality and robot teleoperation systems are major areas where haptic technologies have been employed. However, there are many other fields of research that are beginning to benefit from haptic technologies. The Sarcos Dextrous Arm Master was developed by the departments of Computer Science and Mechanical Engineering at the University of Utah (Maekawa & Hollerbach, 1998)(Nahvi *et al.*, 1998). The Utah haptic device was developed as part of the development of a CAD system that would allow the elimination of the prototyping stage of certain products that are designed for human interface. A good example of such a device is a car dashboard. The Utah system allows a CAD model to be developed in a regular manner, then the designer can test the usability of the device through the use of the haptic interface. The Sarcos Master Dextrous Arm is constructed from a 3 DOF manipulandum attached to the end of 7 DOF redundant manipulator.

Each of the ten joints are hydraulically actuated and resolved by the use of poten-tiometers. Each joint also utilises a torque sensor. Elimination of the expensive and time consuming process of building prototypes, for the iterative testing of the usability of human interfacing devices, is clearly a major cost saving venture. This is of particular importance to the automotive industry where design cost savings and faster time to market are important goals. Similar research in the field of CAD and product prototyping has been carried out by Caldwell et al (Caldwell *et al.*, 1998). An 18 d.o.f. proprioceptive input and feedback exoskeleton was developed as a virtual environment interface. The exoskeleton provides monitoring of the motion of the human arm from the spine to the wrist with very little restriction of natural motion. In addition, the proprioceptive inputs are augmented by tactile feedback of contact pressure at 8 different points on the upper and lower arm seg-ments and pressure, texture, slip, edges/ridges/corners and thermal parameters to the hand via the glove based interface.

2.5 Automotive industry

Haptic interface technology has benefited the automotive industry by providing a means of enabling steering wheel torque feedback on both research simulation sys-tems and "steer-by-wire" power steering systems. Liu and Chang (Liu & Chang, 1995) used a driving simulator with a haptic steering wheel interface to study driver performance both with and without steering system torque feedback. Setlur et al (Setlur *et al.*, 2002) and Nakamura et al (Nakamura *et al.*, 1989) propose the use of haptic steering systems in "steer-by-wire" vehicle power steering systems. Configurable levels of torque feedback to the driver is cited as an advantage of such systems. Schumann (Schumann, 1993) proposed the use of an active steering wheel as an additional feedback interface as part of a collision warning system. Ryu and Kim (Ryu & Kim, 1999) developed a virtual environment for develop-ment of automotive power steering and "steer-by-wire" systems. The system was proposed as a means of reducing development times for vehicle steering systems.

2.6 Haptic computer pointing interfaces

Desktop computer haptic interfaces have been produced by adding haptic feedback to a regular PC mouse. Akamatsu et al retrofitted a regular mouse with both force and tactile feedback (Akamatsu & MacKenzie, 1996)(Akamatsu & Sato, 1994). The force feedback was generated by locating an electromagnet within the case of

the mouse in conjunction with a mouse mat made of iron. Tactile information was provided to the operator by a small pin, which projects slightly through the left mouse button. The mouse was used to perform several button selection tasks with varying haptic feedback, button size and button approach distance. Performance improvements were noted when using haptic feedback, primarily with small targets. In some cases however, tactile feedback was noted to increase error rates, and force feedback was noted to increase task completion time. Similar research was conducted by Oakley and McGee (Oakley *et al.*, 2000)(Oakley, 1999)(McGee, 1999). Here, a PHANToM haptic interface was used to investigate how operator visual overload could be reduced in a conventional windows-like desktop. Haptic feedback was added to a button based targeting task and a scrolling task. Four different haptic signatures were added to the buttons in the targeting task as follows: texture, friction, recess and gravity well. The scrolling task was evaluated in two different modes: visual only and visual with haptic. The haptic feedback for the scrolling task was formed by adding the gravity well sensation to the arrow buttons and the recess sensation to the scroll bar area. Significant reductions in error rate were noted with the recess and the gravity well modes within the targeting test. However, the texture mode was noted to increase operator error rate. The results from the scrolling task mimicked those from the targeting task where the haptic feedback in the form of the gravity well and the recess showed significant reductions in error rate. Despite improved error rates, no decrease in task completion time was noted.

Further research in the field of haptic pointing devices (haptic PC mice) has been conducted by researchers concerned with the effects of multimodal feedback. McGee et al studied the combination of haptic and auditory feedback (McGee, 2000), whereas Campbell et al of the IBM Almaden Research Centre studied the combination of tactile and visual feedback by adding tactile feedback to a laptop IBM Trackpoint device (Campbell *et al.*, 1999). Campbell performed a series of mouse tunnel following tasks where operators were provided with varying visual and tactile feedback. In some cases the visual and tactile feedback were in concert, whilst in other cases the feedback was unconcerted. As expected, in concert haptic and visual feedback offered performance gains over visual feedback alone. Also, as Campbell hypothesised, unconcerted haptic and visual feedback showed performance that was not significantly different to visual feedback alone. Campbell hence concluded that what you feel must be what you see. McGee et al studied the combination of haptic and auditory information and proposed that multimodal feedback of this form could be categorised as being either complemen-

tary, redundant or in conflict. Possible effects on performance are proposed for each.

2.7 Haptic interfaces for disabled computer users

It has also been noted that haptic interface technologies could be used to aid disabled people. Yu et al developed a haptic interface to allow visually impaired people to be able to experience data graphs (Yu *et al.*, 2000). Yu et al noted that visual impairment makes data visualisation techniques inappropriate and thus proposed strategies to tackle the problem. Experiments were conducted using both sighted and non-sighted participants to evaluate the usability of a haptic graph presentation system.

2.8 VR applications

An overview of the state-of-the-art in multimodal technology was presented by Burdea in 1996 (Burdea *et al.*, 1996). The paper reviews VR input/output devices such as trackers, sensing gloves, 3-D audio cards, stereo displays and haptic interfaces. Integration of I/O devices with VR systems is also discussed. In later publications, Burdea et al (Burdea *et al.*, 1997a)(Burdea *et al.*, 1997b) proposed an innovative approach to human hand rehabilitation that uses a VPL Data Glove retrofitted to a Rutgers Master (RM-I). The Data Glove measures the hand gesture and position and the RM-I provides the force feedback via pneumatic actuators. The rehabilitation routine consists of virtual reality exercises such as rubber ball squeezing, individual digit exercising and "peg in the hole" type operations. The latter is intended to test hand eye co-ordination. Force and motion data from the hand is recorded during the exercises and then used in later analysis.

Medical applications for haptic technologies are discussed by Burdea (Burdea, 1996). Again, training is a major area that can benefit from haptic VR systems. Spinal anaesthesia or "Epidural" procedures are recognised as being very difficult to perform. Mistakes made during the procedure can be very painful or even lethal for the patient. Due to the nature of the procedure, i.e. the insertion of a long needle into the base of the spine, an anaesthetist has to rely entirely on haptic feedback. Recognition of the correct haptic "signature" involved with the insertion of the needle into the spine is crucial for a successful procedure and thus training on a virtual patient is more preferable to training on a real person. A commercial haptic device available from Immersion Co. was incorporated in an Epidural Anaesthesia

Training Simulation by Stredney et al (Stredney *et al.*, 1996). The system uses the Immersion haptic device to provide the user with a resistive force that is co-axial to the needle. A more recent training system was developed by Ayache et al (Ayache *et al.*, 1997). Here, a Laparoscopic Impulse Engine from Immersion Co. was used in a surgery simulation system. The simulation system presents the user with a dynamic, visual and haptic simulation of an organ. A highly realistic haptic sensation is reported from the visco-elastic behaviour of the virtual organ. Research in this field has not been limited to human surgery. Researchers from the different departments of the University of Glasgow have worked together to develop a Horse Ovary Palpation System (HOPS) (Crossan *et al.*, 2000)(Brewster *et al.*, 1998). The system uses a PHANToM haptic interface to present an operator with the haptic sensation of conducting a common veterinarian examination procedure. HOPS is intended to be used as a training system that allows students to experience and learn palpation procedures in a safe and humane manner. It is stated that a future aim is to add a second PHANToM to the system to allow more complex interaction between the student and the virtual patient.

It is clear that there are far more applications for the haptic interface technology than is apparent from an initial glance. Another emerging application is the use of haptic technologies in the display of complex scientific data or theoretical principles (Brooks Jr. *et al.*, 1990). Teaching of science requires that the environmental model of the world, held in the mind of a student, be as correct as possible. But it is often the case that this mental model is fundamentally flawed due to our everyday erroneous observations of the environment around us. Dede at al (Dede *et al.*, 1994) propose that physical immersion and multiple sensory perception in a virtual environment may lead to an improved understanding of the world of science. Subjects that are traditionally difficult to master, such as relativity and quantum mechanics could possibly be made more intuitive by the application of VR immersion and learning-by-doing.

2.9 Manipulator teleoperation

General research into the field of remote manipulator teleoperation has focused on the following fields:

- Real-time position and force control

- Real-time obstacle avoidance

- Manipulator kinematic design (to ensure that the manipulator can achieve the tasks required)

- Human-machine interface

Real-time control of the Cartesian motion and forces at the manipulator end effector provides the user with a highly intuitive control method. The operator can control the end effector in Cartesian space without needing to know the, often complex, motion of the manipulator joints that are required to achieve the demanded motion (Whitney, 1969), (Nakamura & Hanafusa, 1986), (Craig, 1986), (Whitney, 1987), (Khatib, 1987), (Nakamura, 1991), (Deo & Walker, 1997), (Freund & Pesara, 1998). Similarly, real-time obstacle avoidance can be used to further simplify the task of the operator by ensuring that collisions between the manipulator links and environment do not occur (Khatib, 1986)(Seraji & Bon, 1999). With redundant manipulators, this can often be achieved as a secondary task by moving links away from obstacles whilst simultaneously ensuring that the end effector motion command supplied by the operator is achieved (Glass *et al.*, 1993).

Teleoperation requires manipulators that are well suited to the tasks that they are to perform and the environment within which they are to function. Manipulator kinematic design, i.e. the choice of link lengths, joint positions and joint motion capabilities, is an important aspect of teleoperation system design since it has a large effect on the ability of the manipulator to reach the desired positions within the workspace. Research in this field has investigated kinematic design optimisation and evaluation to ensure that teleoperation tasks can be performed within the particular workspace of the manipulator. (Gosselin & Angeles, 1991)(Paredis, 1993)(Basavaraj & Duffy, 1993)

Research into human-machine interfaces for remote manipulator teleoperation has addressed the goal of providing the operator with an intuitive means of controlling the remote manipulator. Research has shown that performance improvements are offered by end effector Cartesian position control over joint space control (Wallersteiner *et al.*, 1988) and that in general, Cartesian position control is preferable to Cartesian rate(velocity) control (Kim *et al.*, 1987). Based on these conclusions, Hopper et al (Hopper *et al.*, 1996) developed a complete control system for a redundant manipulator. The system provides the operator with Cartesian position control with force feedback and the option to use several different visual feedback methods such as a VR style stereo headset, regular cameras or a manipulator mimic that is generated on a Silicon Graphics machine. Liu et al (Liu *et al.*, 1991)(Liu *et al.*, 1993) studied the effect of teleoperation system time delay and

visual display refresh rates on operator performance. A head-mounted display was used as an input device and also as a visual feedback device. The orientation of the operator's head was used to control the movement of a pan and tilt camera. Remote manipulation was achieved using a joystick interface system. The study confirmed that communication delays in the teleoperation system and display update rates lower than 10Hz can have an adverse effect on operator performance. However, it was also noted that highly experienced operators can often learn to deal with such deficiencies and still achieve acceptable performance levels.

Many researchers have focused on the application of haptic feedback to robot teleoperation systems. Since the 1950's manipulator teleoperation systems have been developed for remote hazardous area operations. The first systems relied on mechanics and hydraulics that directly linked the kinematics of the master and the slave (Goertz, 1952)(Goertz, 1954)(Flatau, 1965)(Hill, 1977)(Ostoja-Starzewski & Skibniewski, 1989)(Goertz, 1964)(Hamel & Feldman, 1984)(Vertut, 1964). This method of generating haptic feedback relied on close proximity of the master to the slave. The scaling down of the manipulator joint torques was only possible in the mechanical/hydraulic feedback link. As computer performance increased and cost decreased, the direct mechanical link method of haptic feedback was replaced with a computer system containing sensing and actuation, termed now as the haptic interface. This important transition in the evolution of haptic teleoperation systems allows increased distance between operator and manipulator and much increased flexibility in the generation and display of the haptic sensation. The master and the slave no longer need to be kinematically similar. Nor do they need to be similar in size. The manipulator can now be used as a means of extending our dextrous capabilities to both larger and smaller scales (Flatau, 1973). Research in the field of haptic teleoperation systems has been extensive, however little work has focused on nuclear decommissioning related tooling tasks (Daniel *et al.*, 1993)(Daniel & McAree, 1998).

Very often, Fitts style tapping or peg insertion tasks have been used to evaluate the performance of haptic teleoperation systems (Howe & Kontarinis, 1992)(Draper *et al.*, 1999). Howe and Kontarinis (Howe & Kontarinis, 1992) developed an identical master and slave teleoperation system to test the performance gains provided by force feedback over vision alone for a simple one-hole high tolerance peg insertion task. They also looked at the role of force bandwidth in the performance of the task by using low pass filters to narrow the force display bandwidth to 2Hz, 8Hz and 32Hz. Howe and Kontarinis recorded time for completion and also sampled the forces for the duration of the test. They found that force feedback

provided a significant decrease in both completion time and mean force magnitude, even at the 2Hz and 8Hz bandwidths. The 32Hz bandwidth, generally, only provided small gains over the 8Hz bandwidth in comparison with the gains seen between vision alone and the 2Hz bandwidth. Howe and Kontarinis concluded as follows: "These results demonstrate that force feedback improves performance of precision contact tasks in dextrous telemanipulation. Task completion times and error rates decrease as force reflection bandwidth increases. Most of the benefit appears between 2Hz and 8Hz, although some improvement is seen at 32Hz. These experiments also indicate that even low bandwidth force feedback improves the operator's ability to moderate task forces". Howe and Kontarinis have shown that haptic/force feedback improved the performance of their particular teleoperation system.

Despite the research that suggests that force feedback improves man/machine performance, there have been results obtained that suggest that the reverse can also be true. Draper et al (Draper *et al.*, 1999) used a Fitts tapping test to evaluate the performance of their Autonomous/Teleoperated Operations Manipulator, both with their feedback system engaged and disengaged. They used time for completion of a set number of taps as their only performance metric. They found that force reflection increased the mean time for task completion, however they did not measure contact forces during the test, and so had no way of evaluating the effect of force feedback on the system's "man in the loop" force control. Also it appears that there was no attenuation of the slave forces that were displayed on the master and hence the operator felt the full real magnitudes of the forces. Draper et al estimate that the reason for the reduction in performance is due to the increased resistance of motion when using the force feedback. They suggest that the increased force response required by the operator caused an increase in the motor neuron noise associated with any movement and thus a decrease in performance. They also suggest that if the force feedback to the operator was scaled down, then the reduction in performance may not have been seen. Commenting on the Fitts tapping task, Draper noted that it is an excellent tool for evaluating the trajectory-generating portion of a system, however it does not adequately assess the impedance control part of the system. Thus, variations of the task that involve more peg insertions and hence more contact with the environment are better suited to assessing a teleoperation systems impedance control. Examples of such variations on the Fitts theme that are suitable to assessing the performance of haptic feedback can be seen in Massimino and Sheriden (Massimino & Sheriden, 1994), Repperger, Remis and Merril (Repperger *et al.*, 1990) and Draper et al (Draper

et al., 1988). Repperger et al performed an experiment using a passive exoskeleton device. The experiment was similar to the "Disk Transfer" experiment conducted by Fitts (Fitts, 1954), where the amplitude of movement is constant, however, the insertion tolerance differs from one experiment to the next. Massimino and Sheriden used a variation of the Fitts theme that involved the insertion of a peg into a single hole. This task was used to evaluate the performance of an operator when presented with different levels of visual and haptic feedback. The tasks were conducted using a 7 d.o.f slave manipulator, and a 7 d.o.f master hand controller. Massimino and Sheriden found that force feedback made significant improvements to the task completion time.

Salcudean et al, Lawrence et al, Parker et al addressed the problem of adding haptic/force feedback to a heavy-duty hydraulic excavator/tree feller machine (Lawrence *et al.*, 1995)(Salcudean *et al.*, 1997)(Parker *et al.*, 1993). The standard joint by joint rate control interface was removed. In its place Sulcudean et al tested both a haptic Cartesian velocity input device and also a Cartesian position controlling device. They noted that the addition of coordinated control and force feedback improved operator performance, particularly with inexperienced operators. Improvements were noted in terms of time-to-completion, lower operator training times and less environmental damage (damage to trees that are being felled). The velocity input device used was a 6 d.o.f magnetically levitated joystick that was developed by the University of British Columbia. Direct force feedback was evaluated using the device, but found to be unsuitable due to the instability problems that are associated with presenting direct force feedback on a rate controlling input device. Hence, a novel stiffness sensation was developed that allowed the manipulator forces to be presented to the operator by a means of altering the stiffness of the centring spring action. This method of force feedback was reported to be very successful.

Fischer et al of The University of Oxford, conducted research into the specification and design of input devices for teleoperation (Fischer *et al.*, 1992). The problem of designing input devices for teleoperation systems was approached without reference to the implementation of the final solution. The quantitative specification proposed by Fischer et al covers force and position bandwidths, backlash, workspace, device inertia and forward force threshold. This specification was then compared against the specification of several existing haptic input devices. Following on from this research, Daniel et al used the specification in the development of a high performance parallel input device (Daniel *et al.*, 1993)(Daniel & McAree, 1998). The device that was produced, named as the Bilateral Stewart Platform, is

in essence a small parallel robot, which exhibits six degrees of freedom, workspace of 300mm cubed and a bandwidth of 50Hz for small motion in the region of 1mm or 2deg. The BSP was then successfully incorporated in a Puma/Unimation 760 control system, where the destabilising problem of momentum transfer between slave and master has been successfully addressed. Daniel et al conducted decommissioning type tasks in a simulated environment. A drill and a reciprocating saw were used in size reducing experiments. Although no comparison of visual vs. haptic performance was presented, it was noted that the operator was able to carry out the tooling task with relative ease.

Shinohara et al of the Japan Atomic Energy Research Institute developed a mobile manipulator system for use in decommissioning tasks (Shinohara *et al.*, 1984). The mobile manipulator consists of a tracked vehicle with a 6 degrees of freedom electric manipulator attached on the top. Visual and auditory feedback was provided to the operator by using vehicle mounted cameras and a microphone. The on-board slave manipulator was controlled from a kinematically similar master manipulator where force feedback was presented via a common error system. No mention was made as to whether any of the mobile vehicle data and attributes was fed back to the operator via a haptic communication system, no assessment of the performance of the vehicle is provided and no operator experiments were performed.

As this literature review has shown, previous research has covered the use of haptic interfaces in the control of manipulators. However, there has been very little research into the development of haptic interfaces for manipulators designed to perform real nuclear decommissioning related tasks such as material size reduction and removal/dismantlement (Daniel *et al.*, 1993)(Daniel & McAree, 1998)(Fischer *et al.*, 1992). This is ironic given the fact that most early force feedback systems were developed within the nuclear industry for remote handling tasks (Hill, 1977)(Goertz, 1964)(Hamel & Feldman, 1984)(Vertut, 1964). Other researchers have shown that haptic feedback offers improved operator performance when controlling small scale lab based electric manipulators (Howe & Kontarinis, 1992) and also large scale hydraulic manipulators performing large scale tasks such as excavation and tree felling (Lawrence *et al.*, 1995)(Salcudean *et al.*, 1997)(Parker *et al.*, 1993). However, nuclear decommissioning requires robust and powerful hydraulic manipulators to perform delicate tasks such as drilling and grinding. This research is intended to fill the gap in previous research by assessing haptic feedback in the control of an industrial scale hydraulic manipulator. Unlike existing research, this research focuses directly on nuclear decommissioning related tasks such as grind-

ing and drilling. Chapters 4 and 5 cover the development of a haptic interface and its integration with an industrial manipulator and control system (UK Robotics Ltd ATC system). The decision was made to develop a haptic interface since none of the commercially available interfaces met the exact specification requirements of the research. Most of the commercially available haptic interfaces failed on one or more of the following issues:

- General robustness

- Active degrees of freedom

- Power output

- Lack of information available about device characterisation. Essentially a "black box".

- Cost of purchase/development i.e. economic reasons would rule out its use in a real industrial task.

Chapter 6 then presents a set of experiments and their results. The experiments performed involved operators performing peg insertion, grinding and drilling tasks with varying modes of visual and haptic feedback. The author has no knowledge of any previous research that has focused on assessing haptic feedback for such tasks.

While there has been a reasonable amount of research conducted into haptic manipulator teleoperation systems, the author has no knowledge of any publication that covers the use of haptic interfaces which are used to control mobile robotic vehicles, with the exception of Barnes and Counsell (Barnes & Counsell, 1999) and the research into providing haptic feedback within the automotive industry that was introduced in section 2.5. The distinct lack of work in the field of haptic mobile vehicle teleoperation systems is surprising since it is reasonable to expect that operator performance could be improved by extra sensory immersion. This has been shown to be true by Barnes and Counsell (Barnes & Counsell, 1999). Chapter 3 presents research into the use of haptic feedback within a mobile vehicle teleoperation system. This research is aimed at assessing the performance gains that can be expected from integrating a haptic communication system within a mobile vehicle teleoperation system. Experiments have been performed that involved volunteer operators navigating the mobile vehicle through a cluttered environment using varying modes of teleoperation. Chapter 3 also introduces the novel haptic communication systems that were developed and evaluated as part of this research.

Chapter 3

Assessment of Haptic Communication for Mobile Vehicle Applications

3.1 Introduction

Hazardous environment operations such as nuclear plant decommissioning or bomb disposal require typically the use of a remotely operated mobile vehicle. Visual information concerning the vehicle and its environment is essential if a remote operator is to achieve successfully a given task. However, ideal camera placements within such environments are rarely possible. Often an operator has a very restricted "window" onto the vehicle and its environment and thus many "blind-spots" can exist. The lack of visual information when operating in cluttered environments makes vehicle manoeuvring very difficult, and when this situation is exacerbated by strict time limits for a task, then vehicle/environment collisions and resultant damage can occur. Despite continued advancements in autonomous mobile vehicle systems, the nuclear industry prefers to keep a human in the control loop of any vehicle due to the safety critical nature of the environment. This means that the operator is expected to perform the collision avoidance. Thus the obstacle data must be presented to the operator to allow her/him to change the course of the vehicle accordingly. A haptic interface allows a bi-directional flow of data between operator and teleoperation system. Thus the operator can use the joystick to control the motion of the vehicle whilst the vehicle can send proximity sensor data back to the operator to allow him/her to perform the collision avoidance. Clearly the haptic communication must be intuitive so that the operator can easily understand the data that is being presented.

As previously mentioned, the haptic joystick is not limited to presenting the collision avoidance data. Other data can be presented to the operator via the haptic joystick, such as:

- Behaviour of semi-autonomous element of mobile robot, i.e. collision avoidance

- Alarm status

- Software status

The introduction of a haptic interface may allow an overloaded graphical user interface to be improved by transferring some of the data presentation to the haptic interface.

3.2 Hypotheses

Based upon the investigations into previous haptic research (Massie & Salisbury, 1994)(Buttolo & Hannaford, 1995)(Daniel *et al.*, 1993)(Wilhelmsen, 1997)(Maekawa & Hollerbach, 1998)(Jacobsen *et al.*, 1989)(Burdea *et al.*, 1997a)(Burdea, 1996)(Stredney *et al.*, 1996)(Dede *et al.*, 1994)(Brooks Jr. *et al.*, 1990)(Howe, 1992), and prior experience of teleoperation and autonomous robot control, (Hopper *et al.*, 1996)(Bevan *et al.*, 1996)(Barnes *et al.*, 1997) the following hypotheses regarding performance improvements are proposed:

1. If haptic feedback is present during a teleoperation task, then improved operator performance would be obtained.

2. If a telerobotics approach is adopted, as opposed to teleoperation, then further improved operator performance would be obtained.

3. If haptic feedback is present during a telerobotics task, then even greater operator performance improvements would be obtained.

The hypotheses refer to performance improvement, which in this context, is used to imply that fewer errors are made, higher efficiency is achieved and possibly, task completion time is reduced. The hypotheses also refer to telerobotics. Telerobotics is generally used to refer to teleoperation systems that have a degree of autonomous operation, such as collision avoidance. In this context, telerobotics is used specifically to imply teleoperation with autonomous collision avoidance, i.e.

the vehicle is capable of taking the necessary actions to avoid collisions within its environement. To test these hypotheses, experiments were conducted with five different modes of controlling a mobile vehicle as follows:

1. Teleoperation, without haptic feedback and without semi-autonomous collision avoidance;

2. Teleoperation, with environmental haptic feedback and without semi-autonomous collision avoidance;

3. Teleoperation (Telerobotics), without haptic feedback and with semi-autonomous collision avoidance;

4. Teleoperation (Telerobotics), with environmental haptic feedback and with semi-autonomous collision avoidance;

5. Teleoperation (Telerobotics), with behavioural haptic feedback and with semi-autonomous collision avoidance;

The first two modes are pure teleoperation, where the operator is in control of the vehicle's motion at all times. The latter three modes are telerobotics modes, where the vehicle is responsible for the collision avoidance. In order to test operator performance for each of the different modes of operation, tests were conducted using eleven different operators. Each operator used each of the control modes consecutively to drive a mobile vehicle through an obstacle course. Time for completion of the course, distance travelled through the course, number of collisions and the path taken were recorded for each trial. All of the data was recorded automatically within the control software, which made the experimentation process simpler.

3.3 Experimental Apparatus

In order to investigate the effect of operator performance gains provided by haptic feedback a mobile vehicle and a cluttered environment was simulated in the Deneb Telegrip robotic simulation software (Deneb Robotics Inc., 2003). A Cybermotion K2A holonomic vehicle was modeled, and simulated in a slalom type obstacle course. This is shown in figure 3.1.

The Cybermotion K2A has two control inputs, velocity and turret rotation velocity. Thus a two degrees of freedom input device is required to control the device. An Immersion Co Impulse Engine 2000 (Immersion Corp., 2000) was chosen as
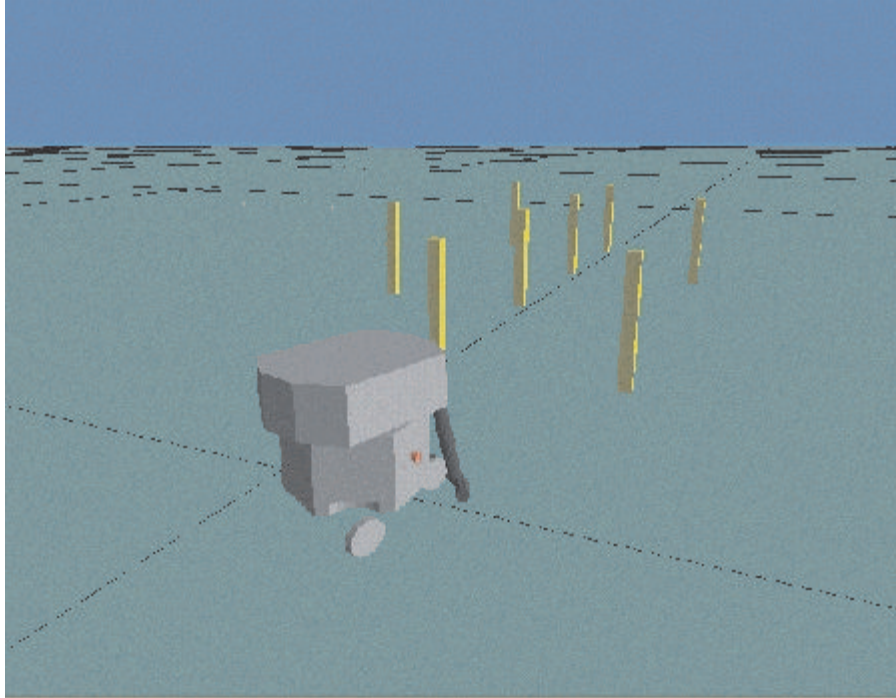
Figure 3.1: Screen shot of the Cybermotion vehicle and the obstacle course

the haptic input device for this research. The Impulse Engine 2000 is shown in figure 3.2.

The Impulse Engine 2000 is a high performance two degrees of freedom haptic device, which is designed for research applications that demand high fidelity and high force bandwidth. Table 3.1 outlines the specification of the device.

PC IO interface	ISA card
Control loop frequency	1KHz
Force bandwidth	120Hz quoted
Position resolution	0.02mm
Maximum continuous force	8.9N
Workspace	152.4mm x 152.4mm

Table 3.1: Specification of the Immersion Impulse Engine 2000

Figure 3.3 shows the simulation system architecture.

Figure 3.2: The Immersion Impulse Engine 2000

| Silicon Graphics

Deneb Telegrip and serial software running in a unix shared library | 80MHz 486PC

Haptic joystick, serial, and environment simulation software | IE 2000 Haptic Joystick |

Rs232 Serial
Update freq 30Hz

ISA Interface
Update freq 1KHz
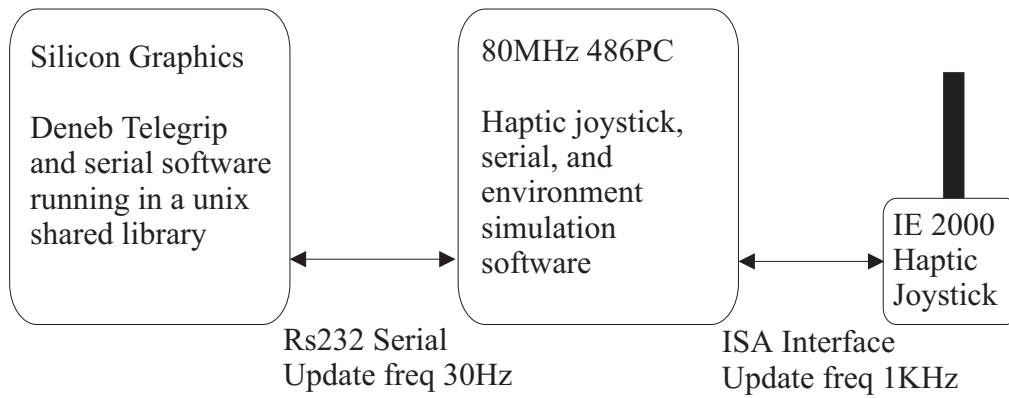
Figure 3.3: The simulation system architecture.

The PC is responsible for generating the haptic sensation, interfacing to the Impulse Engine 2000 (IE2000) and also for modeling the K2A and environment. The position of the K2A in the virtual environment is sent to the Telegrip software via an RS232 serial connection. The haptic display is updated at a frequency of 1KHz whilst the visual display is updated at a frequency of 30Hz. The operator uses the IE2000 to control the motion of the K2A. The y axis of the joystick controls the velocity of the vehicle and the x axis controls the rotational velocity of the turret. Since the vehicle is holonomic it will turn on the spot.

The architecture of the system shown in figure 3.3 is the same as the architecture proposed by Ruspini who conducted research into the field of multi modal visual and haptic systems. (Ruspini & Khatib, 1998)(Ruspini *et al.*, 1997b)(Ruspini *et al.*, 1997a)

3.4   Haptic Feedback

Two different modes of haptic feedback have been developed as follows:

- Environmental haptic feedback

- Behavioural haptic feedback

The environmental haptic feedback provides the user with information on the obstacles that are local to the mobile vehicle, thus allowing the operator to avoid collisions. In contrast to this, the behavioural haptic feedback communicates the operation of the mobile vehicle's collision avoidance algorithm to the operator. The behavioural haptic feedback is provided to allow the operator to understand the operation of the vehicle, and thus allow him/her to over-ride the behaviour if and when it is required.

3.5   Environmental Haptic Feedback

The haptic communication was developed so that the operator could "feel" the proximity of any local obstacles. Virtual range sensors were generated and implemented in the PC environmental model software. The virtual sensors provide range and location data relative to the position and orientation of the mobile vehicle. Figure 3.4 shows a plan view of the mobile and an obstacle.

The range and the orientation of an obstacle must be presented to the operator so that they can perform the obstacle avoidance. When no objects are within the
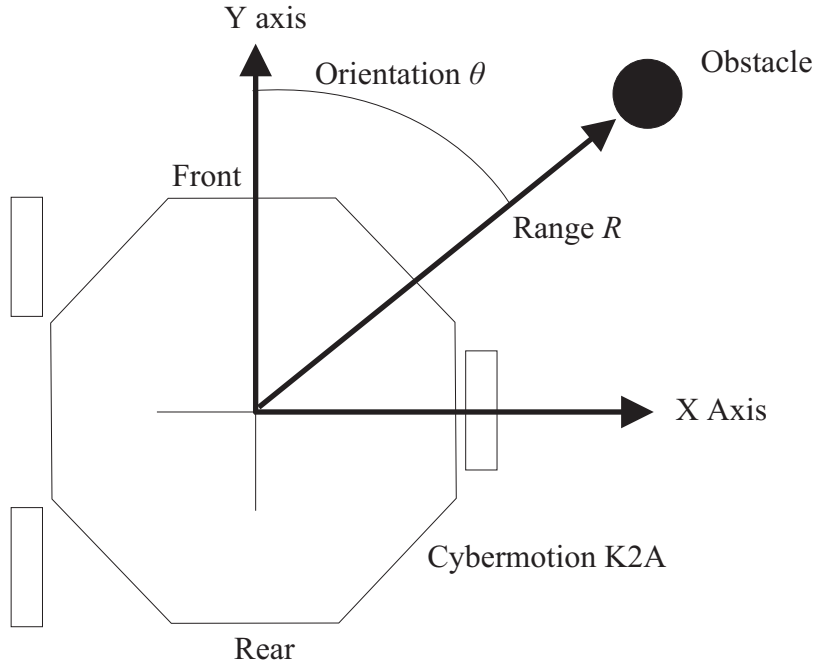
Figure 3.4: Plan view of mobile and obstacle

range of the virtual sensor the joystick is lightly sprung so that it will return to the centre position when displaced, as with a regular joystick. This response is generated as follows.

$$F_x = K_x \times P_x \tag{3.1}$$

$$F_y = K_y \times P_y \tag{3.2}$$

Where F_x and F_y represent the forces felt by the operator, K_x and K_y represent the virtual spring constants and P_x and P_y are the joystick axis positions.

This response can be visualised as shows in figure 3.5.
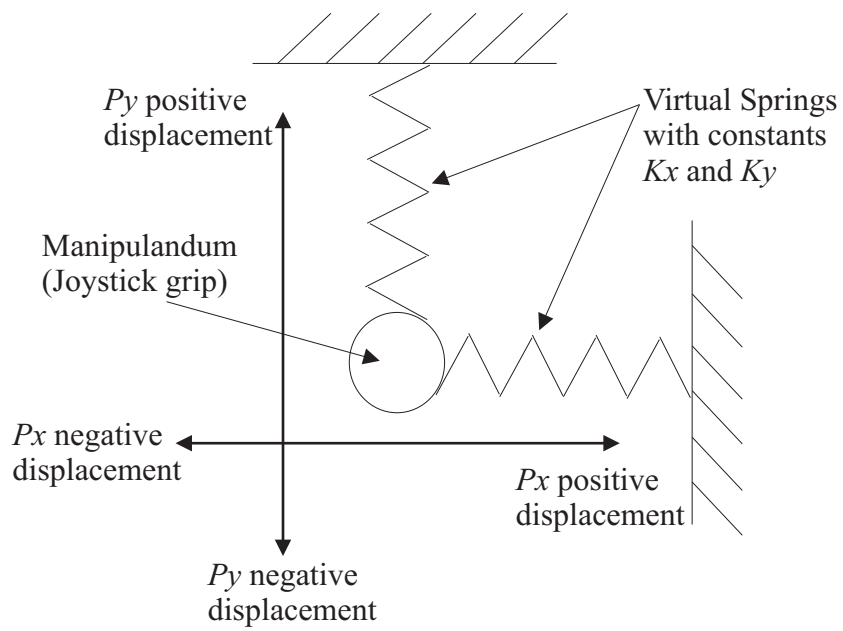
Figure 3.5: Plan view of haptic joystick showing the operation of the virtual springs

The values of K_x and K_y were set so that the behaviour of the joystick was similar to that of a regular passive sprung joystick. The virtual springs behaved as if they were attached to the joystick handle and thus worked under both compression and extension.

When an object is within the range of the virtual sensor, K_x and K_y were modified to generate the haptic communication. The values of K_x and K_y were calculated as follows. Initially the location of the obstacle must be calculated within the vehicles coordinate space.

Calculate the range, normalized between -1 and 1, to the object in the x axis and y axis.

$$R_x = (R/R_{MAX})\sin\theta \qquad (3.3)$$

$$R_y = (R/R_{MAX})\cos\theta \qquad (3.4)$$

Where R_x and R_y are the position of the obstacle within the K2A coordinate frame. R and θ are the outputs from the range sensor. R is the distance to the obstacle and θ is the orientation within the K2A coordinate frame. R_{MAX} is the maximum range of the sensor. R_x and R_y were then used to calculate which frame quadrant the obstacle was in and P_x and P_y were used to calculate which frame quadrant the manipulandum was in. This was performed as follows with reference to the coordinate system as shown in figure 3.6. Figure 3.6 also shows what is meant by coordinate frame quadrant in this context.
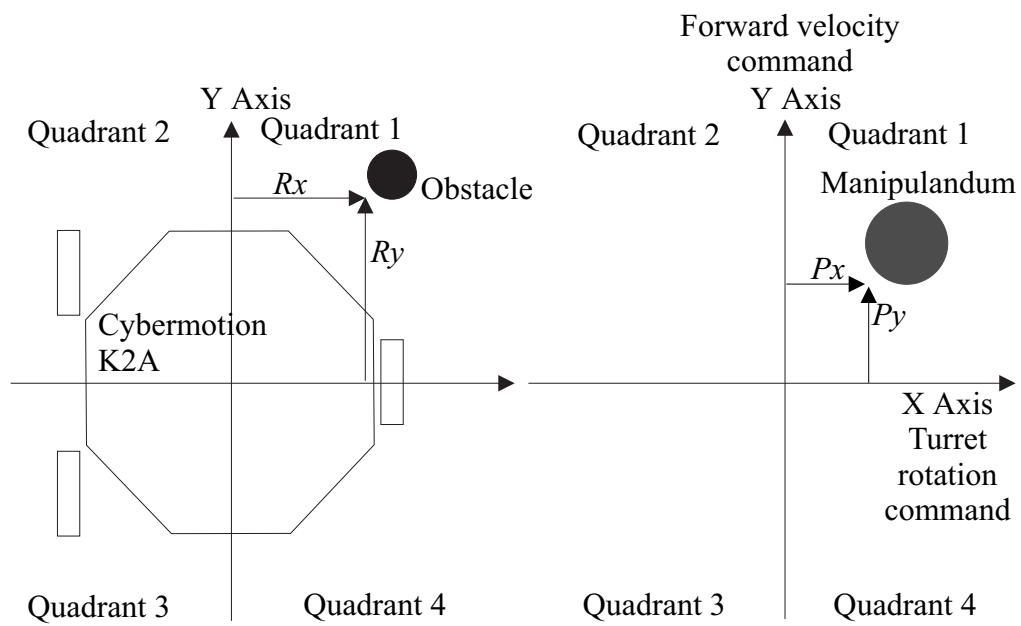
Figure 3.6: Plan view of joystick and mobile/obstacle

To find what coordinate frame quadrant the obstacle is in:

If $R_x \geq 0$ and $R_y \geq 0$: obstacle is in quadrant 1

If $R_x < 0$ and $R_y \geq 0$: obstacle is in quadrant 2

If $R_x < 0$ and $R_y < 0$: obstacle is in quadrant 3

If $R_x \geq 0$ and $R_y < 0$: obstacle is in quadrant 4

To find what coordinate frame quadrant the joystick is in:

If $P_x \geq 0$ and $P_y \geq 0$: joystick is in quadrant 1

If $P_x < 0$ and $P_y \geq 0$: joystick is in quadrant 2

If $P_x < 0$ and $P_y < 0$: joystick is in quadrant 3

If $P_x \geq 0$ and $P_y < 0$: joystick is in quadrant 4

If the obstacle quadrant matches the joystick quadrant the object haptic sensation was generated as follows. If the two quadrants do not match, the passive joystick sensation was generated as shown in equations 3.1 and 3.2.

The values of $K_{xObject}$ and $K_{yObject}$, which are the values of the spring stiffness for the joystick axes, were calculated as follows to generate the obstacle haptic sensation.

$$K_{xObject} = \frac{K_x}{|R_x|} \tag{3.5}$$

$$K_{yObject} = \frac{K_y}{|R_y|} \tag{3.6}$$

Note that, in the case that either R_x or R_y is zero or very close to zero, the value of $K_{xObject}$ or $K_{yObject}$ was set to the maximum possible value of the spring stiffness that did not cause instability. The maximum spring stiffness value was chosen empirically.

The force required on each axis to generate the haptic sensation was then calculated as follows

$$F_x = K_{xObject} \times P_x \tag{3.7}$$

$$F_y = K_{yObject} \times P_y \tag{3.8}$$

Where P_x and P_y are the joystick axis positions and F_x and F_y are the joystick forces.

As the above equations show, the haptic feedback from the obstacle is only present when the manipulandum and the obstacle are in matching quadrants relative to the frame system of the mobile vehicle. This allows the operator to deduce the location of the obstacle. The distance to the obstacle is presented through the stiffness of the springs.

3.6 Collision Avoidance (Semi-Autonomous Behaviour) Generation

A behavioural control approach was adopted to generate the collision avoidance. Whilst many collision avoidance and mobile robot architectures exist (Arkin, 1989)(Brooks, 1986), the Behaviour Synthesis Architecture (BSA)(Barnes *et al.*, 1997)(Barnes, 1996) was used as the basis for the algorithm. This choice was made because there was prior experience of using the architecture within the University of Salford, and also since the architecture has been shown to provide a robust basis for collision avoidance. The collision avoidance algorithm used the virtual sensor data to produce a velocity and turret rotation command that generated motion in order to manoeuvre the mobile vehicle away from a possible collision, and also attenuate any operator commands that direct the vehicle into a possible collision. The output from the collision avoidance algorithm and the operator's motion commands were summed to produce a resultant vehicle motion command.

When an obstacle is in the range of the sensor, the command from the user is created as a function of the joystick position and also the utility values that cause attenuation. This is shown in equations 3.9 and 3.10.

$$V_{user} = P_y \times U_{Ruser} \tag{3.9}$$

$$\omega_{user} = P_x \times U_{Ruser} \times U_{\theta user} \tag{3.10}$$

Where V_{user} is the velocity command, ω_{user} is the rotation velocity command and P_x and P_y are the joystick positions normalized between -1 and 1 for the range of the joystick motion. U_{Ruser} is the utility associated with the range to the obstacle and $U_{\theta user}$ is the utility associated with the angle to the obstacle.

U_{Ruser} is calculated as follows in equation 3.11.

$$U_{Ruser} = R \tag{3.11}$$

Where R is the normalized range to the obstacle, between 0 and 1.

$U_{\theta user}$ is calculated as follows in equation 3.12.

$$U_{\theta user} = |\sin(\theta)| \tag{3.12}$$

Where θ is the angle to the obstacle within the coordinate frame of the vehicle.

The response of $U_{\theta user}$ is shown in figure 3.7. As is shown, the command of the operator is attenuated when the vehicle is alongside an obstacle in order to prevent the operator from turning into a collision. Note that an angle of 90° indicates that the obstacle is directly in front of the vehicle and an angle of 270° indicates that the obstacle is directly behind the vehicle. This can be confirmed from figure 3.6 which shows that the y axis extends from the front of the vehicle.
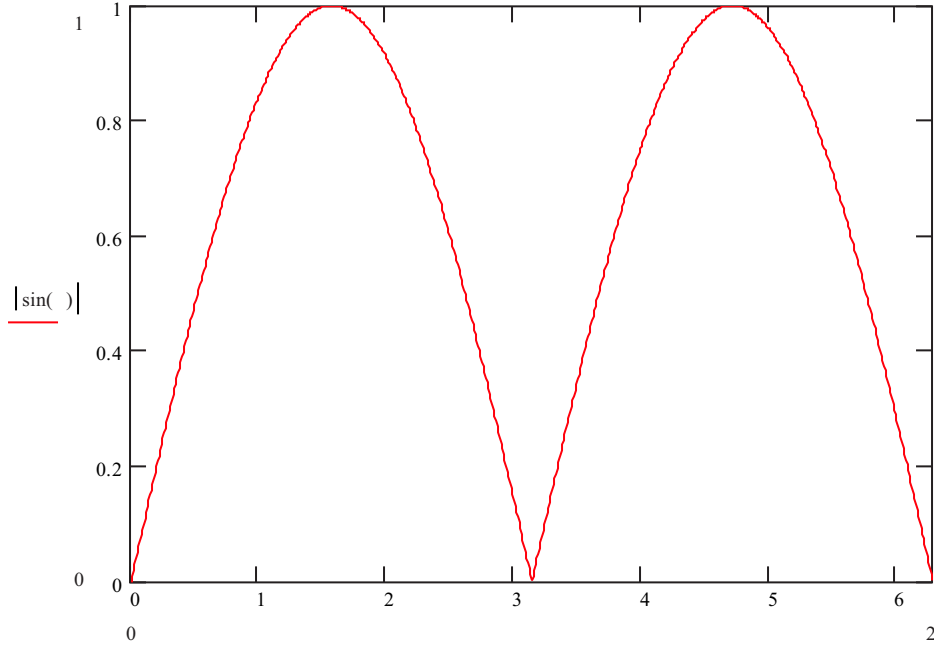
Figure 3.7: Plot of the utility associated with the angle to the obstacle

As stated, V_{user} and ω_{user} are the attenuated commands from the user which are summed with the output from the collision avoidance algorithm to generate the motion commands for the vehicle. The output from the collision avoidance algorithm was generated as follows.

$$V_{collision} = V_{\theta collision} \times U_{Rcollision} \tag{3.13}$$

Where $V_{collision}$ is the velocity command from the collision avoidance algorithm. $V_{\theta collision}$ is the response that is generated due to the angle to the obstacle and

$U_{Rcollision}$ is the utility (priority) that is generated from the range to the obstacle. $U_{Rcollision}$ is generated as shown in equation 3.14.

$$U_{Rcollision} = 1 - R \tag{3.14}$$

Where R is the normalized range to the obstacle, between 0 and 1. Note that as the range value decreases, the value of $U_{Rcollision}$ increases.

$V_{\theta collision}$ is generated as shown in equation 3.15.

$$V_{\theta collision} = \sin(\theta - \pi) \tag{3.15}$$

Where θ is the angle to the obstacle.

Figure 3.8 shows a plot of $V_{\theta collision}$. Note that this plot shows the greatest response at 90° and 270° which correspond to the obstacle being either in front or to the rear of the vehicle. This is confirmed by the coordinate frame that is shown in figure 3.6.
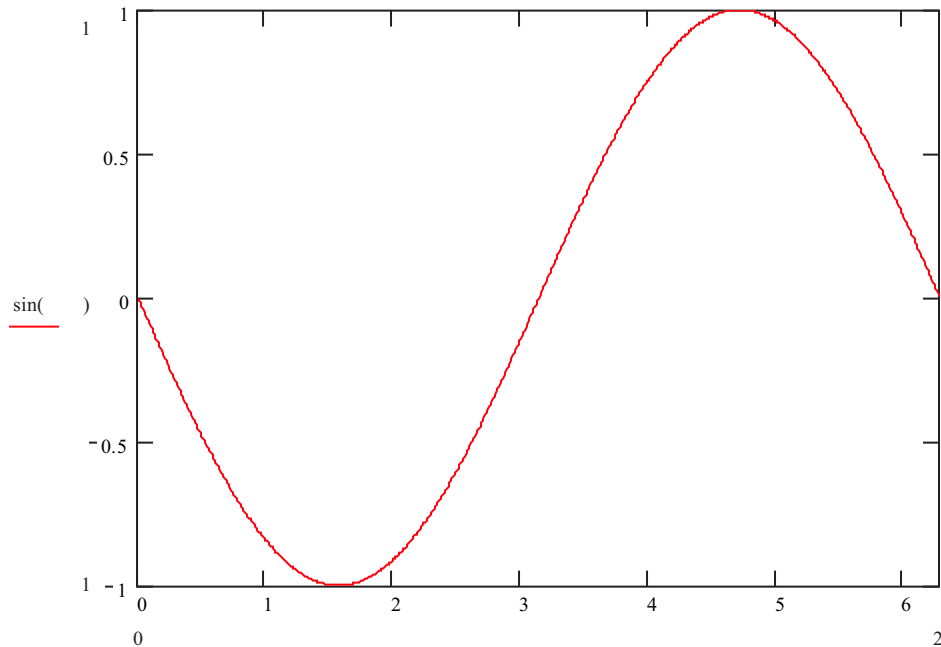
Figure 3.8: Plot of the response associated with the angle to the obstacle

The rotation command from the collision avoidance algorithm, $\omega_{collision}$, is generated as follows.

$$\omega_{collision} = \omega_{\theta collision} \times U_{Rcollision} \qquad (3.16)$$

Where $\omega_{\theta collision}$ is the response that is generated due to the angle to the obstacle and $U_{Rcollision}$ is the utility (priority) that is generated from the range to the obstacle, as shown in equation 3.14.

$\omega_{\theta collision}$ is generated as shown in equation 3.17.

$$\omega_{\theta collision} = \pm(V_{\theta collision}) \qquad (3.17)$$

Where $V_{\theta collision}$ is calculated in equation 3.15 and the polarity of $\omega_{\theta collision}$ is reversed if the vehicle is reversing towards the obstacle. Note that equation 3.17 represents normalized values with no units.

The vehicle velocity and rotation is calculated by summing the command from the operator and the output from the collision avoidance algorithm as follows.

$$V = V_{user} + V_{collision} \qquad (3.18)$$

$$\omega = \omega_{user} + \omega_{collision} \qquad (3.19)$$

Note that V and ω were limited to values between -1 and 1 and then converted to an actual velocity command where values of -1 and 1 correspond to maximum forward and reverse velocities respectively.

Figure 3.9 shows how the above control commands apply to the mobile vehicle.
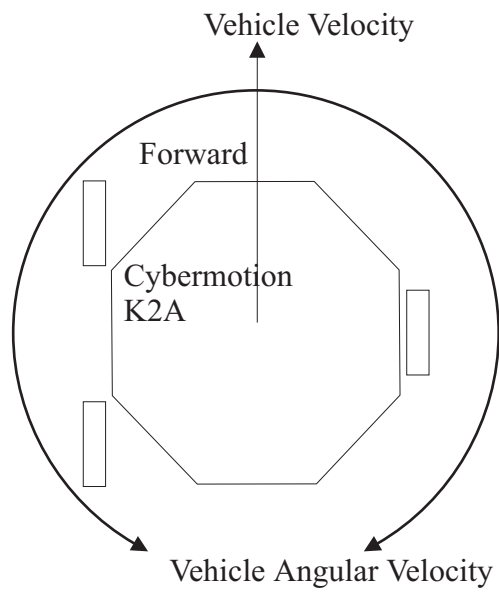
Figure 3.9: Plan view of mobile vehicle showing the motion control inputs

3.7   Behavioural Haptic Feedback

The behavioural haptic feedback is generated in a similar way to the environmental haptic feedback. When there is no obstacle within the range of the virtual sensor the haptic joystick behaves as a regular passive sprung joystick. When an object is within the range of the virtual sensor the behaviour of the collision avoidance algorithm is communicated to the operator rather than the actual obstacle position. Figure 3.10 shows the generation of the haptic feedback and figure 3.11 shows a plan view of the haptic joystick with superimposed virtual springs in order to allow better visualisation.
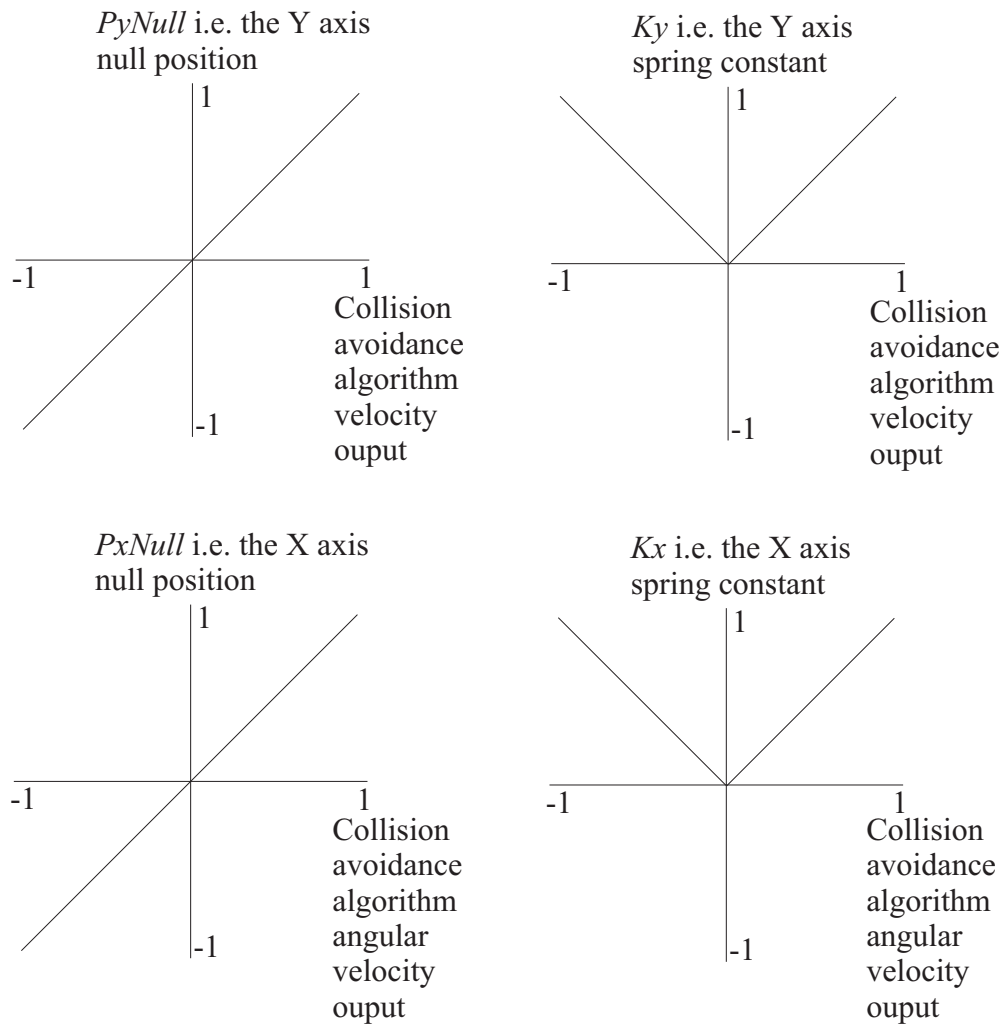
Figure 3.10: Graphs of functions used to generate the behavioural haptic feedback

The following functions show how the force on each axis of the joystick was calculated.
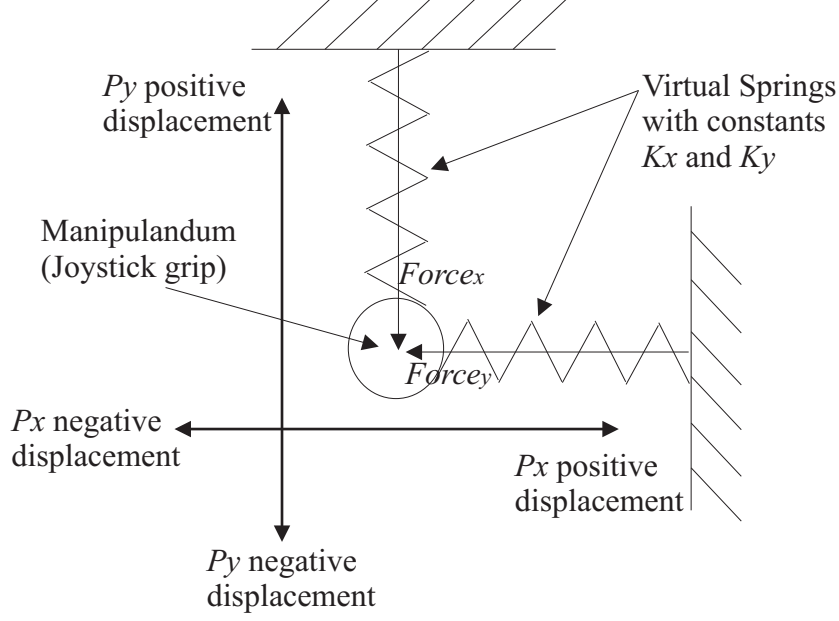
Figure 3.11: Plan view of the haptic joystick showing the superimposed virtual springs

$$Force_x = (P_x - P_{xNull})K_x \qquad (3.20)$$

$$Force_y = (P_y - P_{yNull})K_y \qquad (3.21)$$

P_x and P_y are the positions of the joystick axes, P_{xNull} and P_{yNull} are the pseudo centre positions of the joystick axes and K_x and K_y are the virtual spring constants. The pseudo centre positions of the joystick, P_{xNull} and P_{yNull} require further explanation to ease understanding of the above calculations. The term pseudo is used since the terms P_{xNull} and P_{yNull} do not denote the actual physical centre position of the joystick, as is present in the centre of the workspace of a regular passive joystick. Instead these terms denote the position of equilibrium of the joystick. When the haptic interface is in this haptic mode of operation, the position of equilibrium corresponds to the motion command from the collision avoidance algorithm. Put simply, the centre position of the joystick is used to convey the motion command of the collision avoidance algorithm to the operator. Hence, if the collision avoidance algorithm was to produce a rotational velocity of the vehicle, the centre position of the joystick x axis would be translated to match this command. The operator would thus sense the change in force in the x axis due to the new centre position of this axis.

This mode of operation is interesting when compared to the regular mode of operation of a joystick where the position of the joystick controls the velocity of a vehicle. With the behavioural feedback algorithm the reverse is true since the velocity of the vehicle can control the position of the joystick.

3.8 Experimental Procedure

Eleven operators used each mode of control consecutively to manoeuvre the vehicle around the slalom course. The time for completion, distance travelled, number of collisions and the path through the obstacle course were recorded for each trial. The profile of the operators varied very little. None of the operators were trained in any form of mobile robot operation, however, since all of the operators worked within the robotics industry they all had an appreciation of what teleoperation entails. The primary operator vocation was engineering, exceptions to this were sales engineers and administration staff. Nine of the operators were male, all of the operators were aged between 25 and 50.

Each operator was given the same task instructions prior to the experiment, in addition to two minutes of familiarization time that allowed the operator to become accustomed with the method of controlling the vehicle. The instruction that was given to each operator was as follows: "Drive the vehicle through the slalom course. Try to complete the course as fast as possible without colliding with the posts. The time to complete the course will be recorded along with the number of collisions. The time will start when you pass through the first gate and stop when you pass through the last gate."

In addition to the task instructions, each mode was preceded with an explanation of its operation. Whilst this information was not read from a script, it was kept consistent for each operator.

A "camera" view similar to that shown in figure 3.1 was used throughout.

3.8.1 Mode 0: Teleoperation without haptic feedback

Mode 0 gave the operator complete control of the mobile vehicle and hence the responsibility for avoiding obstacles. Haptic feedback was not present, and therefore an operator had to rely entirely on visual information to manoeuvre the K2A through the slalom course.

3.8.2 Mode 1: Teleoperation with haptic feedback

As with Mode 0 the operator had complete control of the mobile vehicle at all times. However, environmental haptic feedback was present which provided the operator with an extra channel of environmental feedback.

3.8.3 Mode 2: Telerobotics without haptic feedback

This mode included the collision avoidance algorithm as discussed previously. Haptic feedback was not present and hence the joystick behaved as a regular passive sprung device.

3.8.4 Mode 3: Telerobotics with obstacle haptic feedback

As with mode 2, this mode provided autonomous collision avoidance. However, it also provided environmental haptic feedback to the operator in the same manner as mode 1. This allowed an operator to sense an obstacle at the same time as the collision avoidance behaviour reacted to it. This provided the operator with a real time understanding of the behaviour of the mobile vehicle.

3.8.5 Mode 4: Telerobotics with behavioural haptic feedback

As with modes 2 and 3, mode 4 incorporated collision avoidance. Behavioural haptic feedback was also present as discussed in section 3.7.

3.9 Results

The run time between the first and last gate, total distance travelled and total number of collisions were recorded for each operator when using each mode of operation. The results are shown in table 3.2, where column u is the user identity, d is the distance travelled in metres, t is the task completion time in seconds and c is the number of collisions. These results were averaged for the eleven operators and are presented as follows in figures 3.12, 3.13 and 3.14.

	Modes														
u	0			1			2			3			4		
	d	t	c	d	t	c	d	t	c	d	t	c	d	t	c
1	7.58	39	3	5.14	33	2	5.05	15	0	5.54	17	0	5.62	15	0
2	5.75	19	1	5.77	21	0	5.9	23	0	5.94	27	0	6.78	35	0
3	5.39	9	1	5.88	10	0	5.21	10	0	6.66	17	0	5.2	14	0
4	5.58	11	0	5.82	11	0	5.9	12	0	6.2	15	0	5.9	17	0
5	5.03	19	1	5.19	27	0	5.28	26	0	5.5	24	0	5.82	25	0
6	6.81	32	2	5.13	19	1	5.03	15	0	5.2	21	0	4.8	11	0
7	5.11	7	0	4.8	5	0	5.01	7	0	5.42	8	0	4.73	7	0
8	5.28	10	2	6.38	16	2	5.65	15	0	6.32	13	0	5.71	18	0
9	5.7	11	2	4.75	10	0	5.31	11	0	5.45	12	0	5.42	11	0
10	5.12	11	1	5.69	13	1	6.00	15	0	5.85	15	0	5.46	14	0
11	4.99	8	2	5.72	8	1	6.20	13	0	5.30	13	0	6.81	37	0

Table 3.2: Results from the slalom task, where u is the user, d is the distance travelled in metres, t is the time in seconds and c is the number of collisions
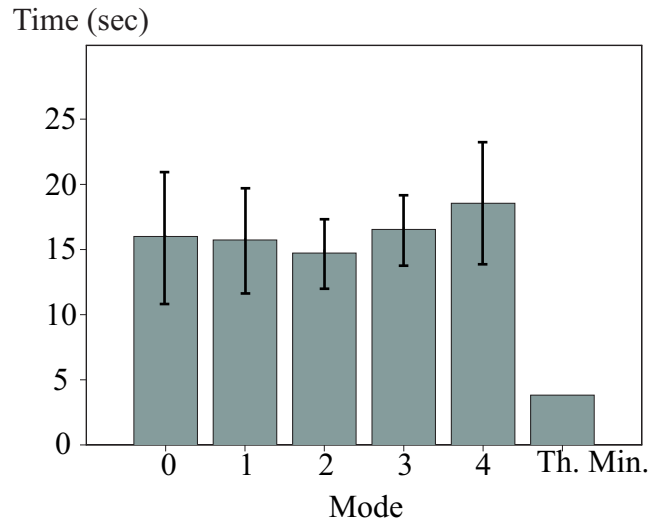
Figure 3.12: Bar chart of average time taken showing standard deviation and theoretical minimum
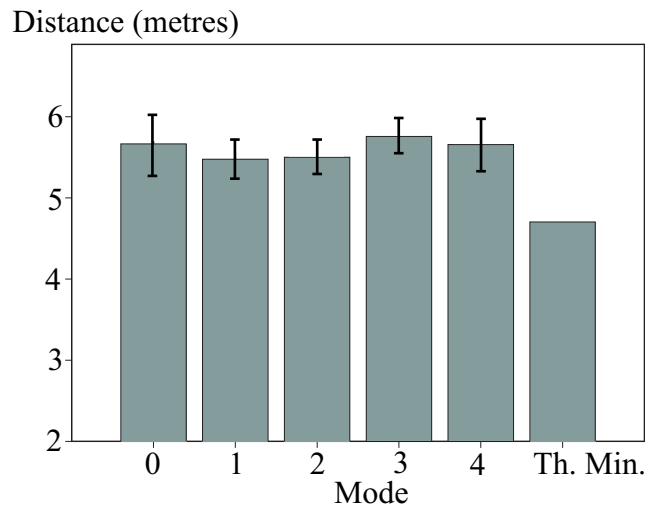
Figure 3.13: Bar chart of average distance travelled showing standard deviation and theoretical minimum
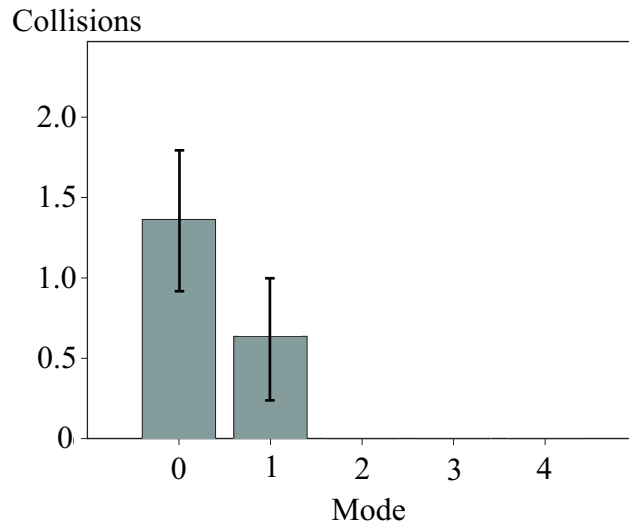
Figure 3.14: Bar chart of average number of collisions showing standard deviation

The Wilcoxon T Test for Dependant Samples (Kirk, 1999) was chosen and carried out on the data from the operator testing. This test is used to test the hypothesis that two population distributions are identical. It is appropriate for dependent samples. Such samples can result from:

- Obtaining repeated measures from the same participant (as with this experiment)

- Using participants matched on a variable that is known to be correlated with the dependent variable

- Using identical twins or littermates

- Obtaining pairs or participants who are matched by mutual selection.

The following levels of alpha (significance) were considered for the Wilcoxon T Test, 0.1, 0.05 and 0.01. When choosing a significance level one should consider the possible consequences of making either a Type I or Type II error. A Type I error is defined as rejecting a true null hypothesis and a Type II error is accepting a false null hypothesis. In some situations, in particular medicine, one can attach a cost to the consequence of making a Type I or II error. For example, if the cost of making a Type I error was possible harm to a patient, then it would be advisable to put tighter control on the possibility of making the error by lowering the value of alpha. Since there is no apparent danger or cost associated with making a Type I or II error within the scope of this research, alpha was chosen to 0.05. This value is a widely accepted and common value for alpha in many fields of research. Tables 3.3 through to 3.5 show the results of the Wilcoxon T tests.

Mode	0 No Haptic + Manual Control	1 Environmental Haptic + Manual Control	2 No Haptic + Collision Avoidance	3 Environmental Haptic + Collision Avoidance
1 Environmental Haptic + Manual Control	Not Significant	no data	no data	no data
2 No Haptic + Collision Avoidance	no data	Not Significant	no data	no data
3 Environmental Haptic + Collision Avoidance	no data	no data	Not Significant Borderline	no data
4 Behavioural Haptic + Collision Avoidance	no data	no data	Not Significant	Not Significant

Table 3.3: Statistical significance within the time for completion data

Mode	0 No Haptic + Manual Control	1 Environmental Haptic + Manual Control	2 No Haptic + Collision Avoidance	3 Environmental Haptic + Collision Avoidance
1 Environmental Haptic + Manual Control	Not Significant	no data	no data	no data
2 No Haptic + Collision Avoidance	no data	Not Significant	no data	no data
3 Environmental Haptic + Collision Avoidance	no data	no data	Significant $p < 0.05$	no data
4 Behavioural Haptic + Collision Avoidance	no data	no data	Not Significant	Not Significant

Table 3.4: Statistical significance within the distance travelled data

Mode	0 No Haptic + Manual Control	1 Environmental Haptic + Manual Control	2 No Haptic + Collision Avoidance	3 Environmental Haptic + Collision Avoidance
1 Environmental Haptic + Manual Control	Significant $p < 0.005$	no data	no data	no data
2 No Haptic + Collision Avoidance	no data	Significant $p < 0.05$	no data	no data
3 Environmental Haptic + Collision Avoidance	no data	no data	Not Significant	no data
4 Behavioural Haptic + Collision Avoidance	no data	no data	Not Significant	Not Significant

Table 3.5: Statistical significance within the collision data

3.10 Discussion

The three metrics allow a good evaluation of operator performance for each trial. Clearly, minimisation of the number of collisions is of great importance, while savings in completion time and distance travelled are also desirable since most tasks carried out in hazardous environments are carried out within strict time limits.

Figure 3.14 shows that for the teleoperation modes 0 and 1, collisions did occur. The haptic feedback of mode 1 reduced the average number of collisions. However, it is important to note that an operator is still able to ignore this information and drive the K2A into a collision.

Modes 2, 3 and 4 show that the introduction of the collision avoidance algorithm reduced the number of collisions to zero. Table 3.5 shows significant differences in the collision data between modes 0 and 1 ($p < .005$) and also modes 1 and 2 ($p < .05$). Thus it can be seen that whilst the addition of haptic feedback greatly reduced the number of collisions, there is still scope for further improvement as shown by mode 2. However, it should be noted that this research was carried out under simulation, thus the collision avoidance system could be tuned to the specific environment and hence its performance was very good. Similar real systems may not perform as well. In addition, it is possible that trained teleoperation operators from the nuclear industry may have produced different performance results. Unfortunately, it was not possible to use trained operators for this research since none were available, hence, this should be taken into consideration when evaluating the results of this research.

The collision data shows that for modes 0, 1 and 2 there is a gradual improvement in performance, with no significant change in the distance travelled or time taken. As mode 2 produced no collisions, one can conclude that this mode generated the best operator performance. However, it is important to note that this does not necessarily mean that this is the best mode of control for teleoperation in hazardous environments. As previously noted, it is desirable that an operator should be able to understand the operation of any autonomous behaviour in order to allow her/him to override the behaviour if and when it is needed. Hence modes 3 and 4 are of particular interest. As with mode 2, there were no collisions when using modes 3 and 4. Furthermore, the Wilcoxon T test showed that there are no significant differences between the distance travelled and time taken between modes 2, 3 and 4. This suggests that the haptic feedback in mode 3 and mode 4 does not offer any great performance improvement over the autonomous operation

of mode 2. One may conclude from this that the haptic feedback is not necessary since the collision avoidance system can achieve a high level of performance alone. This, however, relies on the idea that the collision avoidance system can be trusted at all times and in all situations. This may not be the case in a safety critical environment. Therefore it is desirable that the operator can understand the behaviour of the vehicle. This is why the operation of modes 3 and 4 are important. One can imagine a situation where the operator is providing the high-level motion commands and the vehicle is responsible for avoiding obstacles at a lower level. With haptic feedback, the obstacle avoidance can be monitored and overridden by the operator, thus ensuring that he/she has overall control of the vehicle. While the haptic feedback provides an operator with greater information regarding the vehicle's environment, and hence the knowledge that the vehicle may be about to take some avoiding action, quite what this action will be is unknown until after the event has occurred. This situation may be satisfactory provided an operator has complete trust in the autonomous behaviour of the robot. The collision avoidance algorithm used in the trials was very simple; if the behaviour was made more complex, then mode 3 may be less attractive. Mode 4 on the other hand, does inform an operator as to the motion of the K2A as it is occurring, but the operator may in some situations have to rely upon any available camera information to appreciate why the K2A is executing this motion.

Figures 3.12 and 3.13 also show the theoretical minimum for the time taken and the distance travelled. Note, theoretical does not necessarily mean practical or desirable as these figures are based upon the K2A travelling at its maximum velocity (0.75m/sec), while just skimming past the posts. However, these values do highlight the fact that even greater performance improvements are possible.

3.11 Conclusion

A number of experiments have been performed to test the hypotheses:

1. Teleoperation performance can be improved upon if haptic feedback is introduced.

2. Telerobotics yields improved performance over teleoperation alone.

3. Telerobotics when combined with haptic feedback yields improved operator performance over that of telerobotics alone.

Although the results obtained have substantiated hypotheses 1 and 2, hypothesis 3 has proved more illusive. When a remote robot is equipped with some autonomous behaviour, e.g. collision avoidance, then this telerobotic capability is extremely useful when manoeuvring the vehicle in a cluttered environment. In the absence of ideal camera placements, haptic communication can be used effectively to augment the information available to an operator. However, when this communication method is combined with telerobotics, the data has shown that there is not the expected further increase in operator/system performance. The results of the statistical analysis show that there was no significant performance difference between modes 2(Telerobotics), 3(Telerobotics with Environmental Haptic Feedback) and 4(Telerobotics with Behavioural Haptic Feedback). Hence it would appear that there is no strong argument in favour of using haptic feedback with telerobotics. However, as stated in the analysis of the results, this conclusion would not take into account the advantages offered by haptic feedback in extenuating circumstances, that are beyond the scope of normal data collection and experimentation. In this context, an extenuating circumstance is defined as an event where the normal condition of the robot of environment is changed to the abnormal for whatever reason. An example would be a situation where the collision avoidance algorithm fails and allows the vehicle to get too close to an obstacle, or due to a change in the environment, the vehicle gets caught in a local minima. These kind of situations are difficult to predict and thus difficult to simulate and assess. One can imagine that in these situations, the operator may need to be able to take complete control of the operation of the robot, hence, she/he would require additional assistance to be able to perform the task. In this situation, it is known that haptic feedback would offer assistance to the operator. Thus, in conclusion, it is recommended that for increased fault tolerance in real life systems, either modes 3 or 4 should be chosen.

This research has shown that haptic feedback can offer performance improvements to mobile vehicle teleoperation systems. Thus it is natural to assume that the same technology can be applied to manipulator teleoperation systems. Chapter 4 documents the development of a high quality three degrees of freedom haptic interface. Chapter 5 covers the integration of the haptic interface with an industry standard teleoperation system. Chapter 6 then covers the use of the system in a series of performance evaluations experiments. Performance evaluations were carried out with peg insertion, grinding and drilling tasks.

Chapter 4

Development of the Three Degrees of Freedom Haptic Manipulandum

4.1 Introduction

Force reflection requires a manipulandum that can present the operator with forces and torques that mimic those that are present at the manipulator end effector. The feedback that is presented to the operator is usually scaled to an acceptable human level (approximately 10N for forces, 0.1Nm for torques). True force reflection generally requires a manipulandum that has six degrees of freedom. Many haptic interfaces that have been developed are capable of force reflection (Daniel *et al.*, 1993)(Wilhelmsen, 1997)(Hannaford *et al.*, 1991)(Maekawa & Hollerbach, 1998)(Nahvi *et al.*, 1998). Although such systems present the operator with a highly intuitive interface, the complexity and production costs of such devices are similar to that of a regular manipulator. Highly intuitive control is achieved at a high cost, which some consider to be a valid reason for compromise (McKinnon & King, 1988).

Very early manipulator teleoperation systems often used masters that were kinematically identical to the slave (Hill, 1977)(Goertz, 1964)(Goertz *et al.*, 1961). The reason for this was that if both the master and the slave shared the same kinematics, then there did not need to be any computation carried out to calculate the required joint velocity or position of the slave arm for any given motion of the master arm, i.e. the slave should always mimic the motion of the master. This allowed the production of early servomanipulators that used electrical servo systems to link the motion of the master to the slave. Figure 4.1 shows the general

principle of an early teleoperation system.
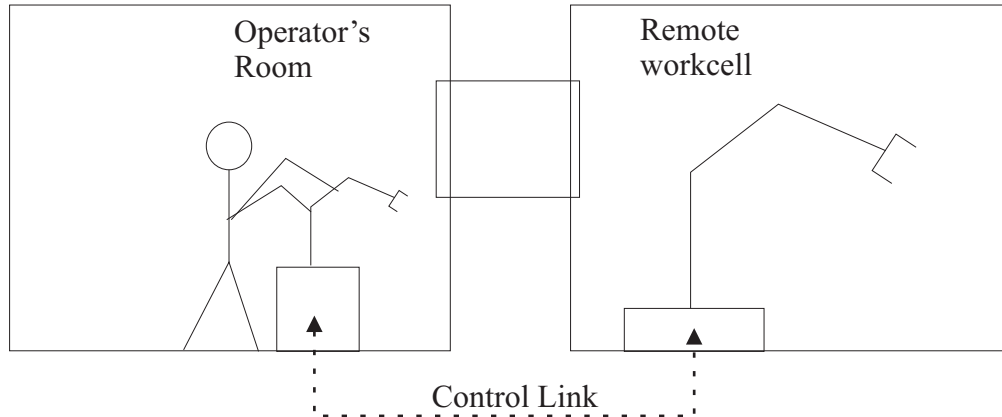
Figure 4.1: An early teleoperation system

Advances in computer technology allowed the use of dissimilar master and slave devices, with the motion coupling calculated and performed by the computer. Hence the computer could carry out both force and motion scaling, thus eliminating the need for often complicated and expensive mechanical linkages (Hamel & Feldman, 1984)(Vertut, 1964). Teleoperation systems, where the master is very similar to the slave, offer an operator a very intuitive means of controlling a remote manipulator, which, due to the inherent mechanical link, naturally presents the operator with force reflection. However, due to the large operational volume, and the fact that the operator has to support the master, they can often be very tiring to use (Siva *et al.*, 1988).

Similar operator fatigue problems are not present with regular joysticks (Zhu & Salcudean, 1995) and hence joystick control systems are generally favoured over kinematically similar master/slave systems. Despite continued high quality research into the development and use of exoskeleton and anthropomorphic control interfaces, joysticks are currently the accepted teleoperation man machine interface in the space, offshore and nuclear industries.

In the design of a joystick, there is a trade off between number of axis and cost of production. For haptic interfaces, this trade off is even more pronounced. Single degree of freedom haptic interfaces are often little more than a handle attached to an actuator (Colgate & Brown, 1994), whereas six degrees of freedom devices are best visualised as a regular robotic manipulator (Maekawa & Hollerbach, 1998)(Nahvi *et al.*, 1998).

Three degrees of freedom joysticks are widely accepted for controlling manipulator position and orientation. Example systems include the UK Robotics Ltd ATC

system and the Brokk AB (Brokk AB., 2003) mobile manipulator control system. Figure 4.2 shows the UK Robotics Ltd ATC system.

Figure 4.2: The UK Robotics Ltd Advanced Teleoperation Controller

Both the UK Robotics system and the Brokk system utilise two, three degrees of freedom joysticks. The UK Robotics system uses the first joystick to control the manipulator tool Cartesian position and the second to control the tool's orientation, i.e. roll, pitch and yaw. Currently the Brokk system does not exhibit resolved Cartesian motion and thus each joystick degree of freedom controls a single manipulator joint. Systems such as these allow six channels of data transfer between the man and the machine without the need for a complex six-axis joystick. However, the use of two, three-axis joysticks is clearly not as intuitive as one six-axis joystick. Also, six-axis joysticks are sometimes more suitable due to the fact that they allow single-handed operation. The offshore industry often prefers single-handed manipulator controllers that allow the operator to use their second hand for controlling the motion of the R.O.V to which the manipulator is attached.

Daniel et al (Daniel *et al.*, 1993) of the University of Oxford have developed a six degrees of freedom haptic interface and position control teleoperation system. Position control requires manipulanda that exhibit relatively large workspaces. Due to stability issues, this fact is pronounced with haptic feedback systems. In order to satisfy the requirement for a large manipulandum workspace, Daniel et

al developed a six degrees of freedom Bilateral Stewart Platform (BSP). The BSP is in essence a parallel manipulator with six degrees of freedom that has a regular joystick manipulandum attached to the end effector. This high performance manipulator/manipulandum with a relatively large workspace coupled to position control offers a high performance and highly intuitive system. However, due to the fact that the haptic interface is effectively a high performance manipulator, the actual development cost of such a system is very high.

After considering all the previous research into teleoperation haptic interfaces and also commercial non-haptic teleoperation control interfaces, a three degrees of freedom device was chosen for the manipulator research. This decision is justified as follows:

- Passive, three degrees of freedom devices are accepted by the industry

- Allows performance comparisons with passive three degrees of freedom systems

- Using two, three degrees of freedom devices to control both position and orientation provides an even split of work between both hands, i.e. one hand controls x, y and z, whilst the other hand controls roll, pitch and yaw

- The mobile robot research proved the effectiveness of the two degrees of freedom device, thus adding an extra degree of freedom is a simple logical step

- It is likely to be more cost effective to produce two, three degrees of freedom haptic interfaces than one, six degrees of freedom haptic interface. Given that six are required for simultaneous control of x, y and z and roll, pitch and yaw

As with the two degrees of freedom device used in the mobile research, three degrees of freedom commercial haptic joysticks exist on general sale, however, it was noted that whilst high performance devices are available (Massie & Salisbury, 1994), they are still in essence a black box. In this context, the phrase "black box" is used to identify a system that is closed and not extensible by end developers. It should also be noted that use of such systems is often hampered by a lack of device characterization data. In order to fully understand the haptic device, the decision was made to develop a device rather than purchase an "off the shelf device". This decision also allows the devices characteristics to precisely meet the requirements of the research.

4.2 Development

4.2.1 Desired Device Characteristic Specification

Two similar designs of three degrees of freedom haptic devices exist and both are similar in construction to the Immersion IE2000. The first, as shown in figure 4.3 exhibits roll, pitch and yaw and the second as shown in figure 4.4 exhibits roll, pitch and z-axis degrees of freedom.
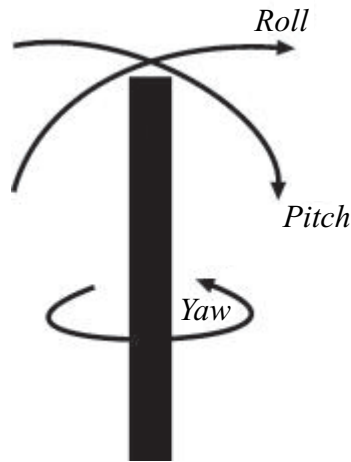
Figure 4.3: 3 DOF haptic joystick configuration with z wrist twist
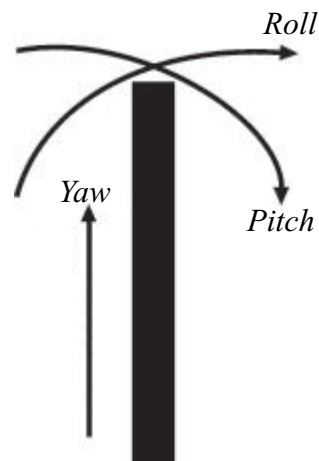
Figure 4.4: 3 DOF haptic joystick configuration with vertical z motion

The roll, pitch and yaw configuration, as shown in figure 4.3, was chosen. This is because this configuration is the same as the passive joysticks that are used

in existing and industry accepted teleoperation systems such as the UK Robotics ATC and also the Brokk AB mobile manipulator control interface. Choosing this design allows direct performance comparisons between the haptic and regular passive joystick interfaces.

From a literature search into haptic joystick production (Massie & Salisbury, 1994)(Buttolo & Hannaford, 1995)(Maekawa & Hollerbach, 1998)(Hannaford *et al.*, 1991)(Colgate & Brown, 1994)(Ellis *et al.*, 1996)(Smith, 1998)(Fischer *et al.*, 1992)(Daniel *et al.*, 1993), and also from the Internet published specifications of commercially available devices (Microsoft SideWinder Force Feedback Pro, 2002)(Immersion Corp., 2000)(Cybernet Systems, 2000)(Sensable Technologies, 2000)(Haptic Technologies Inc. MouseCAT(TM), 2000)(Virtual Technologies Inc. CyberGrasp(TM), 2000), a specification was generated for the haptic joystick design. This specification is outlined in table 4.1.

Max Continuous Torque Roll and Pitch axis:	1Nm
Max Continuous Torque Yaw (Wrist Twist) axis:	0.1Nm
Force Resolution	$\geq$9bit signed
Position Resolution	$\approx$0.01 Degrees
Joystick displacements	-40 to +40 Degrees
Sample and update rate	$\geq$1 KHz

Table 4.1: The desired haptic device specification

In designing a high performance haptic interface there are many design considerations. Ellis et al (Ellis *et al.*, 1996) proposed eleven characteristics that a high performance haptic device should exhibit:

1. Low apparent mass/inertia

2. Low friction

3. High structural stiffness

4. Apparent backdriveability

5. Zero (or very low) backlash

6. High force bandwidth

7. High force dynamic range

8. Absence of mechanical singularities

9. Accessibility to the operator

10. Compactness

11. Isotropic, i.e. even "feel" throughout the workspace.

From the above list, points 1 and 2 are primarily due to the actuation system and the device mechanics. Points 4 and 5 are highly dependent on the torque transmission system design. Here optimisation can be achieved if there is no transmission system i.e. in a direct drive system. Points 6 and 7 primarily rely on the actuation system but they are also affected by the device mechanics and transmission system.

As noted by Ellis et al (Ellis *et al.*, 1996) and also Fischer et al (Fischer *et al.*, 1992), many of the specification requirements for a haptic interface design are in contradiction with other specification requirements. For example, a direct drive actuation system would provide minimal backlash, friction, and high backdrive-ability. However, in order to achieve large forces, a larger actuator would be required which would thus increase the apparent mass/inertia of the device.

4.2.2   Actuator Choice

Electrical actuation, via high quality DC motors, is the most common source of actuation for haptic devices. Pneumatic and hydraulic actuation have also been used. As with robotic actuation, pneumatics is generally used where relatively small forces are required and hydraulics is used where large forces are required. In haptic interface design, pneumatic actuation is generally used for the actuation of the human finger (Burdea *et al.*, 1997a), while hydraulic actuation is generally used for actuation of the human arm (Maekawa & Hollerbach, 1998).

Electrical actuation via DC motors was chosen for the three degrees of freedom joystick. Ease of control and high availability of robust high performance products are the main influence, as well as the fact that it is generally accepted that motors are best suited to provide the level of torques that are required from a hand based haptic system.

Electric DC motors vary in quality depending on their design and intended use. High performance robots such as haptic interfaces require high quality motors that exhibit high torque, low torque ripple, linear torque response and no cogging. Iron-less core Maxon DC motors were chosen to meet these criteria. Maxon iron-less core motors exhibit no magnetic cogging, low rotor inertia, high torque due to the use of rare earth magnets, and a highly linear torque versus speed response. Long brush and commutator life is achieved by the reduction of brush arcing by using capacitors that are built into the armature of the motor.

The motor chosen was a 10 Watt, Maxon RE25. Table 4.2 outlines some important technical data for the Maxon RE25 10 Watt DC motor.

Product code	118743
Nominal voltage (V)	12
Max. continuous current (A)	1.26
Max. continuous torque (mNm)	29.61
Rotor Inertia (gcm)	10.6
Motor Weight (g)	130

Table 4.2: Maxon RE25 10W Technical Data

Since the chosen motor does not generate sufficient torque to meet the desired specifications for the haptic interface, a reduction mechanism was required to increase the total torque generated.

4.2.3 Torque Transmission Factors

From the eleven desirable characteristics put forward by Ellis et al (Ellis *et al.*, 1996) there are five points that are dependent on the choice of torque transmission:

- Low apparent mass/inertia

- Low friction

- Apparent backdriveability

- Zero (or very low) backlash

- Compactness.

Initially, it appears that these five characteristics can be maximised by having no reduction mechanism between the actuator and joystick handle, however, as stated previously, a direct drive system would require larger and more powerful actuators that would also require more power. Since this is also not desirable, there is a trade off to be met between large high power, high inertia actuators and small low power, low inertia actuators running through torque increasing transmissions.

In order to meet the specified force and torque requirements that are detailed in table 4.1 (The desired haptic device specification), a high quality Maxon 28:1 planetary gearhead was chosen as the reduction mechanism. The Maxon gearhead is specifically designed to be interfaced with the chosen Maxon RE25 DC motor. Other alternatives to the chosen planetary gearhead are:

- belt drives

- wire and gimbal mechanisms.

An excellent example of a wire and gimbal mechanism can be found in use on the Immersion Co. Impulse Engine 2000 (Immersion Corp., 2000). Figure 4.5 shows this system.
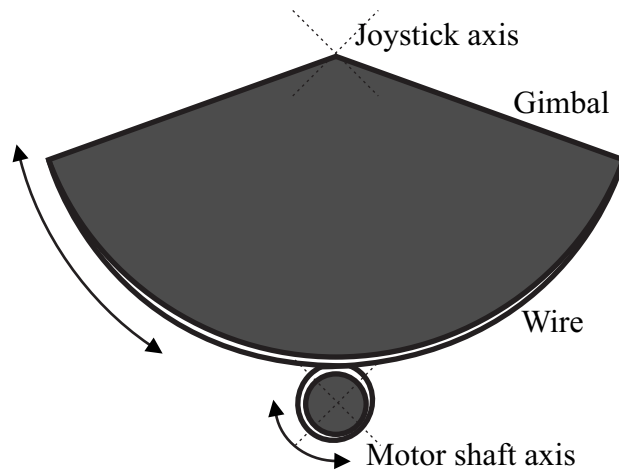
Figure 4.5: Wire and gimbal torque transmission

Table 4.3 outlines the strengths and weaknesses of the three suggested means of torque transmission. It should be noted that this performance evaluation is the opinion of the author, from previous experience of using similar systems. Also, there may be exceptions to the evaluation provided in this table, which were not considered.

	Planetary Gearhead	Belt Drive	Wire and Gimbal
Low inertia	Good	Excellent	Excellent
Low friction	Excellent	Fair	Excellent
Backdriveability	Excellent	Excellent	Excellent
Zero/low backlash	Fair/Good	Good	Excellent
Compactness	Excellent	Good	Poor
Robustness	Excellent	Fair	Poor

Table 4.3: Table showing the strengths and weaknesses of the different types of torque transmission

Table 4.3 shows that the planetary gearhead performs well in every area except inertia and backlash. The manufacturer quotes the amount of backlash exhibited by the Maxon 28:1 gearhead to be not greater than 2.6 degrees. This equates to approximately 4.5 mm of linear backlash at a radial distance of 100mm from the output shaft. Fischer et al (Fischer *et al.*, 1992) quote 2mm as being an acceptable amount of backlash for a haptic manipulandum in a review on the specification and design of input devices for teleoperation. Although there is no doubt that an operator can easily perceive 4.5mm of free motion between two hard stops or virtual walls, this does not necessarily imply that all haptic sensations will be greatly corrupted by the level of backlash. In environments where unilateral constraints are the primary source of haptic sensations, the amount of backlash in the haptic display is far less critical than in many other environments.

The chosen gearhead was a Maxon 32mm 28:1 Planetary Gearhead. Table 4.4 outlines the relevant technical data for the Maxon gearhead.

Product code	114472
Reduction	28:1
Number of stages	2
Backlash	<2.6 degrees
Max continuous torque	2.25 Nm
Max efficiency	75%

Table 4.4: Maxon 32mm Planetary Gearhead Technical Data

4.2.4 Motor Control

Control of a DC motor's torque can be achieved by two very different principles.

- Pulse Width Modulation

- Linear Amplification

Table 4.5 outlines the strengths and weaknesses of both pulse width modulation amplifiers and linear amplifiers.

Pulse Width Modulation	Linear Amplification
Can be difficult to implement, or expensive to buy	Cheap and easy off the shelf implementation
Very efficient	Inefficient due to excessive heat dissipation
Does not require any hardware for connection to a control computer	Requires a D/A for connection to a control computer
Compact	Less compact
Update time limited by modulation frequency	Update time limited only by D/A conversion time
Can cause auditory noise and electrical noise	Produces no noise.

Table 4.5: Strengths and weaknesses of PWM and linear amplifiers

4.2.4.1 Linear Amplifiers

Linear amplifiers rely on transistors to control the current being supplied to a motor. This can be inefficient due to the power transistors being operated in the linear region where excess power is dissipated as heat. Figure 4.6 shows an approximate plot of efficiency for a linear amplifier.

Since linear amplifiers convert an analogue voltage to a motor current they need a D/A to interface to a digital control system, which adds cost and increases size. The major advantage of linear amplifiers is that they produce negligible electrical noise.
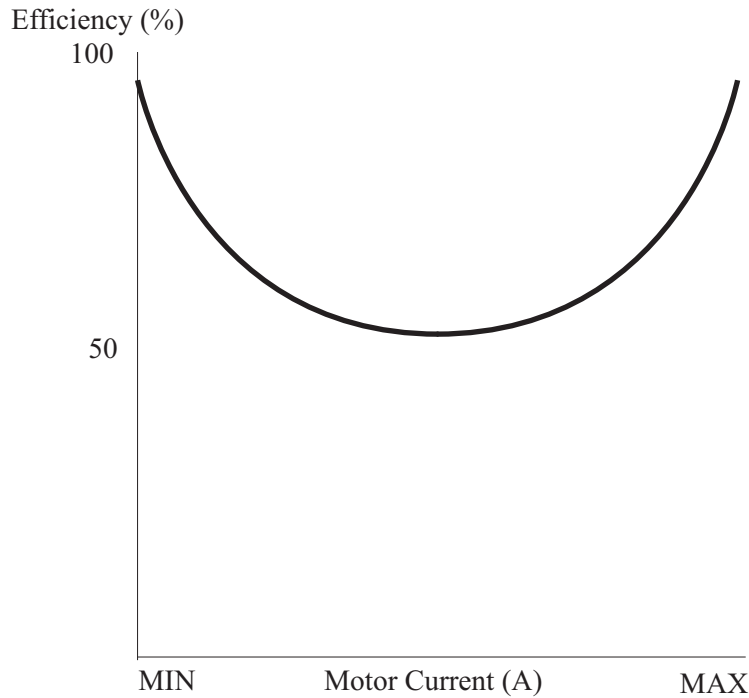
Figure 4.6: An approximate plot of efficiency for a linear amplifier

4.2.4.2   Pulse Width Modulation

Pulse width modulation (PWM) is a very efficient means of controlling the current
supplied to a motor because no power is purposely lost as dissipated heat, as with
linear amplifiers (Kenzo, 1996). PWM or switched mode controllers operate by
switching from full current to no current at high frequencies. The ratio of the
"on" time versus the "off" time gives the percentage of maximum current that
the motor is supplied with. If the switching rate is generated at a high enough
frequency, then oscillations of the armature are of a very low amplitude and the
fundamental result is that the current supplied to the motor is proportional to the
mark/space ratio (on/off ratio). Figure 4.7 shows three PWM signals of differing
mark/space ratio.

PWM requires no D/A converters, and can often be simply implemented in
a microcontroller or Programmable Logic Device (PLD) with no extra devices
other than the power transistor drivers. Since the transistor drivers operate in the
saturated region they dissipate very little power. Often the most important aspect
of a PWM motor controller is the modulation frequency, since this governs the
update time (a cycle must end before a new mark/space ratio is used in the next
cycle) and the dynamic behaviour of the motor. If the modulation frequency is
too low, then large amplitude oscillations will occur in the motor armature. This

60
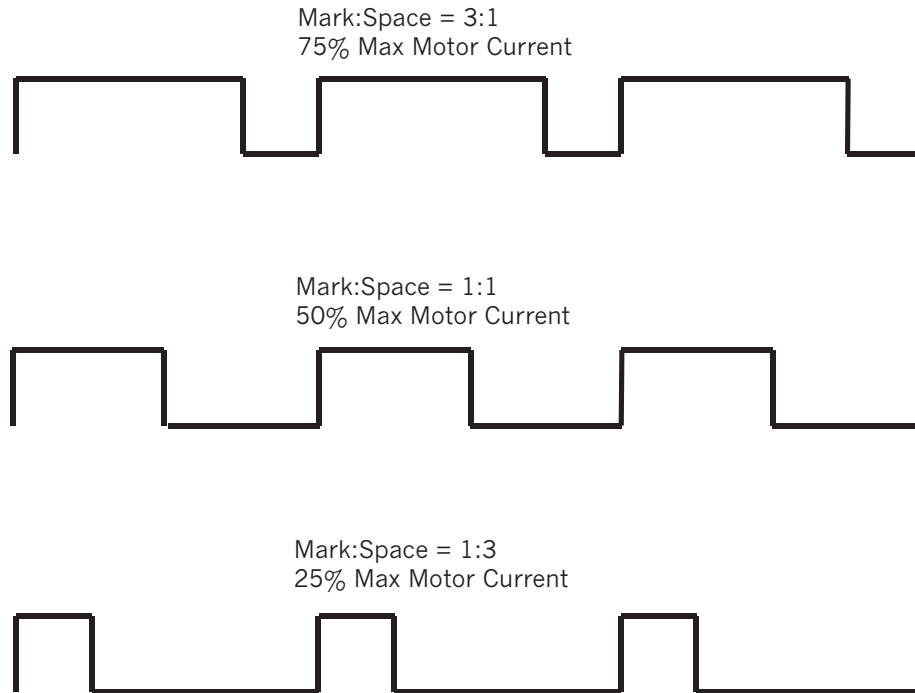
Figure 4.7: Example PWM cycles and the resulting approximate motor currents

will cause some or all of the following problems:

1. System oscillations

2. Auditory noise

3. Poor current control

For a haptic joystick, point 1 is clearly very undesirable because the operator may be able to perceive these oscillations. Point 2 is less of a problem since all motors make noise when in use, and we are usually surrounded by PCs and other equipment that often produce small amounts of auditory noise. Point 3 however is the most influential since we require an accurate, linear motor controller for the haptic device.

Despite the fact that linear amplifiers are simpler to implement, PWM was chosen for efficiency.

4.2.4.3   Pulse Width Modulation Implementation

Appendix D documents the development of a prototype Motorola 68HC11 micro-controller based PWM generator.

Different PWM frequencies were tested to evaluate the highest frequency that could be felt as an oscillation via the hand and finger tips. PWM frequencies in the range of 500Hz to 1KHz were found to be the highest frequencies that could cause palpable oscillations. Very high PWM excitation frequencies are as undesirable as very low frequencies, since the efficiency of the drive transistors is reduced as the switching rate is increased. This is due to the fact that as the PWM frequency increases, the rate at which the transistors switch from the off state to the on state via the linear operating region increases. As the linear operating time increases, thus the efficiency decreases. Accepted PWM frequencies range between 1KHz and 20KHz, where frequencies in the region of 16KHz or greater are usually acceptable (Kenzo, 1996)(Gottlieb, 1994). The chosen modulation frequency was 14Khz, while this produces some low amplitude auditory noise, no oscillations of the manipulandum can be perceived. These findings correlate with Ellis et al (Ellis *et al.*, 1996), where it is quoted that the maximum palpable frequency is in the region of 300Hz to 1Khz for very small amplitude vibrations at the fingertip. The chosen PWM frequency allows a maximum motor torque update rate of 14KHz, which far exceeds the required specification for the device.

Initially, a microcontroller based PWM solution was produced that utilized interrupts to generate the control signal. Appendix D documents this development. However, since the microcontroller uses software to generate the PWM signal, the maximum achievable frequency was found to be 8KHz. Thus a new system was developed for the final three degrees of freedom haptic interface that used an Altera Programmable Logic Device (PLD) to generate the PWM signal. The chosen PLD was an EPM7128SLC84-15 device. This device was chosen for the following reasons:

- Relatively high number of logic macro cells

- Relatively high number user i/o pins

- Very low cost

- In system programmable

- Since the PWM generation relies on logic, the required PWM rate of 14KHz is achievable.

The "in-system" programming procedure uses the JTAG (Joint Test Action Group IEEE 1149.1 standard) port on the PLD. The JTAG port connects to the parallel port on a PC via a simple buffer. Appendix D shows the connection

required between the PC parallel port and the JTAG port on the PLD. In system programming allows a PLD to be inserted in to a board, and then never removed again. This eliminates bad connections due to chip socket connection wear, and also eliminates the need for chip labels and chip logging. Implementing the PWM generators in a PLD rather than using microcontrollers or discrete logic chips saves PCB board space and reduces PCB build time. Figure 4.8 shows the logic schematic for a single PWM generator.
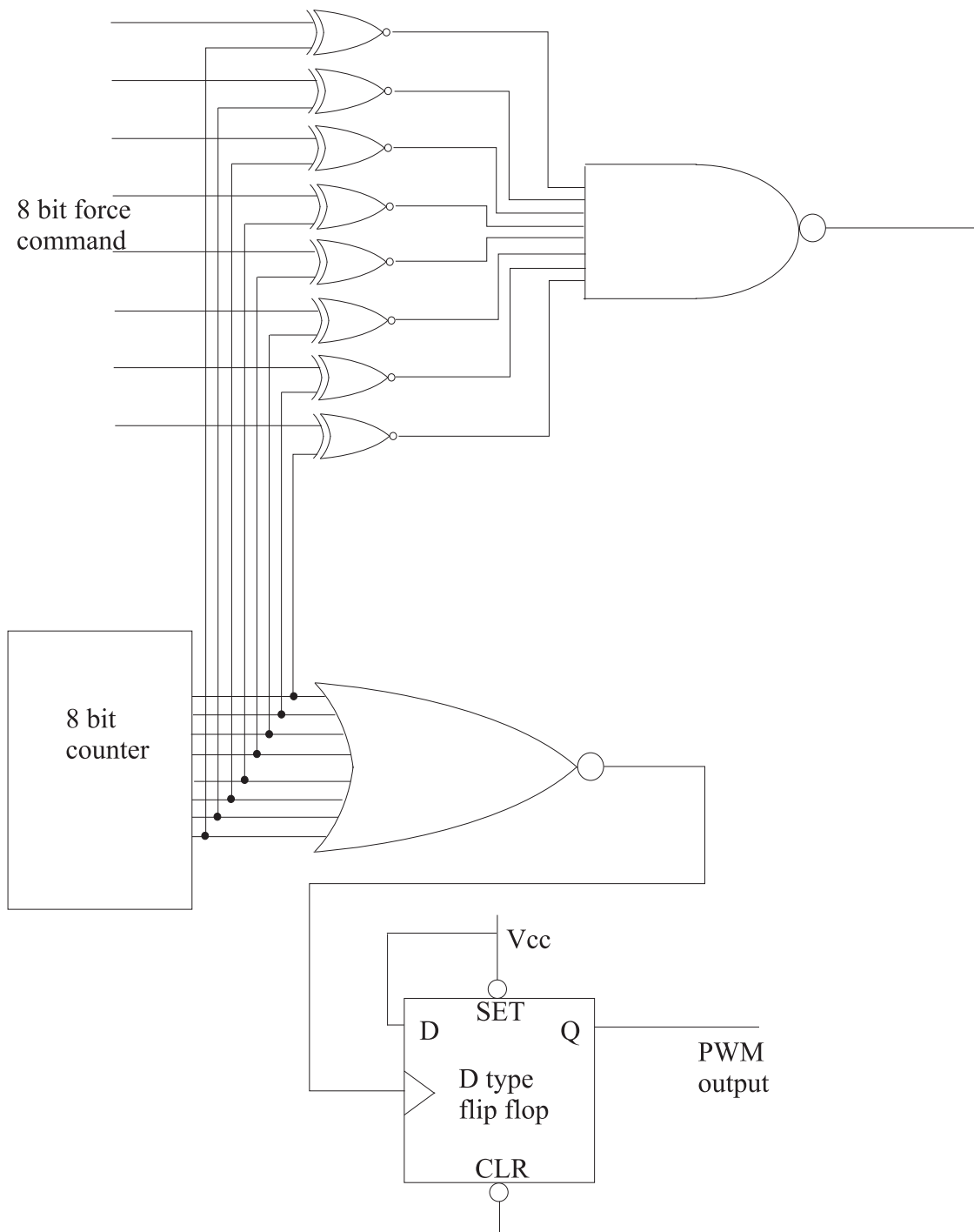
Figure 4.8: The logic schematic for a single PWM generator.

Figure 4.8 shows how the lower eight bits of the force command are used to generate the PWM signal. The ninth bit, which is the polarity indicator, is connected directly to the motor control H bridge which controls the direction of the current that is supplied to the motor. The H-bridge is discussed in detail later in this chapter.

4.2.5   Position Resolving

There are many sensors suitable for position resolving, each with their own strengths and weaknesses. These are outlined in table 4.6.

	Incremental Optical Encoders	Resolvers	Hall effect sensors
Resolution	Excellent	Good	Good
Robustness	Fair	Excellent	Excellent
Temp. Range	Fair	Excellent	Fair
Speed Range	Good	Excellent	Poor
Size	Fair	Good	Excellent

Table 4.6: Outline of the strengths and weaknesses of different position sensors

For haptic device applications, temperature range, robustness and speed are not as important as resolution. Thus it is widely recognised that optical encoders are best suited for position resolving in haptic devices. The choice of encoder resolution was governed by the haptic device specifications outlined in section 4.2.1. A 500 step per revolution, two channel, Hewlett Packard encoder was chosen. The encoder can be supplied fitted to the chosen Maxon motor. With quadrature decoding the encoder resolution is 2000 steps per revolution.

4.2.5.1   Encoder Handling

Appendix D describes the development of the prototype single degree of freedom haptic device. The encoder in the prototype was initially handled by a microcontroller. This worked at slow speeds, but despite optimising the software with respect to execution time, the microcontroller was not fast enough to deal with the high speed rotations of the encoder which can produce cycle rates in excess of 30KHz. Thus, this approach was discarded in favour of logic/firmware encoder handlers. As with the PWM generation, the encoder handlers are implemented in an Altera EPM7128SLC84-15 PLD. Figure 4.9 shows the logic schematic for a single encoder handler. The PLD encoder handler can handle encoder cycle rates in excess of 1MHz, which is far higher than required.
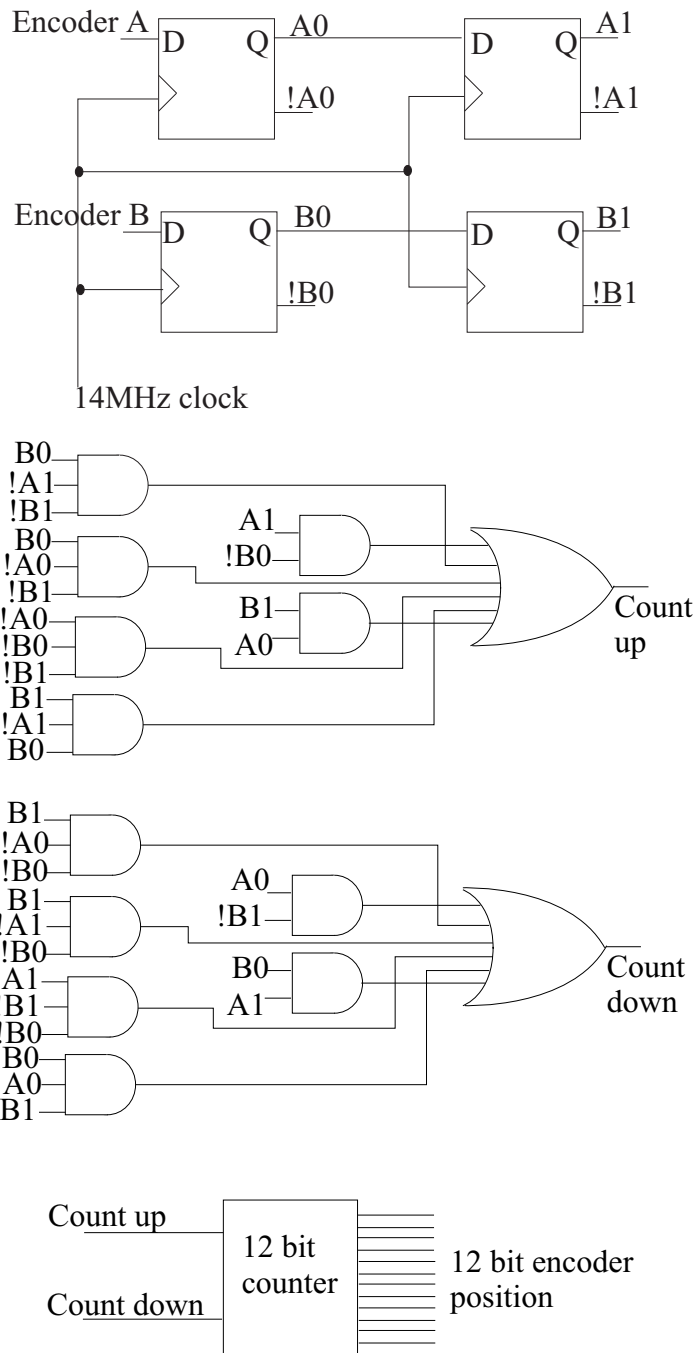
Figure 4.9: The logic schematic for a single channel quadrature encoder handler.

The encoder handlers are quadrature decoding state machines, where a change in state seen between the two sets of D type flip flops is used to either increment or decrement a 12 bit counter. The final implementation that was loaded into the PLD also allowed the counter output to be zeroed to allow the centre position of the joystick axis to be set at any given time.

4.2.6 PC Interface

The PC interface is a critical part of the haptic joystick design since the PC is inside the control loop. If the PC interface cannot read the encoder handler hardware, and write to the motor controller fast enough, then the control loop rate will be limited and thus the haptic sensation will be impaired.

In order to update all three axes of the joystick the PC must read 3, 12 bit values for the encoder positions, and also write 3, 9 bit values to the motor PWM controller. This equates to a total transfer of 63 bits. To allow the control loop rate to be 1KHz, this transfer must occur in 1 millisecond. Thus, the required data rate is 63,000 bits per second. A data rate of 63Kbps is too high for a regular serial connection, thus the decision was made to develop an ISA (PC bus) card. Appendix D shows the single degree of freedom 8 bit ISA card that was developed for the prototype haptic interface. The three degree of freedom ISA card was developed using the knowledge that was gained from the prototype ISA card development. The three degree of freedom ISA card's functionality is achieved completely in logic, which is implemented in an Altera PLD as with the encoder and PWM handlers. The ISA card uses the full 16 bits (AT architecture) of the ISA bus which allows it to transfer either the 12 bit encoder position or 9 bit motor current command in one step. Figure 4.10 shows the schematic of the ISA bus interface.

AEN   Address Lines   Address   IO   IO   IO16
       A9   –   A4   Lines   Read   Write

Address decoding logic. Output low when card base address 220h is present on the address bus

The card uses these address lines to determine the nature of the read or write command.
0000 = Force1
0010 = Force2
0100 = Force3
0110 = Encoder1
1000 = Encoder2
1010 = Encoder3
1110 = Zero force output
1111 = Zero encoder position

These lines are used to control the operation of the tri-state buffers that interface with the ISA data bus

Indicates that a 16 bit data transfer is occurring

AEN. Address Enable, asserted to stop IO cards from responding to memory access instructions

CE (Card Enable). Card is enabled when this line is low. Base address of 220h.

Encoder   Encoder2   Encoder   Force1   Force2   Force3

Encoder multiplexing   Force multiplexing

Encoder tri-state buffer   Force tri-state buffer

Data Bus

Figure 4.10: Schematic of the ISA Bus interface

All of the logic shown in figure 4.10, except for the tri-state buffers, is implemented in an Altera PLD. In order to save space on the printed circuit board, both the bus interface logic and the encoder handlers are implemented within the same PLD chip. A second chip carries the PWM generation logic. Both PLD chips are mounted on the ISA card. Figure 4.11 shows the two Altera PLD chips on the three degrees of freedom ISA card.
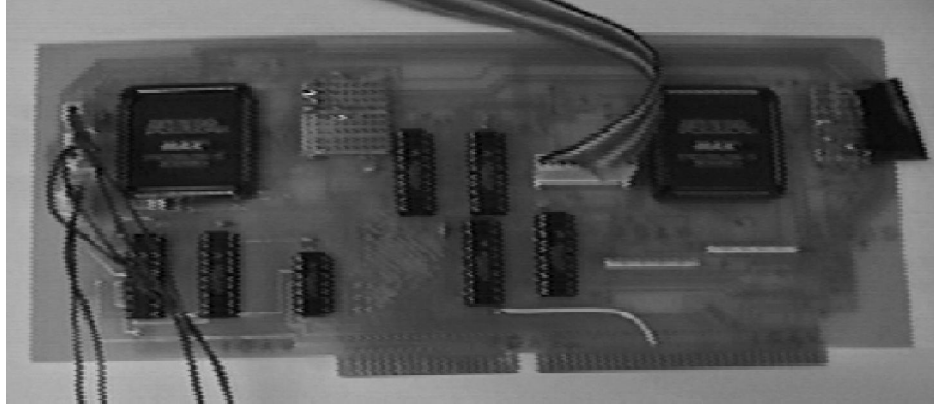
Figure 4.11: Photograph of the three degrees of freedom ISA card.

4.2.7   Motor Drivers

The motor drivers are responsible for switching the current to the motors. Figure 4.12 shows the schematic for one motor driver circuit.
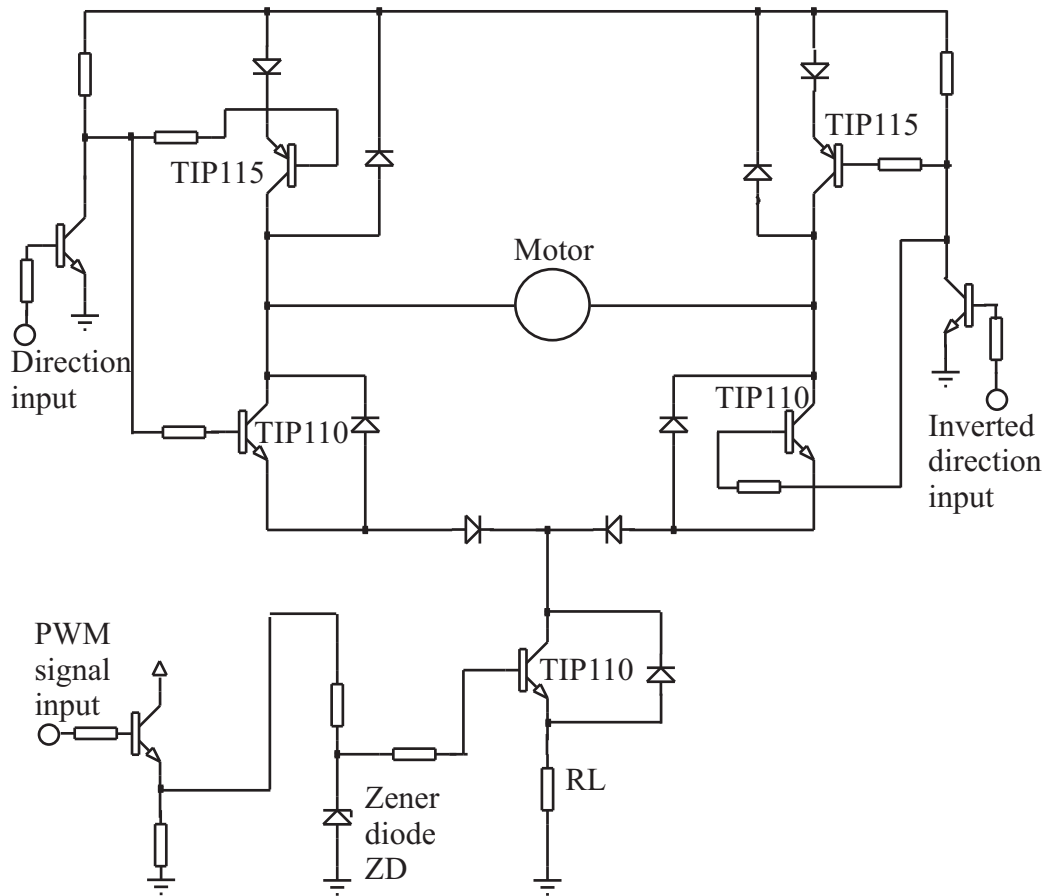
Figure 4.12: The schematic for one motor driver H bridge circuit

The circuit is a simple H bridge where the direction signal controls which pair of transistors are active and thus which direction the current flows through the motor. One side of the H bridge is supplied with the direction signal directly, whereas the other is supplied with the inverted direction signal. The PWM signal controls the switching of the current through the complete H bridge. The resistor RL and the Zener diode ZD are used to control the maximum continuous current through the motor. For the roll and pitch axis RL is effectively 1.6 Ohm and the Zener Diode has a drop of 3.3Volts. For the yaw axis RL is 1 Ohm and the Zener Diode is replaced with three forward biased diodes that equate to a voltage drop of approximately 2.1Volts.

4.2.8 Device Mechanics

Key requirements of the mechanics of a high performance haptic device are as follows:

- Low apparent mass/inertia

- Low friction

- High structural stiffness

- Absence of mechanical singularities

- Accessibility to the operator

- Compactness

- Isotropic, i.e. even "feel" throughout the workspace.

Given that the device mechanics must exhibit three degrees of freedom, several different mechanical configurations are possible.

Three degrees of freedom could be achieved by connecting three actuators in series as shown in figure 4.13.
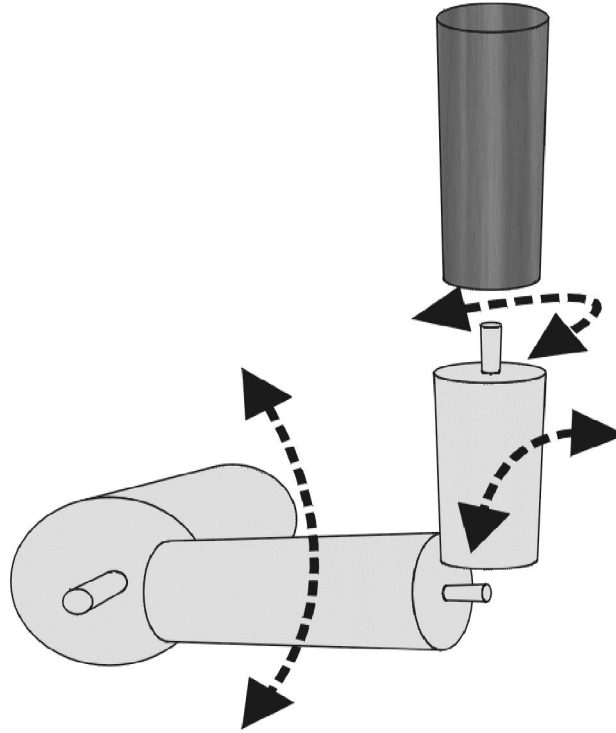
Figure 4.13: Serial mechanical configuration (Exploded view, motor connections left out to aid viewing)

This design would be relatively simple to manufacture since each actuator is attached to the next and thus the bodies of the actuators form integral load bearing parts of the mechanics. However, certain key features are not met by this design. Since two of the actuators move with the manipulandum, the total inertia of the device is increased which is clearly undesirable. Furthermore, since the output shaft of each motor carries the load of the motor and the subsequent motors in the chain, the structural stiffness is relatively low. The device would be highly unbalanced unless the motors could be mounted so that they moved around their centre of gravity. This means that the control of the motors would have to compensate for the unbalance.

In contrast to the serial mechanism shown above in figure 4.13, parallel mechanisms generally exhibit high structural stiffness and low inertia since the actuators are not moving parts. Figure 4.14 and figure 4.15 show two, three degrees of freedom parallel mechanisms.
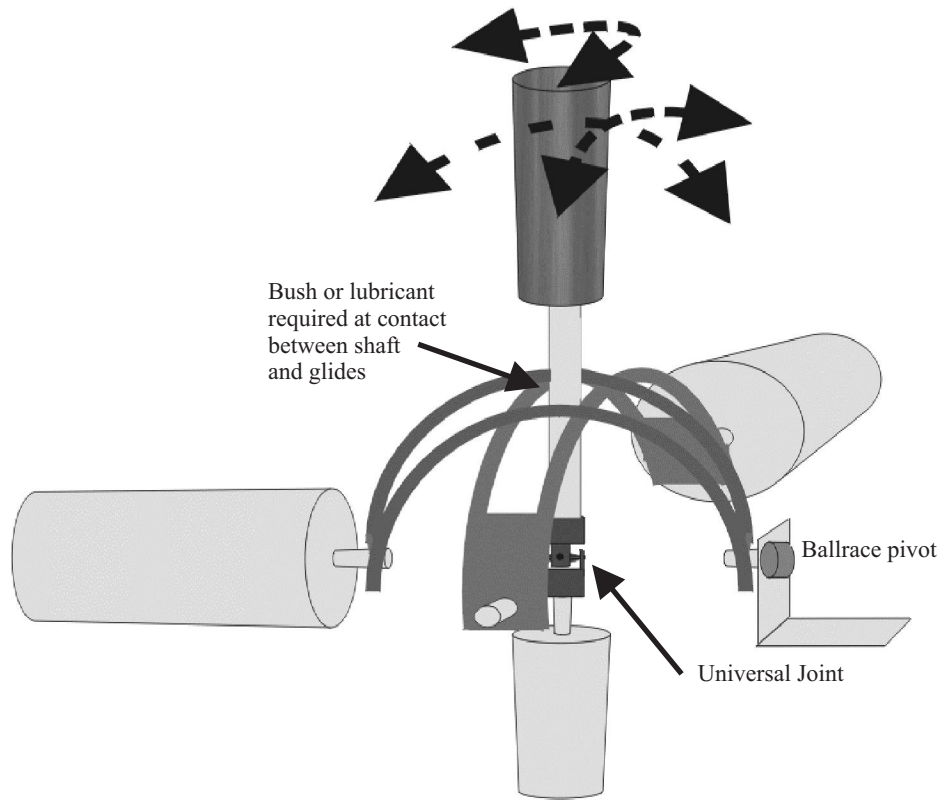
Figure 4.14: Parallel mechanical configuration B (Exploded view, some parts left out to aid viewing)
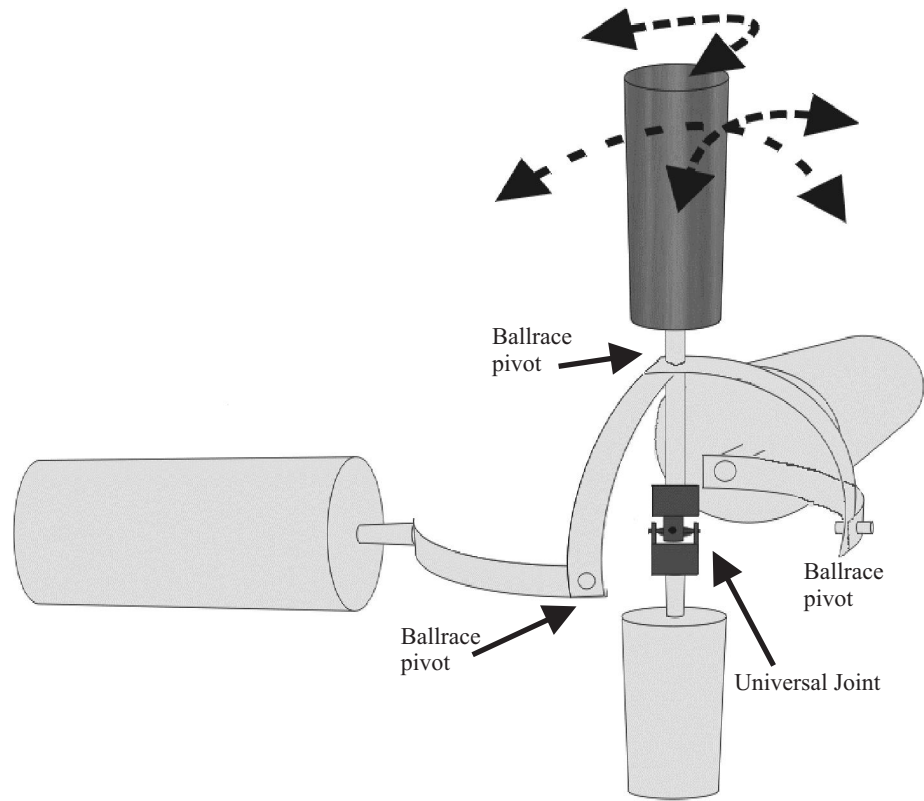
Figure 4.15: Parallel mechanical configuration A (Exploded view, some parts left out to aid viewing)

In comparison to the serial mechanical configuration, both the above mechanisms offer the advantage of very low inertia and high structural stiffness. However, production costs are higher since more parts are required. Both parallel mechanisms offer similar characteristics except for their frictional characteristics. Figure 4.14 relies on two glides to transfer the torque to the manipulandum. Even when the glides are highly lubricated, high levels of friction are introduced which is clearly undesirable. This fact was confirmed by manufacturing both mechanisms. A simple test was performed by commanding a high torque on the x axis whilst simultaneously moving the other axis by hand. Figure 4.14 showed considerably higher levels of frictional cross talk than figure 4.15. It should be noted that it may be possible to use a better glide system on figure 4.14, however it is expected that this would substantially increase the cost of the mechanism. After considering all the advantages and disadvantages of each configuration, the design as shown in figure 4.15 was chosen.

4.2.8.1 Mechanical Design

The device mechanics were produced from aluminium and steel. A Huco universal joint was purchased along with several ballraces. Figure 4.16 shows a close up photograph of the mechanics, and figure 4.17 shows the complete three degrees of freedom haptic device.
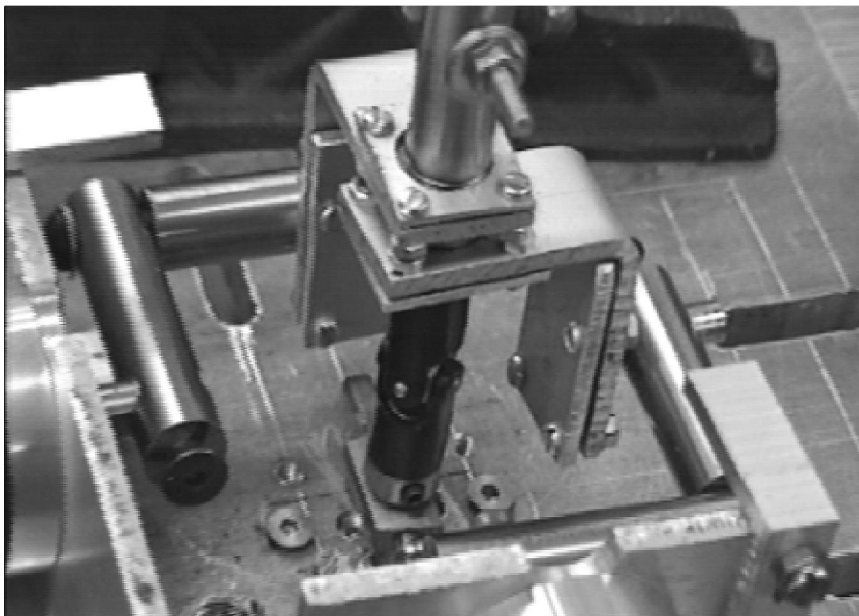
Figure 4.16: A close up photograph of the device mechanics

Figure 4.17: The complete three degrees of freedom haptic device

An inexpensive P.C. games joystick was purchased and then dismantled, the joystick handle was then modified and used as the haptic device handle.

Use of the universal joint in the wrist twist axis has a consequence on the torque that is felt by the operator. Universal joints are commonly used to transfer torques through changes in shaft axes. However, the speed and torque of the output shaft changes relative to the angle between the two shaft axes and the angular orientation of the joint itself. The relationship of the torques on the two axes is given by the following equation which is taken from "Universal Joints and Driveshafts" by Schmelz et al(Schmelz *et al.*, 1992).

$$T_2 = \frac{\cos \beta}{1 - \sin^2 \beta \sin^2 \theta_1} T_1 \tag{4.1}$$

Where T_1 and T_2 are the torques on the two axes, β is the angle between the two axes and θ_1 is the angular orientation of the universal joint. An angle of 50° causes a fluctuation of $\pm 55.6\%$ between the input and output torques, which is clearly undesirable. This problem can be resolved either by removing the universal joint or closed loop force control. Removal of the universal joint would require the actuator to be mounted within the handle of the joystick. This would increase the inertia of the device and cause a large unbalance that would need to be resolved within the control software. Closed loop force control would require the use of torque sensors on the manipulandum, this would increase the complexity of the control system but would provide a means of ensuring accurate control of the force that is felt by the user. Neither approach was adopted in the final interface design. However, this issue is mitigated due to the way in which the haptic joystick was used in the experimentation. None of the three tasks that were used required simultaneous displacement of the wrist twist axis combined with either of the other two axes. Thus, the angle of the universal joint was always zero when a torque was being generated via the wrist twist axis. Clearly, to enable the interface to be used for a broader range of applications the issue of the universal joint would need to be solved, preferably by the addition of closed loop force control or a software based compensation algorithm based on the model of a universal joint.

4.2.9 Safety Issues

As with all robotic devices that operate either close to, or in contact with humans, safety should always be a very important issue. General common sense was used to ensure the operator safety when designing the three degrees of freedom haptic

interface. Primarily, this involved ensuring that the maximum force output from the device was not sufficient to either injure or trap the operator.

4.3   Performance Evaluation

Haptic devices can be characterised in a similar manner to regular robotic manipulators, where measures such as maximum force, force bandwidth, positional accuracy and positional repeatability are used to assess and compare the performance of one device with another.

Table 4.7 shows the desired specification of the haptic device that was set out in section 4.2.1 and table 4.8 shows the actual specification of the device.

Max Continuous Torque Roll and Pitch axis:	1Nm
Max Continuous Torque Yaw (Wrist Twist) axis:	0.1Nm
Force Resolution	≥9bit signed
Position Resolution	≈0.01 Degrees
Joystick displacements	-40 to +40 Degrees
Sample and update rate	≥1 KHz

Table 4.7: The desired haptic device specification

Max Continuous Torque Roll and Pitch axis:	0.829Nm
Max Continuous Torque Yaw (Wrist Twist) axis:	0.489Nm
Force Resolution	9bit signed
Position Resolution Roll and Pitch axis:	0.0128 Degrees
Position Resolution Yaw (Wrist Twist) axis:	0.0064Degrees
Joystick displacements Roll and Pitch axis:	-50 to +50 Degrees
Joystick displacements Yaw (Wrist Twist) axis:	-40 to +40 Degrees
Sample and update rate	1 KHz(And greater if required)

Table 4.8: The actual haptic device specification

Table 4.8 shows that the device meets the desired specifications. However, in order to test the actual performance of the haptic interface, performance characterisation was required. Ellis et al (Ellis *et al.*, 1996) developed a high performance three degrees of freedom haptic interface and then devised a methodology for carrying out a performance evaluation. Ellis et al suggested the methodology to be used by other researchers to allow device performance comparisons. From the methodology proposed by Ellis et al, the following characteristics were evaluated:

- Force bandwidth

- Positional accuracy

- Positional repeatability

- PI controller stiffness.

4.3.1 Force bandwidth

Due to the fact that the haptic interface does not contain integral force sensing, a strain gauge rig was built that attached to the haptic interface and allowed individual axis torque data to be measured. The strain gauge was connected as per the schematic shown in appendix C.

Figure 4.18 shows the strain gauge rig.
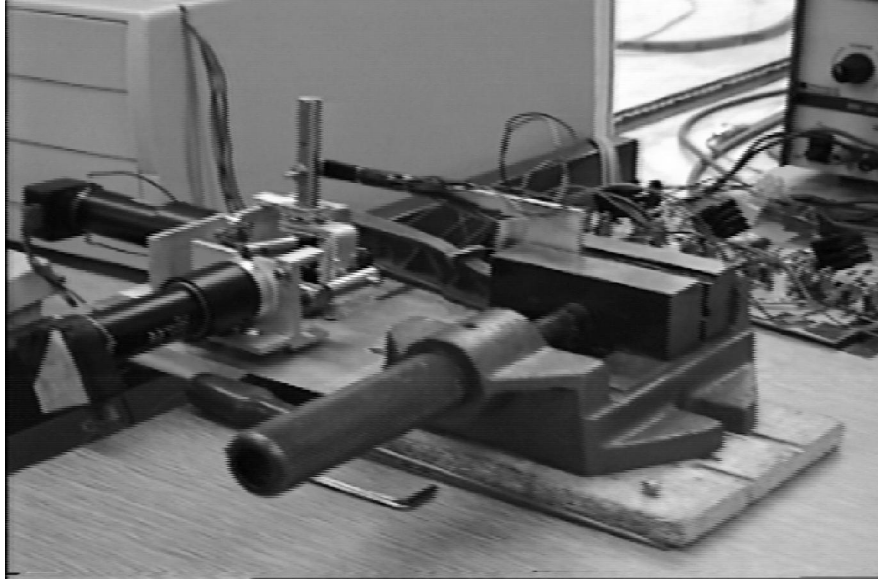
Figure 4.18: The strain gauge rig

An application was written in the "C" programming language that generated a sinusoidal force signal on an individual axis of the haptic joystick. The software was written so that the amplitude and frequency of the signal could be varied. The software was then used to scan through a range of frequencies while the amplitude of the output from the strain gauge amplifier was read on an oscilloscope. The procedure was carried out for one of the two identical axes and a second time for the wrist twist (yaw) axis. As per Ellis et al, the signal that was used to excite the motors was sinusoidal with a maximum amplitude of 50%. The bandwidth to -3dB was found to be very similar for all three axes. The roll and pitch axes exhibit a force bandwidth of 24Hz whilst the yaw axis exhibits a force bandwidth of 20Hz.

Figure 4.19 shows the force bandwidth plot for the roll/pitch axes and figure 4.20 shows the force bandwidth plot for the yaw (wrist twist) axis.
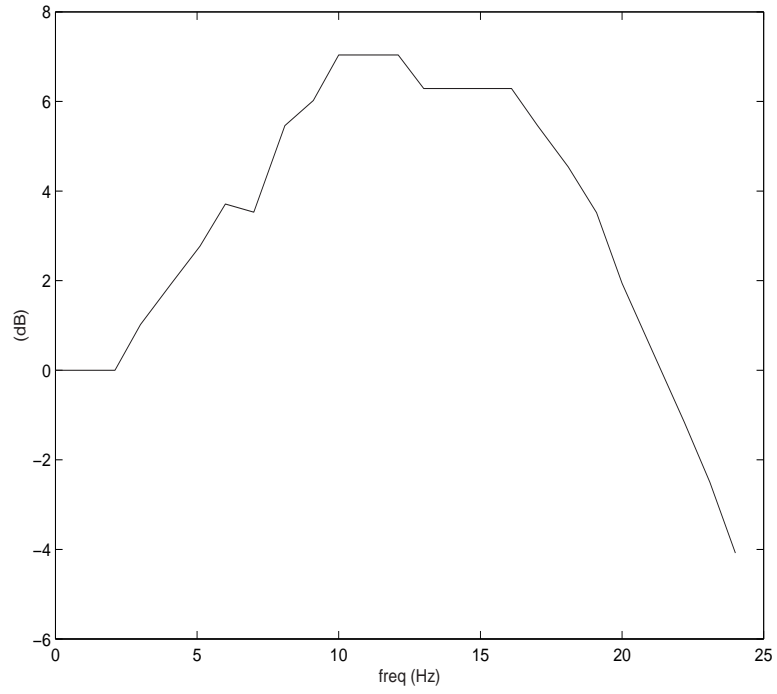
Figure 4.19: Force bandwidth plot for the roll/pitch axes
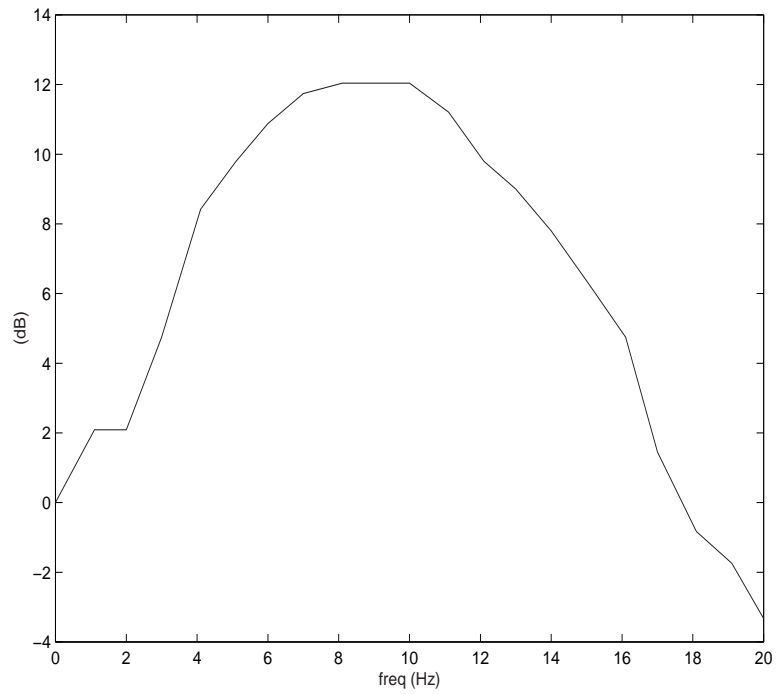
Figure 4.20: Force bandwidth plot for the yaw (wrist twist) axis

4.3.2 Positional accuracy, and repeatability

The mechanical device end stops were used to produce fiducial reference positions within the device workspace. The device was then moved by hand (motor power off) to these reference positions. Multiple readings were taken to determine the accuracy and repeatability of the position sensing. For all three axes, positional accuracy and repeatability were found to be 0.25 degrees. For the roll and pitch axes (x and y), this equates to 0.44mm of motion at a distance of 100mm from the axis of the motor and gearhead i.e. at the centre of the manipulandum.

4.3.3 PI controller stiffness

As with the bandwidth experiment, specific software was produced to allow the evaluation of the maximum controller stiffness. The software emulates a PI servo with a control loop frequency of approximately 1KHz. The integral term was set so that it did not cause saturation. The value of the P term was then increased to the point at which the system was close to the limit of stability, whilst an operator was gripping the manipulandum. As with Ellis et al (Ellis *et al.*, 1996), a human gripping the joystick handle was unable to induce instability. This joystick axis was then displaced until the maximum force was being applied. The displacement was then measured using a micrometer. The maximum controller stiffness was then calculated from the displacement and the force measurement. A value of $1896 \mathrm{Nm}^{-1}$ was recorded as the maximum possible stiffness.

4.3.4 Conclusion on Performance Characterisation

The performance of the haptic device has been evaluated in a manner that allows direct comparison with similar devices. Table 4.9 shows the results of the performance evaluation.

In comparison with the performance criteria of Ellis et al, the maximum stiffness, positional repeatability and positional accuracy are notably different. Ellis et al quote a figure of $24 \mathrm{KNm}^{-1}$ for maximum stiffness and 0.03mm for positional accuracy and repeatability, both of which are roughly ten times better than the figures shown in table 4.9. It is believed that this difference is primarily due the difference in transmission system backlash between the two devices. Ellis et al used a cable transmission system, which may exhibit considerably less backlash than the gearhead transmission that was used in the device that was developed for this research. Unfortunately, no figures were quoted for the backlash of the cable transmission system.

Force bandwidth for roll and pitch axes	24Hz at -3dB
Force bandwidth for yaw axis	20Hz at -3dB
Max. PI stiffness	$1896\mathrm{Nm}^{-1}$ (Limited by backlash in gearhead)
Position accuracy	0.25deg
Position repeatability	0.25deg
Maximum continuous force for roll and pitch axes	8.4N (At 100mm, centre of grip)
Maximum continuous torque for yaw axis	0.489Nm
Joint travel: roll, pitch, yaw	50deg, 50deg, 40deg

Table 4.9: The results of the performance evaluation

Chapter 5

Integration of the three degrees of freedom haptic interface with the ATC and Schilling manipulator

5.1 Introduction

This chapter covers the integration of the three degrees of freedom haptic device with an industry accepted manipulator and teleoperation controller system. The manipulator was a Schilling Titan II and the teleoperation controller was a UK Robotics Ltd Advanced Teleoperation Controller (ATC) (UK Robotics Ltd, 2003).

5.2 System Architecture

Figure 5.1 shows the manipulator teleoperation system architecture that comprises of the Schilling Titan II manipulator, the UK Robotics ATC teleoperation controller and the three degree of freedom haptic interface. The haptic interface is shown comprising of the control PC and the haptic joystick/manipulandum.
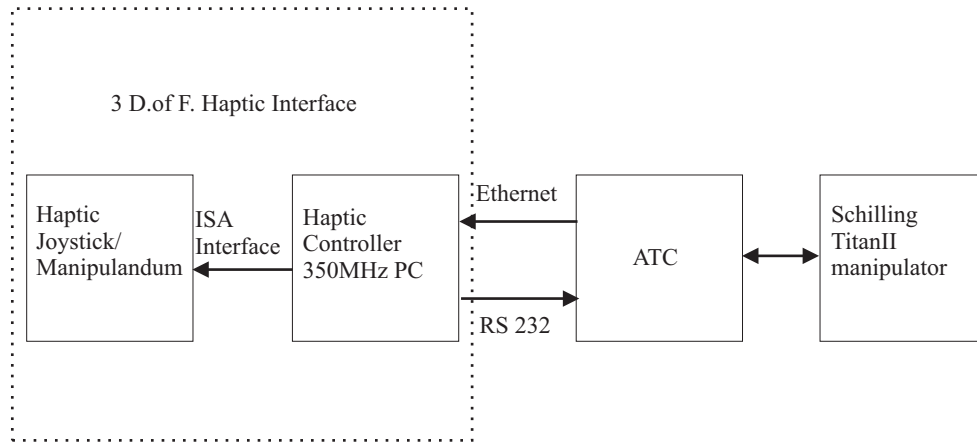
Figure 5.1: Manipulator teleoperation system architecture

5.3 Communications

The interface between the haptic PC and the ATC system utilises a TCP/IP over 10Mbps Ethernet connection and an RS232 serial connection. User motion of the manipulandum is transferred to the ATC via the RS232 serial connection operating at 19200 Baud. The manipulandum position is sent to the controller every 30ms. The haptic control PC produces a dead band region by sending zero motion commands to the ATC system when the joystick axes are very near to their centre position. The ATC system implements Cartesian rate control with varying velocity scale depending on the task that is to be performed.

Raw force-torque data is transferred from the teleoperation controller to the haptic control PC using TCP/IP over a 10Mbps Ethernet connection at a rate of 500Hz. Every 2 milliseconds, 24 bytes of data (6 four-byte values) are sent to the haptic control PC, which equates to a data rate of 96Kbps. This rate was easily achieved and maintained on the Ethernet connection, despite the overhead of using TCP.

The TCP socket was used to provide a reliable channel for the data. Since the haptic PC runs the Win3.1 operating system, Trumpet Winsock was required to provide the communication protocol stack. Figure 5.2 shows the architecture of the haptic PC.
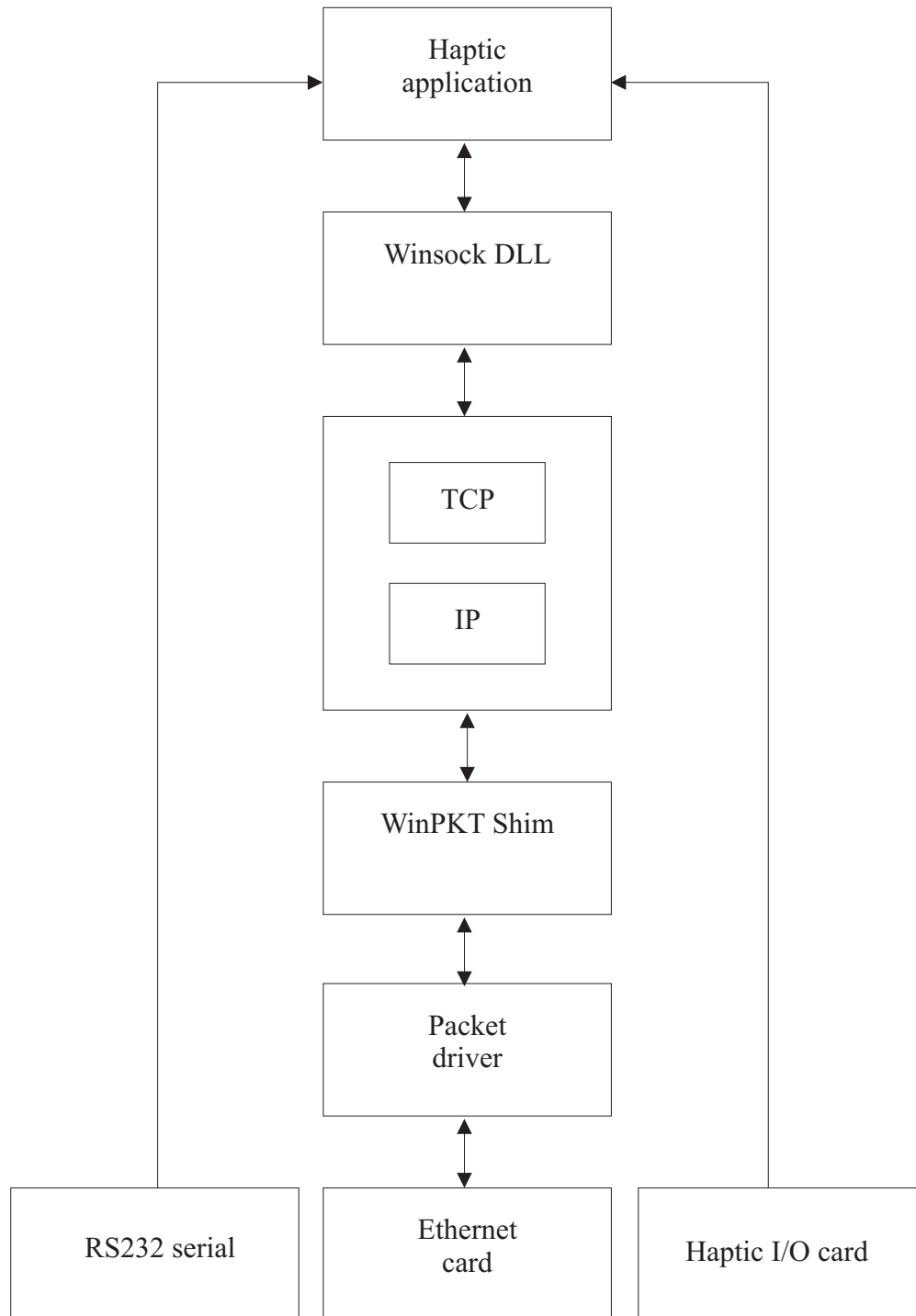
Figure 5.2: The software architecture of the haptic PC

During teleoperation, only the force/torque data was present on the Ethernet, thus there was no contention that could reduce the actual data rate beneath the required rate.

The serial connection between the ATC system and the haptic PC was primarily used to transfer the position of the joystick from the haptic PC to the ATC and the position of the manipulator from the ATC to the haptic PC. The connection was also used to transfer status information from the ATC to the haptic PC. Information was sent to the haptic PC on the status of:

- Axis locks

- Tool choice (Grinder, Drill or Gripper)

- Cartesian operating frame.

The axis lock information was used to generate axis locks on the haptic interface that mimic the axis locks on the manipulator. This information provided intuitive feedback on the status of the ATC systems axis lock feature.

The haptic software used the information regarding the tool that was in use to scale the level of the force/torque feedback.

The information on the Cartesian operating frame informed the haptic PC as to whether the operator was working in world frame or tool frame. This information was used to ensure that as the operating frame moved in relation to the force/torque sensor frame, the operator perceived a consistent force mapping on the haptic interface.

5.4   Force Transformation, Sensor to Tool Tip

The haptic PC performed the force-torque transformation on the raw data depending on what tool was being used. The rotation between the gripper, which was mounted on the 6th axis, and the force/torque sensor was also handled in the transformation. Figure 5.3 shows the position of the force/torque sensor relative to the tool tip.
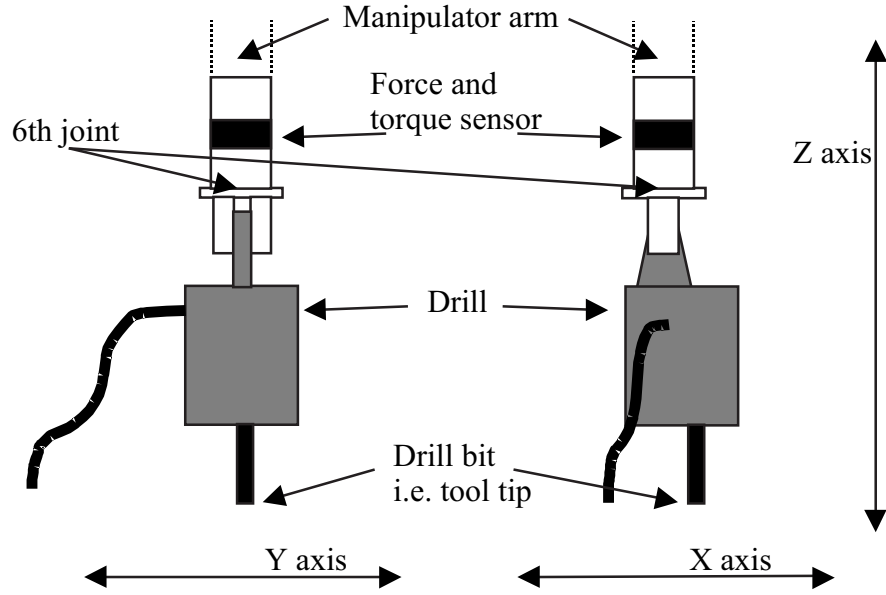
Figure 5.3: The position of the force/torque sensor relative to the tool tip

Figure 5.3 shows the drill being held by the Schilling as an example of the offset between the tool tip and the force/torque sensor. J. J. Craig, "An Introduction to Robotics, Mechanics and Control Methods"(Craig, 1986) was used as a reference to derive the transformation that maps the sensor frame to the tool tip frame. The transformation is as follows.

$$^{T}F_{T} = {}_{S}^{T}T^{T} \times {}^{S}F_{S} \tag{5.1}$$

Where $^{T}F_{T}$ is the matrix of tool forces and torques and $^{S}F_{S}$ is the matrix of sensor forces and torques.

$_{S}^{T}T^{T}$ is the transformation matrix which is given by:

$$_{S}^{T}T^{T} = \begin{bmatrix} {}_{S}^{T}R & 0 \\ {}^{T}P_{S} \times {}_{S}^{T}R & {}_{S}^{T}R \end{bmatrix} \tag{5.2}$$

Where $_{S}^{T}R$ is the rotation transformation from the sensor to the tool frame

$$_{S}^{T}R = \begin{bmatrix} \cos\theta & -\sin\theta & 0 \\ \sin\theta & \cos\theta & 0 \\ 0 & 0 & 1 \end{bmatrix} \tag{5.3}$$

$^{T}P_{S}$ is the position of the tool frame origin within the sensor frame.

$$^T P_S = \begin{bmatrix} X \\ Y \\ Z \end{bmatrix} \tag{5.4}$$

X, Y and Z are the tool axis offsets and θ is the angle of the sixth joint

Hence the full transformation is written as follows.

$$\begin{bmatrix} F_{tx} \\ F_{ty} \\ F_{tz} \\ T_{tx} \\ T_{ty} \\ T_{tz} \end{bmatrix} = \begin{bmatrix} {}^T_S R & 0 \\ {}^T P_S \times {}^T_S R & {}^T_S R \end{bmatrix} \begin{bmatrix} F_{sx} \\ F_{sy} \\ F_{sz} \\ T_{sx} \\ T_{sy} \\ T_{sz} \end{bmatrix} \tag{5.5}$$

Which can be expanded to.

$$\begin{bmatrix} F_{tx} \\ F_{ty} \\ F_{tz} \\ T_{tx} \\ T_{ty} \\ T_{tz} \end{bmatrix} = \begin{bmatrix} \cos\theta & -\sin\theta & 0 & 0 & 0 & 0 \\ \sin\theta & \cos\theta & 0 & 0 & 0 & 0 \\ 0 & 0 & 1 & 0 & 0 & 0 \\ -Z\sin\theta & -Z\cos\theta & Y & \cos\theta & -\sin\theta & 0 \\ Z\cos\theta & -Z\sin\theta & -X & \sin\theta & \cos\theta & 0 \\ (X\sin\theta - Y\cos\theta) & (X\cos\theta - Y\sin\theta) & 0 & 0 & 0 & 1 \end{bmatrix} \begin{bmatrix} F_{sx} \\ F_{sy} \\ F_{sz} \\ T_{sx} \\ T_{sy} \\ T_{sz} \end{bmatrix} \tag{5.6}$$

This transformation was calculated within the haptic PC at a rate of 500Hz, which equals the rate of the force sensor data transfer. The values of the tool axis offsets were updated whenever the tool was changed.

5.5   Haptic communication

The standard joystick interface to the ATC system controlled the velocity of the manipulator's gripper in Cartesian space. As noted by Salcudean et al (Lawrence *et al.*, 1995)(Salcudean *et al.*, 1997)(Parker *et al.*, 1993), haptic feedback implementation on a rate control joystick requires a different approach than haptic feedback implementation on a position control joystick. This is due to the fact that direct force feedback with rate control is impractical due to very limited stability. To circumvent this problem, Salcudean et al proposed a novel stiffness control scheme, which they showed to be very successful when used to control a

heavy duty hydraulic mini-excavator type machine. This joystick stiffness control scheme was used as the basis for the development of the force feedback sensation, but, unlike Salcudean, the value of the actual joystick force was modulated rather than the stiffness. The haptic communication of the force data was calculated as follows when the joystick was moved away from the centre dead band region.

When the motion command from the joystick acts to increase the force applied at the slave:

$$F_M = \frac{F_S}{F_{SMax}} \tag{5.7}$$

When the motion command from the joystick acts to decrease the force applied at the slave:

$$F_M = 0 \tag{5.8}$$

$$\text{IF } F_M \geq 1 \text{ THEN } F_M = 1$$

$$\text{IF } F_M \leq -1 \text{ THEN } F_M = -1$$

$$F_{MOutsideDeadband} = F_M \tag{5.9}$$

F_M is the force felt by the operator, which was normalized between -1 and +1. F_S is the force present at the slave end effector and F_{SMax} is the value of the slave end effector force at which the haptic response saturates. $F_{MOutsideDeadband}$ is used in equation 5.11, shown below. The haptic joystick response is shown graphically in Figure 5.4.
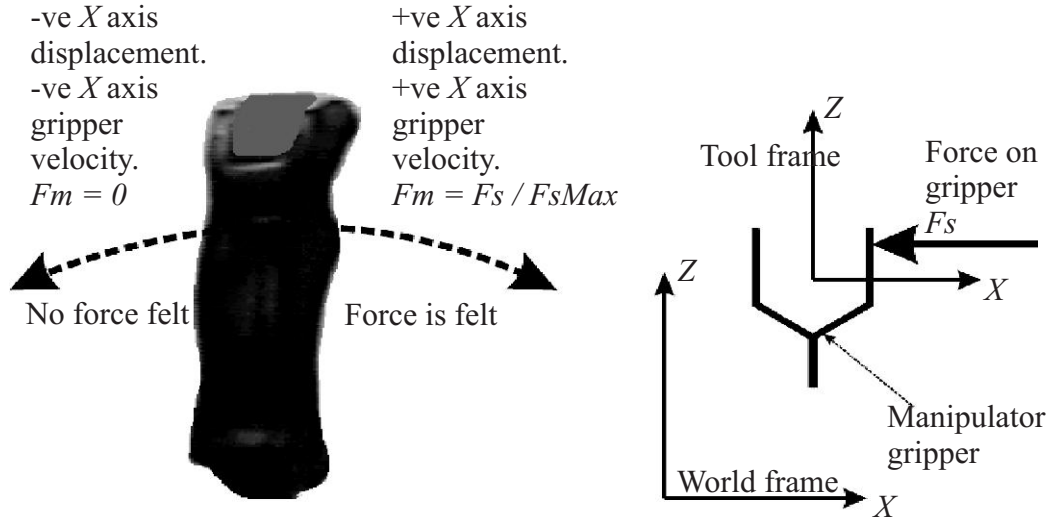
Figure 5.4: The response of the haptic joystick when it is out of the dead band region

Small instability problems could be encountered at the limit of the dead band region if the force just on the outside of the region was larger than the force just on the inside. This was due to step changes in the force response of the joystick. To circumvent this, the dead band behaviour of the joystick was adjusted relative to the normal operating region of the joystick, so that the value of the force across the full range of the joystick was continuous and thus the instability problems were completely eliminated. The calculation of the haptic response in the dead band region is calculated as shown in equations 5.10 through 5.14.

$$F_{MInsideDeadband} = K \times X_{DeadBandLimit} \tag{5.10}$$

where K is the dead band stiffness

$$IF \ F_{MOutsideDeadband} > F_{MInsideDeadband} \tag{5.11}$$

where $F_{MOutsideDeadband}$ is taken from equation 5.9

$$THEN \ K_{adjusted} = \frac{F_{MOutsideDeadband}}{X_{DeadBandLimit}} \tag{5.12}$$

$$F_M = K_{adjusted} \times X \tag{5.13}$$

$$ELSE \ F_M = K \times X \tag{5.14}$$

In the above equations, X is the displacement of the joystick, $F_{MInsideDeadband}$ is the value of F_M at the inner limit of the dead band region and $X_{DeadBandLimit}$ is the value of X at the limit of the dead band. K, which is the stiffness in the centre dead band region, was set so that the operator noted a slight resistance to motion when the joystick was operating in the dead band region. This proportional behaviour in the dead band region felt like a small notch, which helped the operator keep certain axes in their centre position, when displacing other axes. Joystick centring and balance correction were superimposed on all three axis of motion. The forces involved, however, were very small in comparison to the haptic feedback range of forces. Figure 5.5 shows the haptic response when the manipulator is exerting a very small force, and Figure 5.6 shows the haptic response when the manipulator is exerting a large force.
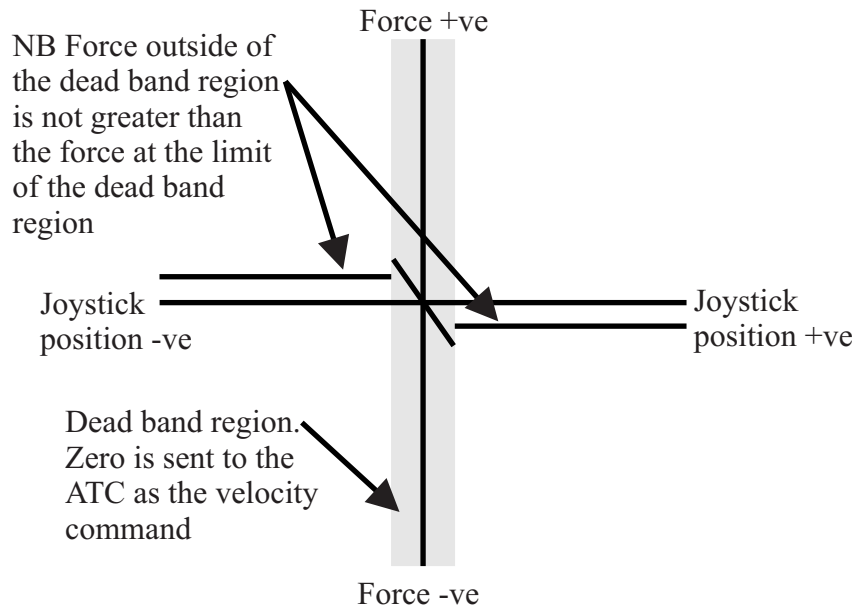
Figure 5.5: Dead band and normal region response with negligible force on slave end effector
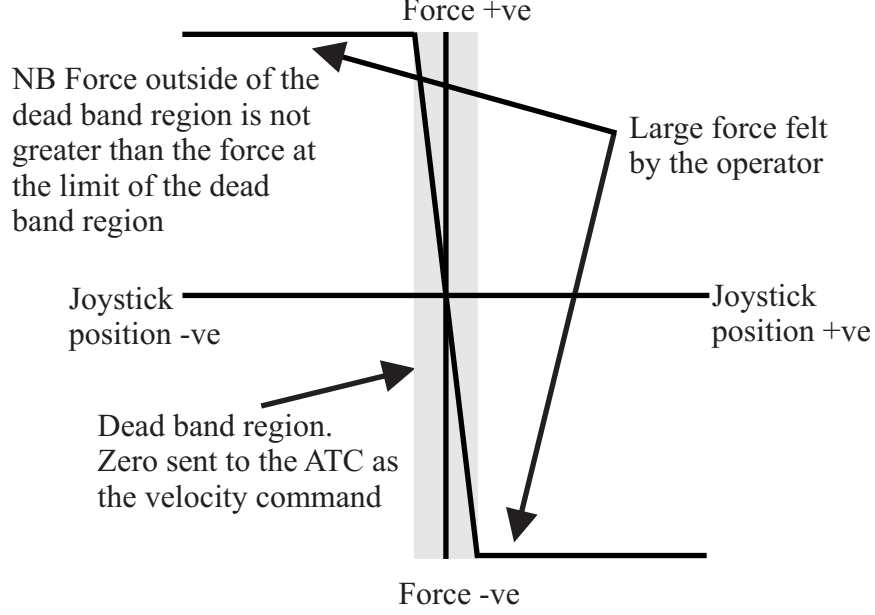
Figure 5.6: Dead band and normal region response with large force on slave end effector

The haptic control scheme proved to be a very effective way of providing information on a rate input device. However, tooling operations such as grinding and drilling also require torque information to be presented to the operator. Since none of the haptic joystick axes controls the rotation of the manipulator gripper, the torque data could not be fed back to the operator in the same manner as the force data and thus a different approach was required. An oscillation of the joystick was chosen as the medium to carry torque information and was generated as follows.

$$T_{SNormalized} = \frac{|T_S|}{T_{Smax}} \tag{5.15}$$

$$A = T_{SNormalized} \times G_{Amplitude} \tag{5.16}$$

$$F = 1 + (1 - T_{SNormalized}) \times G_{Frequency} \tag{5.17}$$

$$X = A \times \sin(t \times F) \tag{5.18}$$

where t is time

In the above equations, T_S is the torque present at the slave end effector, T_{Smax} is the value of T_S at which the response of the haptic feedback saturates and t is used to denote time. T_{Smax} was set according to the specific tooling operation. The value of $G_{Frequency}$ was set so that the frequency range of the oscillation is 20Hz

93

to 80Hz where the lower frequency implies a larger value of torque. The frequency range was chosen so that it did not cross the natural frequency of the device. The value of $G_{Amplitude}$ was set empirically so that the high frequency/low amplitude oscillation was very subtle and the low frequency/high amplitude oscillation felt quite severe. This information was conveyed to the operator via the joystick X axis. In equation 5.18, the result X is the displacement of the axis from its centre position.

5.6   Data Capture

During each experiment, data was recorded to allow the analysis of operator performance.

For the peg insertion experiment that is documented in chapter 6, the following data was recorded:

- Manipulator force value in x, y, and z axes

- Manipulator end effector position

- Haptic joystick position

- Time to completion.

For the drilling and grinding experiments that are documented in chapter 6, the following data was recorded:

- Manipulator force value in the z-axis

- Tool torque generated by the motor

- Manipulator end effector position

- Haptic joystick position

- Time to completion.

The data was recorded at a rate of 33Hz for the duration of each experiment. During the experiment the data was stored to RAM and then persisted to a flat file at the end of the experiment. The data was recorded in this manner since any write actions to the hard disk during the experiment would cause disruption of the real time joystick control system.

Chapter 6

Assessment of Haptic Communication for Manipulator Robotic Operations

6.1   Introduction

Nuclear decommissioning involves the use of remotely deployed manipulators controlled via teleoperation systems. These manipulators are used to perform tasks such as:

- Waste sorting

- Grinding

- Drilling

- Shearing (cutting through objects with a large scissors-like tool)

- Swabbing (sampling dust and dirt from within a cell)

- Plasma arc cutting.

  Teleoperations in hazardous environments are often hampered by a lack of visual and auditory information. Ideal camera locations are generally not possible. Also, visual feedback is often of limited use because it does not generally provide the operator with information regarding the forces and torques that are being applied by the manipulator to the environment or a tool. Damage to the manipulator, tool or environment can be very expensive and dangerous within a hazardous environment such as a nuclear plant. This chapter presents the results of operator

performance tests that have been carried out using the haptic teleoperation system. Operator performance has been studied for peg in the hole, grinding and drilling tasks, both with and without haptic communication and both with one camera and two camera views.

6.2 Background research

Many previous researchers have developed haptic teleoperation systems and evaluated the performance of the system both with and without haptic feedback (Howe & Kontarinis, 1992)(Ouh-young *et al.*, 1989)(Barnes & Counsell, 1999)(Lawrence *et al.*, 1995)(Massimino & Sheriden, 1994)(Salcudean *et al.*, 1997)(Parker *et al.*, 1993)(Hannaford *et al.*, 1991). Where suitable, most researchers have used peg insertion type tasks in order to evaluate the performance of their teleoperation system. Task data usually consists of time to completion and applied manipulator force and torque. From this, operator performance is analysed.

Peg insertion tasks are generally very simple and widely used. The task requires an operator to use many different senses and skills in order to perform the task both swiftly and accurately. Many peg insertion experiments using non-force feedback systems are carried out using a matrix of holes with micro switches attached to the bottom of the hole. The micro switches are used to record the precise moment at which the peg is successfully inserted into the hole. Operators are instructed to move the peg between holes and thus the whole experiment is a mixture of gross Cartesian motion between holes and then precise motion to allow peg insertion. This gives a good measure of the usability of a teleoperation system. However, in order to assess the performance of the haptic feedback element of a teleoperation system, the performance of the system needs to be assessed without the gross Cartesian motion between holes as this will provide no useful data. So rather than the traditional Fitts (Fitts, 1954)(MacKenzie, 1992) type tapping test with more then one hole/tapping region, a haptic peg insertion tasks requires just one hole.

High tolerance peg insertion tasks require good control of contact forces for successful execution, hence force feedback systems should offer improvements over visual feedback only systems. Howe and Kontarinis (Howe & Kontarinis, 1992) developed an identical master and slave teleoperation system to test the performance gains provided by force feedback over vision alone for a simple one-hole high tolerance peg insertion task. They also looked at the role of force bandwidth in the performance of the task by using low pass filters to narrow the force display

bandwidth to 2Hz, 8Hz and 32Hz respectively. Howe and Kontarinis recorded time for completion and also sampled the forces for the duration of the test. They found that force feedback provided a significant decrease in both completion time and mean force magnitude, even at the 2Hz and 8Hz bandwidths. The 32Hz bandwidth, generally, only provided small gains over the 8Hz bandwidth, compared to the gains seen between vision alone, and the 2Hz bandwidth force feedback. Howe and Kontarinis concluded as follows: "These results demonstrate that force feedback improves performance of precision contact tasks in dextrous telemanipulation. Task completion times and error rates decrease as force reflection bandwidth increases. Most of the benefit appears between 2 and 8Hz, although some improvement is seen at 32Hz. These experiments also indicate that even low bandwidth force feedback improves the operator's ability to moderate task forces". Howe and Kontarinis have shown that haptic/force feedback improved the performance of their particular teleoperation system. Given this, is it possible to improve the performance of a teleoperation system, where the master is a regular three axis joystick, and the slave is a six axis hydraulic industrial manipulator?

Despite the research that suggests that force feedback improves man/machine performance, there have been results obtained that suggest that the reverse can also be true. Draper et al (Draper *et al.*, 1999) used a Fitts tapping test to evaluate the performance of their Autonomous/Teleoperated Operations Manipulator, both with their feedback system engaged and disengaged. They used time for completion of a set number of taps as their only performance metric. Draper et al found that force reflection increased the mean time for task completion, however they did not measure contact forces during the test, and so had no way of evaluating the effect of force feedback on the system's "man in the loop" force control. Also it appears that there was no attenuation of the slave forces that were displayed on the master and hence the operator felt the full real magnitudes of the forces. Draper et al hypothesised that the reason for the reduction in performance was due to the increased resistance of motion when using the force feedback. They suggested that the increased force response required by the operator caused an increase in the motor neuron noise associated with any movement and thus a decrease in performance. They also suggested that if the force feedback to the operator was scaled down, then the reduction in performance may not have been seen. Commenting on the Fitts "tapping task", Draper noted that it is an excellent tool for evaluating the trajectory-generating portion of a system but that it does not adequately assess the impedance control part of the system. Thus, variations of the task that involve more peg insertions and hence more contact with

the environment are better suited to assessing a teleoperation system's impedance control. Examples of such variations on the Fitts theme that are suitable to assessing the performance of haptic feedback can be seen in Massimino and Sheriden (Massimino & Sheriden, 1994), Repperger, Remis and Merril (Repperger *et al.*, 1990) and Draper et al (Draper *et al.*, 1988). Repperger et al (Repperger *et al.*, 1990) performed an experiment using a passive exoskeleton device. The experiment was similar to the "Disk Transfer" experiment conducted by Fitts (Fitts, 1954), where the amplitude of movement is constant but the insertion tolerance differs from one experiment to the next. Massimino and Sheriden (Massimino & Sheriden, 1994) used a variation of the Fitts theme that involved the insertion of a peg into a single hole. This task was used to evaluate the performance of an operator when presented with different levels of visual and haptic feedback. The tasks were conducted using a 7 d.o.f. slave manipulator, and a 7 d.o.f. master hand controller (the master and slave's 7th d.o.f. was the gripper, i.e. no redundancy). Massimino and Sheriden found that force feedback made significant improvements to the task completion time. Draper et al (Draper *et al.*, 1988) simulated the task of inserting an electrical plug into a socket. An operator used the manipulator to insert a two-prong peg into a socket. Time for task completion was used to evaluate performance.

Salcudean, Lawrence, Parker et al addressed the problem of adding haptic/force feedback to a heavy-duty hydraulic excavator/tree feller machine (Lawrence *et al.*, 1995)(Salcudean *et al.*, 1997)(Parker *et al.*, 1993). The standard joint by joint rate control interface was removed. In its place Sulcudean et al tested both a haptic Cartesian velocity input device and also a Cartesian position controlling device. They noted that the addition of coordinated control and force feedback improved operator performance, particularly with inexperienced operators. Improvements were noted in terms of time-to-completion, lower operator training times and less environmental damage (damage to trees that are being felled). The velocity input device used was a six degrees of freedom magnetically levitated joystick that was developed by the University of British Columbia. Direct force feedback was evaluated using the device, but found to be unsuitable due to the instability problems that are associated with presenting direct force feedback on a rate controlling input device. Hence, a novel stiffness sensation was developed that allowed the manipulator forces to be presented to the operator by a means of altering the stiffness of the centring spring action. This method of force feedback was reported to be very successful.

Fischer et al of The University of Oxford, conducted research into the specifica-

tion and design of input devices for teleoperation (Fischer *et al.*, 1992). The problem of designing input devices for teleoperation systems was approached without reference to the implementation of the final solution. The quantitative specification proposed by Fischer et al covers force and position bandwidths, backlash, workspace, device inertia and forward force threshold. This specification was then compared against the specification of several existing haptic input devices. Following on from this research, the specification was used in the development of a high performance parallel input device (Daniel *et al.*, 1993). The device that was produced, named as the Bilateral Stewart Platform (BSP), is in essence a small electrically actuated parallel robot which exhibits six degrees of freedom. The BSP was then successfully incorporated in a Puma/Unimation 560 Teleoperation system.

The majority of haptic teleoperation systems that have been produced have been position controlling. This is due to the general acceptance that ideal position control is superior to ideal velocity control. This hypothesis has been tested and proved by Kim et al (Kim *et al.*, 1987). Kim et al found that the master/slave workspace ratio had a large effect on the performance of both the position and velocity control systems. For systems where the master workspace was small or similar in size to the human workspace, position control was superior to velocity control. However, where the manipulator was very slow or the workspace was very large, the superiority of position control generally disappeared. Hence velocity control is advisable in these situations, since velocity control does not require the indexing that is associated with position control.

Many papers have been published that document the performance of teleoperation systems when performing Fitts style tests. However, research into the performance of these systems when performing task such as grinding, drilling and other nuclear decommissioning related tasks is uncommon. Since humans rely heavily on haptic feedback to perform every day tasks with their hands, one would expect that the addition of haptic feedback to a teleoperation system should provide performance improvements for these tasks also.

The focus of this chapter is to present the findings in the area of haptic feedback application, when performing peg insertion, grinding and drilling tasks.

6.3 Experimental Methodology

In order to simulate the task of operating a manipulator in a remote hazardous environment, and also to standardise the visual feedback, cameras were used and

direct line of sight of the manipulator was eliminated by blanking-out the laboratory window. Figure 6.1 shows the camera positions relative to the manipulator gripper during each task and figure 6.2 shows the operator workstation, comprising of the haptic joystick and two camera monitors.
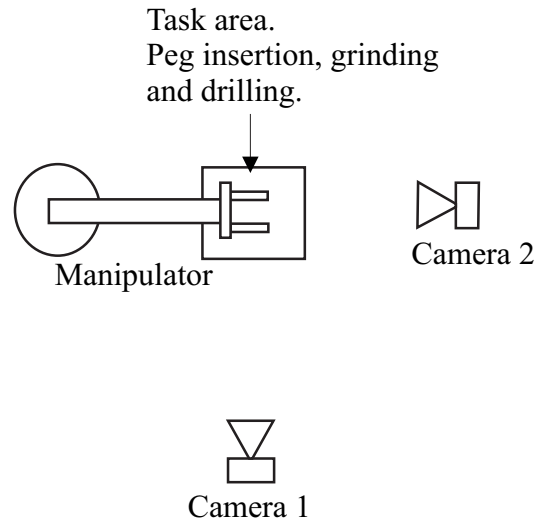
Figure 6.1: Plan view of manipulator work cell showing the camera positions

Figure 6.2: View of the operator workstation, showing the camera monitors and the haptic joystick

Auditory feedback was eliminated so that the operator could not use the sound emitted by the grinder or drill, and thus had to rely entirely on haptic and visual feedback. Ear plugs and ear defenders where used to eliminate the auditory feedback.

Prior to the start of each test, the manipulator was moved to a consistent start position. For the grinding and drilling tasks the tool was positioned just above the work piece, whilst for the peg insertion task, the manipulator gripper was positioned away from the hole with a consistent offset in all three axis. Figure 6.3 shows the Schilling workcell.

Grinding and drilling table where the workpiece was mounted.

Figure 6.3: The Schilling workcell.

All of the experiments were conducted in the laboratory of UK Robotics Ltd, which is shown in figure 6.3

Each task was performed in four different modes. These modes were as follows:

- Mode 1, 1 Camera, no haptic feedback

- Mode 2, 2 Cameras, no haptic feedback

- Mode 3, 1 Camera, with haptic feedback

- Mode 4, 2 Cameras, with haptic feedback.

As documented in section 5.6, data was captured during the experiments. For the peg insertion experiments, the end effector forces and positions in the x, y and z axes were recorded along with the position of the joystick and the time to completion. The same data was recorded for the grinding and drilling tasks, in addition to the torque due to the tool.

6.3.1 Statistical Analysis

The modes of operation allow analysis of performance gains/losses offered by both haptic feedback and increased visual feedback. The results taken from each task were analysed using two different statistical methods. Significance due to haptic feedback was tested using the Mann-Whitney U Test and significance due to visual feedback was tested using the Wilcoxon T Test for Dependent Samples. Each task operator was randomly assigned to the haptic or non-haptic group. Each task operator then performed the task twice, the first time with one camera and the second time with two cameras. Hence analysis of the results requires two separate methods. The analysis of the effect of the haptic feedback requires a test that assumes random assignment of test participants (Kirk, 1999), while the analysis of the effect of the visual feedback requires a test that is suitable for matched pairs. The following section provides a brief introduction to both statistical analysis procedures.

6.3.1.1 Mann-Whitney U Test for Two Independent Samples

The Mann-Whitney U test is used to test the hypothesis that two population distributions are identical. The test assumes that the populations are continuous and that random samples have been drawn from each or that the participants have been randomly assigned to two conditions. This test was originally developed by Frank Wilcoxon in 1945 and called the Wilcoxon rank-sum test (Kirk, 1999). This test is used to test for significance due to haptic feedback since the operators were randomly assigned to either the haptic or non-haptic group.

Appendix E shows an example of using this test.

6.3.1.2 Wilcoxon T Test for Dependent Samples

The Wilcoxon T test is used to test the hypothesis that two population distributions are identical. The test is suitable for samples that result from:

- Repeated measures on the same participant

- Participants matched on a variable that is known to be correlated with the dependant variable

- Identical twins

- Obtaining pairs of participants who are matched by mutual selection.

The Wilcoxon T test makes the assumption that the populations are continuous and that a random sample of paired elements has been obtained or that the paired elements have been randomly assigned to the conditions. This test is used to test for significance due to visual feedback since each operator performed the task twice, once with a single camera and a second time with two cameras.

Appendix F shows an example of using this test.

6.3.1.3   Chosen Level of Significance (Alpha)

As with the mobile vehicle research, careful consideration was made when choosing the level of alpha for the tests. The values of alpha that where considered are as follows: 0.1, 0.05 and 0.01. As was noted in the mobile vehicle research one should consider the possible consequences of making either a Type I Error or a Type II Error, and thus choose the level of alpha accordingly. Within the medical field, the effect of a Type error on a patients health is considered, and if required, alpha is adjusted to control the possibility of making an error. Since there is no apparent cost associated with making a Type I or II error, alpha was chosen to be 0.05. This value is a widely accepted and common value in many fields of research.

6.4   Peg Insertion Task

6.4.1   Design

The peg insertion experimentation was split into two studies, namely A and B. Study A focused on highlighting the performance gains offered by haptic communication, while study B aimed to highlight the effect of haptic communication on operator learning and familiarisation.

Figure 6.4 shows a photo of the peg and the hole that were used in the experiment. The peg has a diameter of 17.59mm and the hole has a diameter of 20.05mm.

As previously mentioned, sound can be a valuable source of feedback when performing drilling and grinding tasks. However, sound did not provide any in-
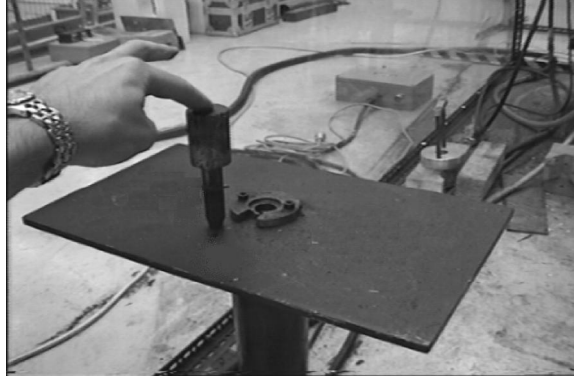
Figure 6.4: The peg and hole that where used in the peg insertion experiments

formation to the operator during the peg insertion experiments, and so ear plugs were not required.

Each operator was required to insert the peg into the hole as gently but as quickly as they possibly could. Crash insertions were not allowed. Prior to each experiment, the manipulator was driven so that the peg was above the front left corner of the table, as viewed by the operator. The orientation of the peg was also set so that it matched that of the hole, and hence, would slide into the hole when the position was correct. During the test, the operator had control of all of the three end effector axes of motion.

The operators were given instructions according to whether they were using the haptic mode or not. Instructions for the non-haptic mode were as follows.

- The joystick controls the velocity of the manipulator gripper, the twist axis controls the velocity in the vertical direction and the other two axes control velocity in the horizontal plane

- You are required to insert the peg into the hole by applying as little force as possible

- You will be timed and you must perform this task as fast as possible

- The forces that you exert using the manipulator and the time it takes for you to complete the task will be recorded

Instructions for the haptic mode were exactly the same as shown in the previous list with the following addition.

- Force feedback will be presented to you by the joystick in all three directions of motion

6.4.2   Study A

6.4.2.1   Hypothesis

Given the four modes of operation, the following two sets of hypothesis are proposed. The first set concerns haptic feedback:

- H_{H0}: Haptic feedback does not improve operator performance

- H_{H1}: Haptic feedback does improve operator performance.

The second set concerns visual feedback:

- H_{V0}: Increased visual feedback does not improve operator performance

- H_{V1}: Increased visual feedback does improve operator performance.

6.4.2.2   Participants

Six operators performed the task using teleoperation modes 1 and 2 while another six operators performed the tasks using modes 3 and 4.

A reminder of the modes of teleoperation follows:

- Mode 1: 1 Camera, no haptic

- Mode 2: 2 Cameras, no haptic

- Mode 3: 1 Camera, with haptic

- Mode 4: 2 Cameras, with haptic.

None of the operators were trained in teleoperation, however, since all of the operators worked within the robotics industry they all had an appreciation of what teleoperation entails. The primary operator vocation was engineering, exceptions to this were sales engineers and administration staff. Eleven of the operators were male, all of the operators were aged between 25 and 50.

6.4.2.3   Results

The following sections show the results of the experiments and also the statistical calculations that were performed to test for significance. As was stated previously, significance due to haptic feedback was tested using the Mann-Whitney U Test and significance due to visual feedback was tested using the Wilcoxon T Test for Dependent Samples.

6.4.2.4 Results and comparison of the maximum z axis force recorded for groups 1 and 3

Mann-Whitney U Test to test for significance where $\alpha = 0.05$. Table 6.1 shows the results for this experiment.

- H_{H0}: Haptic feedback does not improve operator performance.

- H_{H1}: Haptic feedback does improve operator performance.

No haptic, 1 camera. (N)	Rank R_1	Haptic, 1 camera. (N)	Rank R_2
196	8	145	2
450	12	165	5
158	3	186	7
214	10	164	4
214	10	167	6
214	10	130	1
$n_1 = 6$	$\Sigma R_1 = 53$	$n_2 = 6$	$\Sigma R_2 = 25$
$mean = 241$		$mean = 159.5$	

Table 6.1: Results and comparison of the maximum z axis force recorded for groups 1 and 3

Perform the computational check:

$$53 + 25 = \frac{(6+6)(6+6+1)}{2} \tag{6.1}$$

Calculate the test statistic:

$$U(6,6) = Smallest\ of \left[\begin{array}{c} (6)(6) + \dfrac{6(6+1)}{2} - 53 \\[2mm] (6)(6) + \dfrac{6(6+1)}{2} - 25 \end{array} \right] = 4 \tag{6.2}$$

$$U_{0.05/2;6,6} = 7 \tag{6.3}$$

Since the test statistic $U(6,6) = 4$ is less then the critical value $U_{0.05/2;6,6} = 7$, H_{H0} is rejected and thus H_{H1} is accepted.

6.4.2.5 Results and comparison of the maximum z axis force recorded for groups 2 and 4

Mann-Whitney U Test to test for significance where $\alpha = 0.05$. Table 6.2 shows the results for this experiment.

- H_{H0}: Haptic feedback does not improve operator performance.

- H_{H1}: Haptic feedback does improve operator performance.

No haptic, 2 camera. (N)	Rank R_1	Haptic, 2 camera. (N)	Rank R_2
234	10	136	4
531	11	143	5
162	7	156	6
195	8.5	45	2
595	12	195	8.5
116	3	13	1
$n_1 = 6$	$\Sigma R_1 = 51.5$	$n_2 = 6$	$\Sigma R_2 = 26.5$
$mean = 305.5$		$mean = 114.667$	

Table 6.2: Results and comparison of the maximum z axis force recorded for groups 2 and 4

Perform the computational check:

$$51.5 + 26.5 = \frac{(6+6)(6+6+1)}{2} \tag{6.4}$$

Calculate the test statistic:

$$U(6,6) = Smallest\ of\ \left[\begin{array}{c} (6)(6) + \dfrac{6(6+1)}{2} - 51.5 \\ (6)(6) + \dfrac{6(6+1)}{2} - 26.5 \end{array} \right] = 5.5 \tag{6.5}$$

$$U_{0.05/2;6,6} = 7 \tag{6.6}$$

Since the test statistic $U(6,6) = 5.5$ is less then the critical value $U_{0.05/2;6,6} = 7$, H_{H0} is rejected and thus H_{H1} is accepted.

6.4.2.6 Results and comparison of the mean z axis force recorded for groups 1 and 3

Mann-Whitney U Test to test for significance where $\alpha = 0.05$. Table 6.3 shows the results for this experiment.

- H_{H0}: Haptic feedback does not improve operator performance.

- H_{H1}: Haptic feedback does improve operator performance.

No haptic, 1 camera. (N)	Rank R_1	Haptic, 1 camera. (N)	Rank R_2
50.331	12	19.501	5
31.926	8	31.464	7
17.616	3	35.763	9
18.579	4	38.728	11
38.444	10	23.348	6
5.398	1	12.876	2
$n_1 = 6$	$\Sigma R_1 = 38$	$n_2 = 6$	$\Sigma R_2 = 40$
$mean = 27.049$		$mean = 26.947$	

Table 6.3: Results and comparison of the mean z axis force recorded for groups 1 and 3

Perform the computational check:

$$38 + 40 = \frac{(6+6)(6+6+1)}{2} \tag{6.7}$$

Calculate the test statistic:

$$U(6,6) = Smallest\ of \left[\begin{array}{c} (6)(6) + \dfrac{6(6+1)}{2} - 38 \\[2ex] (6)(6) + \dfrac{6(6+1)}{2} - 40 \end{array} \right] = 17 \tag{6.8}$$

$$U_{0.05/2;6,6} = 7 \tag{6.9}$$

Since the test statistic $U(6,6) = 17$ is not less then the critical value $U_{0.05/2;6,6} = 7$, H_{H0} is accepted.

6.4.2.7 Results and comparison of the mean z axis force recorded for groups 2 and 4

Mann-Whitney U Test to test for significance where $\alpha = 0.05$. Table 6.4 shows the results for this experiment.

- H_{H0}: Haptic feedback does not improve operator performance.

- H_{H1}: Haptic feedback does improve operator performance.

No haptic, 2 camera. (N)	Rank R_1	Haptic, 2 camera. (N)	Rank R_2
35.044	12	5.786	2
14.991	6	2.727	1
22.2	9	22.875	10
21.793	8	14.475	5
18.81	7	27.684	11
6.511	3	6.555	4
$n_1 = 6$	$\Sigma R_1 = 45$	$n_2 = 6$	$\Sigma R_2 = 33$
$mean = 19.892$		$mean = 13.35$	

Table 6.4: Results and comparison of the mean z axis force recorded for groups 2 and 4

Perform the computational check:

$$45 + 33 = \frac{(6+6)(6+6+1)}{2} \tag{6.10}$$

Calculate the test statistic:

$$U(6,6) = Smallest\ of \left[\begin{array}{c} (6)(6) + \dfrac{6(6+1)}{2} - 45 \\ (6)(6) + \dfrac{6(6+1)}{2} - 33 \end{array} \right] = 12 \tag{6.11}$$

$$U_{0.05/2;6,6} = 7 \tag{6.12}$$

Since the test statistic $U(6,6) = 12$ is not less then the critical value $U_{0.05/2;6,6} = 7$, H_{H0} is accepted.

6.4.2.8 Results and comparison of the task completion time for groups 1 and 3

Mann-Whitney U Test to test for significance where $\alpha = 0.05$. Table 6.5 shows the results for this experiment.

- H_{H0}: Haptic feedback does not improve operator performance.

- H_{H1}: Haptic feedback does improve operator performance.

No haptic, 1 camera. (sec)	Rank R_1	Haptic, 1 camera. (sec)	Rank R_2
250.53	11	224.82	10
85.02	6	282.63	12
53.91	3	152.61	9
82.62	5	47.7	2
99.66	8	85.05	7
78.69	4	27.66	1
$n_1 = 6$	$\Sigma R_1 = 37$	$n_2 = 6$	$\Sigma R_2 = 41$
$mean = 108.405$		$mean = 136.745$	

Table 6.5: Results and comparison of the task completion time for groups 1 and 3

Perform the computational check:

$$37 + 41 = \frac{(6+6)(6+6+1)}{2} \tag{6.13}$$

Calculate the test statistic:

$$U(6,6) = Smallest\ of \left[\begin{array}{c} (6)(6) + \dfrac{6(6+1)}{2} - 37 \\ (6)(6) + \dfrac{6(6+1)}{2} - 41 \end{array} \right] = 16 \tag{6.14}$$

$$U_{0.05/2;6,6} = 7 \tag{6.15}$$

Since the test statistic $U(6,6) = 16$ is not less then the critical value $U_{0.05/2;6,6} = 7$, H_{H0} is accepted.

6.4.2.9 Results and comparison of the task completion time recorded for groups 2 and 4

Mann-Whitney U Test to test for significance where $\alpha = 0.05$. Table 6.6 shows the results for this experiment.

- H_{H0}: Haptic feedback does not improve operator performance.

- H_{H1}: Haptic feedback does improve operator performance.

No haptic, 2 camera. (sec)	Rank R_1	Haptic, 2 camera. (sec)	Rank R_2
180.6	11	156.81	10
151.95	9	116.04	8
76.68	7	65.7	6
47.01	4	58.53	5
285.51	12	32.94	2
44.04	3	21.3	1
$n_1 = 6$	$\Sigma R_1 = 46$	$n_2 = 6$	$\Sigma R_2 = 32$
$mean = 130.975$		$mean = 75.22$	

Table 6.6: Results and comparison of the task completion time recorded for groups 2 and 4

Perform the computational check:

$$46 + 32 = \frac{(6+6)(6+6+1)}{2} \tag{6.16}$$

Calculate the test statistic:

$$U(6,6) = Smallest\ of \left[\begin{array}{c} (6)(6) + \dfrac{6(6+1)}{2} - 46 \\ (6)(6) + \dfrac{6(6+1)}{2} - 32 \end{array} \right] = 11 \tag{6.17}$$

$$U_{0.05/2;6,6} = 7 \tag{6.18}$$

Since the test statistic $U(6,6) = 11$ is not less then the critical value $U_{0.05/2;6,6} = 7$, H_{H0} is accepted.

6.4.2.10   Results and comparison of the maximum z axis force recorded for groups 1 and 2

Wilcoxon T Test to test for significance where $\alpha = 0.05$. Table 6.7 shows the results and calculations for this experiment.

- H_{V0}: Increased visual feedback does not improve operator performance.

- H_{V1}: Increased visual feedback does improve operator performance.

Pair Id	No haptic, 1 camera. (N) X_1	No haptic, 2 camera. (N) X_2	Diff	Rank of difference ignoring polarity	Rank associated with +ve difference R_+	Rank associated with -ve difference R_-
1	196	234	38	3	3	
2	450	531	81	4	4	
3	158	162	4	1	1	
4	214	195	-19	2		2
5	214	595	381	6	6	
6	214	116	-98	5		5
	mean = 241	mean = 305.5			$\Sigma R_+ = 14$	$\Sigma R_- = 7$

Table 6.7: Results and comparison of the maximum z axis force recorded for groups 1 and 2

Perform the computational check:

$$14 + \left| 7 \right| = \frac{6(6 + 1)}{2} \tag{6.19}$$

Calculate the test statistic:

$$T(6) = Smallest\ of \begin{bmatrix} 14 \\ |7| \end{bmatrix} = 7 \tag{6.20}$$

$$T_{0.05,6} = 2 \tag{6.21}$$

Since the test statistic $T(6) = 7$ is not less then the critical value $T_{0.05,6} = 2$, H_{V0} is accepted.

6.4.2.11 Results and comparison of the maximum z axis force recorded for groups 3 and 4

Wilcoxon T Test to test for significance where $\alpha = 0.05$. Table 6.8 shows the results and calculations for this experiment.

- H_{V0}: Increased visual feedback does not improve operator performance.

- H_{V1}: Increased visual feedback does improve operator performance.

Pair Id	Haptic, 1 camera. (N) X_1	Haptic, 2 camera. (N) X_2	Diff	Rank of difference ignoring polarity	Rank associated with +ve difference R_+	Rank associated with -ve difference R_-
1	145	136	-9	1		1
2	165	143	-22	2		2
3	186	156	-30	4		4
4	164	45	-119	6		6
5	167	195	28	3	3	
6	130	13	-117	5		5
	mean = 159.5	*mean* = 114.667			$\Sigma R_+ = 3$	$\Sigma R_- = 18$

Table 6.8: Results and comparison of the maximum z axis force recorded for groups 3 and 4

Perform the computational check:

$$3 + \left|18\right| = \frac{6(6+1)}{2} \tag{6.22}$$

Calculate the test statistic:

$$T(6) = Smallest\ of \begin{bmatrix} 3 \\ \left|18\right| \end{bmatrix} = 3 \tag{6.23}$$

$$T_{0.05,6} = 2 \qquad\qquad (6.24)$$

Since the test statistic $T(6) = 3$ is not less then the critical value $T_{0.05,6} = 2$, H_{V0} is accepted.

6.4.2.12 Results and comparison of the mean z axis force recorded for groups 1 and 2

Wilcoxon T Test to test for significance where $\alpha = 0.05$. Table 6.9 shows the results and calculations for this experiment.

- H_{V0}: Increased visual feedback does not improve operator performance.

- H_{V1}: Increased visual feedback does improve operator performance.

Pair Id	No haptic, 1 camera. (N) X_1	No haptic, 2 camera. (N) X_2	Diff	Rank of difference ignoring polarity	Rank associated with +ve difference R_+	Rank associated with -ve difference R_-
1	50.331	35.044	-15.287	4		4
2	31.926	14.991	-16.935	5		5
3	17.616	22.2	4.584	3	3	
4	18.579	21.793	3.214	2	2	
5	38.444	18.81	-19.633	6		6
6	5.398	6.511	1.113	1	1	
	mean = 27.049	*mean* = 19.892			$\Sigma R_+ = 6$	$\Sigma R_- = 15$

Table 6.9: Results and comparison of the mean z axis force recorded for groups 1 and 2

Perform the computational check:

$$6 + \left| 15 \right| = \frac{6(6+1)}{2} \tag{6.25}$$

Calculate the test statistic:

$$T(6) = Smallest\ of \begin{bmatrix} 6 \\ |15| \end{bmatrix} = 6 \tag{6.26}$$

$$T_{0.05,6} = 2 \tag{6.27}$$

Since the test statistic $T(6) = 6$ is not less then the critical value $T_{0.05,6} = 2$, H_{V0} is accepted.

6.4.2.13 Results and comparison of the mean z axis force recorded for groups 3 and 4

Wilcoxon T Test to test for significance where $\alpha = 0.05$. Table 6.10 shows the results and calculations for this experiment.

- H_{V0}: Increased visual feedback does not improve operator performance.

- H_{V1}: Increased visual feedback does improve operator performance.

Perform the computational check:

$$1 + \left| 20 \right| = \frac{6(6+1)}{2} \tag{6.28}$$

Calculate the test statistic:

$$T(6) = Smallest\ of \begin{bmatrix} 1 \\ |20| \end{bmatrix} = 1 \tag{6.29}$$

$$T_{0.05,6} = 2 \tag{6.30}$$

Since the test statistic $T(6) = 1$ is less then the critical value $T_{0.05,6} = 2$, H_{V0} is rejected and thus H_{V1} is accepted.

Pair Id	Haptic, 1 camera. (N) X_1	Haptic, 2 camera. (N) X_2	Diff	Rank of difference ignoring polarity	Rank associated with +ve difference R_+	Rank associated with -ve difference R_-
1	19.501	5.786	-13.715	4		4
2	31.464	2.727	-28.737	6		6
3	35.763	22.785	-12.888	3		3
4	38.728	14.475	-24.254	5		5
5	23.348	27.684	4.336	1	1	
6	12.876	6.555	-6.321	2		2
	$mean = 26.947$	$mean = 13.35$			$\Sigma R_+ = 1$	$\Sigma R_- = 20$

Table 6.10: Results and comparison of the mean z axis force recorded for groups 3 and 4

6.4.2.14 Comparison of task completion time for groups 1 and 2

Wilcoxon T Test to test for significance where $\alpha = 0.05$. Table 6.11 shows the results and calculations for this experiment.

- H_{V0}: Increased visual feedback does not improve operator performance.

- H_{V1}: Increased visual feedback does improve operator performance.

Pair Id	No haptic, 1 camera. (sec) X_1	No haptic, 2 camera. (sec) X_2	Diff	Rank of difference ignoring polarity	Rank associated with +ve difference R_+	Rank associated with -ve difference R_-
1	250.53	180.66	69.87	5	5	
2	85.02	151.95	-66.93	4		4
3	53.91	76.68	-22.77	1		1
4	82.62	47.01	35.61	3	3	
5	99.66	285.51	-185.85	6		6
6	78.69	44.04	34.65	2	2	
	mean = 108.405	*mean* = 130.957			$\Sigma R_+ = 10$	$\Sigma R_- = 11$

Table 6.11: Comparison of task completion time for groups 1 and 2

Perform the computational check:

$$10 + \left| 11 \right| = \frac{6(6+1)}{2} \tag{6.31}$$

Calculate the test statistic:

$$T(6) = Smallest \ of \begin{bmatrix} 10 \\ |11| \end{bmatrix} = 10 \tag{6.32}$$

$$T_{0.05,6} = 2 \tag{6.33}$$

Since the test statistic $T(6) = 10$ is not less then the critical value $T_{0.05,6} = 2$, H_{V0} is accepted.

6.4.2.15 Comparison of task completion time for groups 3 and 4

Wilcoxon T Test to test for significance where $\alpha = 0.05$. Table 6.12 shows the results and calculations for this experiment.

- H_{V0}: Increased visual feedback does not improve operator performance.

- H_{V1}: Increased visual feedback does improve operator performance.

Pair Id	Haptic, 1 camera. (sec) X_1	Haptic, 2 camera. (sec) X_2	Diff	Rank of difference ignoring polarity	Rank associated with +ve difference R_+	Rank associated with -ve difference R_-
1	224.82	156.81	68.01	4	4	
2	282.63	116.04	166.59	6	6	
3	152.61	65.7	86.91	5	5	
4	47.7	58.53	-10.83	2		2
5	85.05	32.94	52.11	3	3	
6	27.66	21.3	6.36	1	1	
	mean = 136.745	mean = 75.22			$\Sigma R_+ = 19$	$\Sigma R_- = 2$

Table 6.12: Comparison of task completion time for groups 3 and 4

Perform the computational check:

$$19 + \left| 2 \right| = \frac{6(6+1)}{2} \tag{6.34}$$

Calculate the test statistic:

$$T(6) = Smallest \; of \begin{bmatrix} 19 \\ |2| \end{bmatrix} = 2 \tag{6.35}$$

$$T_{0.05,6} = 2 \tag{6.36}$$

Since the test statistic $T(6) = 2$ is less then the critical value $T_{0.05,6} = 2$, H_{V0} is rejected and thus H_{V1} is accepted.

6.4.2.16 Discussion

The previous results sections showed the results data and the statistical calculations that were performed to test for significance. The results of the statistical analysis is shown in the following tables, alongside the section number that contains the calculation of the result.

			Mode 2	Mode 3	Mode 4
			Non-Haptic	Haptic	Haptic
			2 Cameras	1 Camera	2 Cameras
Mode 1	Non-Haptic	1 Camera	Not Significant (6.4.2.10)	Significant $p < 0.025$ (6.4.2.4)	no data
Mode 2	Non-Haptic	2 Cameras	no data	no data	Significant $p < 0.05$ (6.4.2.5)
Mode 3	Haptic	1 Camera	no data	no data	Not Significant (6.4.2.11)

Table 6.13: Statistical significance within the maximum force in z-axis data

			Mode 2	Mode 3	Mode 4
			Non-Haptic	Haptic	Haptic
			2 Cameras	1 Camera	2 Cameras
Mode 1	Non-Haptic	1 Camera	Not Significant (6.4.2.12)	Not Significant (6.4.2.6)	no data
Mode 2	Non-Haptic	2 Cameras	no data	no data	Not Significant (6.4.2.7)
Mode 3	Haptic	1 Camera	no data	no data	Significant $p < 0.05$ (6.4.2.13)

Table 6.14: Statistical significance within the mean force in z-axis data

			Mode 2	Mode 3	Mode 4
			Non-Haptic	Haptic	Haptic
			2 Cameras	1 Camera	2 Cameras
Mode 1	Non-Haptic	1 Camera	Not Significant (6.4.2.14)	Not Significant (6.4.2.8)	no data
Mode 2	Non-Haptic	2 Cameras	no data	no data	Not Significant (6.4.2.9)
Mode 3	Haptic	1 Camera	no data	no data	Significant $p < 0.05$ (6.4.2.15)

Table 6.15: Statistical significance within the time for completion data

Table 6.13 shows that haptic feedback significantly reduced the level of the maximum recorded insertion force, whereas extra visual feedback did not. In contradiction to this, tables 6.14 and 6.15 show that haptic feedback did not show any performance advantages to the mean force in the z-axis or task completion time. All of the above tables show that adding an extra camera when there was no haptic feedback did not produce significant improvements. However, adding an extra camera when haptic feedback was present did show improvements to task completion time and mean force in the z-axis. This is possibly not the result that one would initially expect. Most people would possibly expect that improving visual feedback would make the task easier for the operator and thus reduce insertion force and task completion times. However the results show that this is not necessarily true. Possibly the most important of the three metrics is maximum insertion force. This is due to the fact that if one can keep the force levels low, then damage to tools, manipulator and environment will be reduced. This is clearly a key concern of the nuclear industry. Haptic feedback showed significant improvements by reducing the peak insertion forces, however increasing visual feedback did not yield similar results. Although a second camera gave the operators depth of view and allowed them to line up the peg with the hole against two fields of reference, it did not improve their performance. This is likely to be due to the basic fact that when a slight misalignment occurred between the peg and the hole, the only indication of this was that the manipulator stopped, i.e. the peg made contact with the rim of the hole and thus movement in the z-axis was stopped. Clearly adding a second camera does not allow the operator to notice this halt in motion any quicker. Ironically if the peg/hole contact occurred in the short time while the operator was moving his/her eyes from one camera to the second, the reaction time of the operator may actually be increased very slightly by the addition of the second camera. Conversely, the addition of haptic feedback serves the operator with immediate notice of any contact between the peg and hole thus allowing the operator to stop the motion of the manipulator immediately.

As noted by Draper et al (Draper *et al.*, 1999), haptic/force feedback does not generally improve the time to complete a task, but does generally lower the forces applied by the slave end effector. This is confirmed by these results from the peg insertion experiments.

6.4.3 Study B

6.4.3.1 Hypothesis

Given the nature of the task, one would expect that the operators would become more skilled each time they performed the task thus lowering the time to completion and also the number of errors with each trial. It would also be expected that the learning rate (rate of performance improvement) would be higher for haptic modes of teleoperation.

6.4.3.2 Participants

The peg insertion task was performed by two operators. Each operator performed the task ten times for each mode of teleoperation. Both operators were male engineers who had no previous training in teleoperation but were familiar with what teleoperation entails. Both operators were aged between 25 and 50.

6.4.3.3 Statistical Analysis

Least squares regression analysis was performed on the results data in order to test for performance improvements that arise with increased operator experience. MatLab was used to fit a 2nd order least squares linear regression to the maximum z axis force data and the time to completion data. Analysis of variance (ANOVA) with alpha set to 0.05 was used to verify that the chosen model matches the data(Weisberg, 1985). This procedure is documented in appendix H.

6.4.3.4 Results

Figures 6.5 through to 6.8 show the regression plots for time to completion and maximum z axis force for haptic and non-haptic modes of teleoperation.
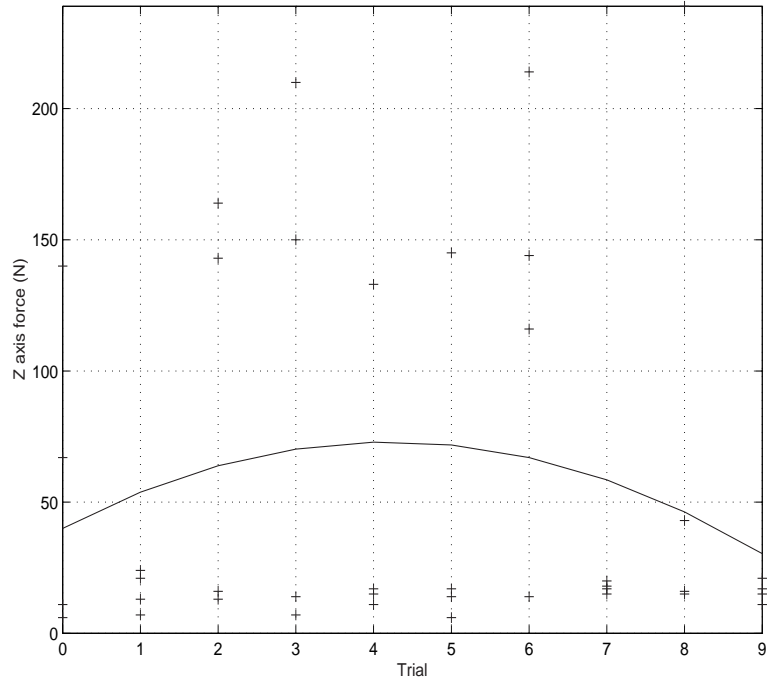
Figure 6.5: 2nd order regression plot for maximum z axis force, modes 1 and 2. Since the observed $F = 0.1209$ is smaller than the critical value $F(0.05; 28, 10) = 2.70$ the fit is accepted.
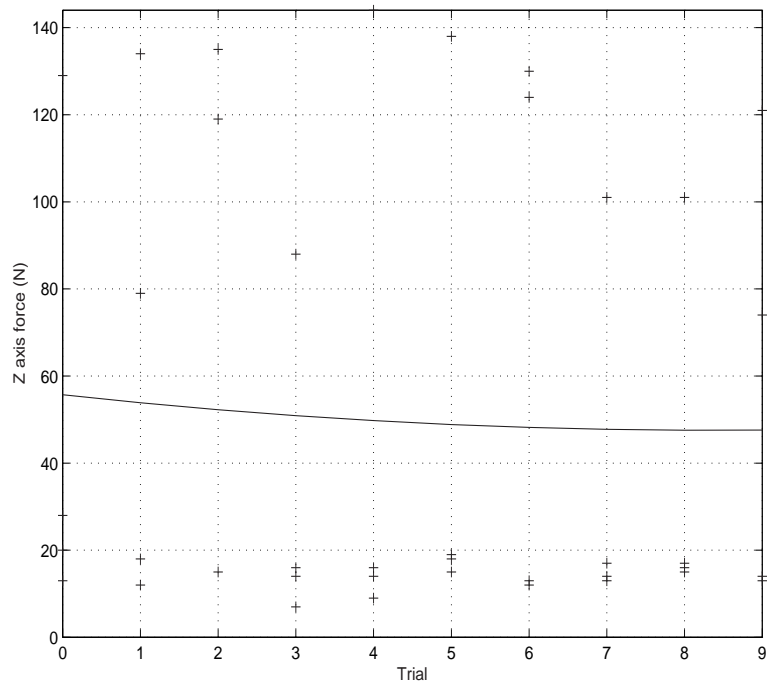
Figure 6.6: 2nd order regression plot for maximum z axis force, modes 3 and 4. Since the observed $F = 0.0255$ is smaller than the critical value $F(0.05; 28, 10) = 2.70$ the fit is accepted.
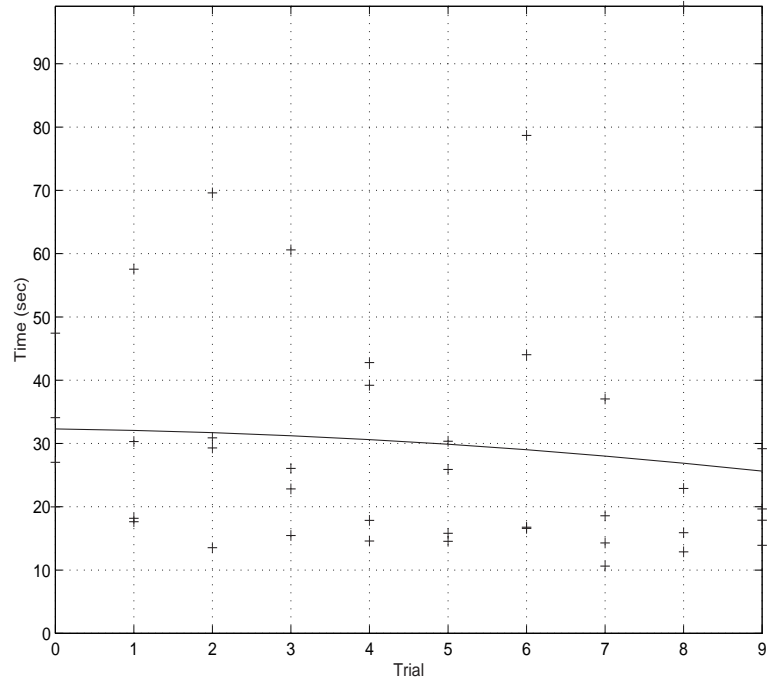
Figure 6.7: 2nd order regression plot for completion time, modes 1 and 2. Since the observed $F = 0.0428$ is smaller than the critical value $F(0.05; 28, 10) = 2.70$ the fit is accepted.
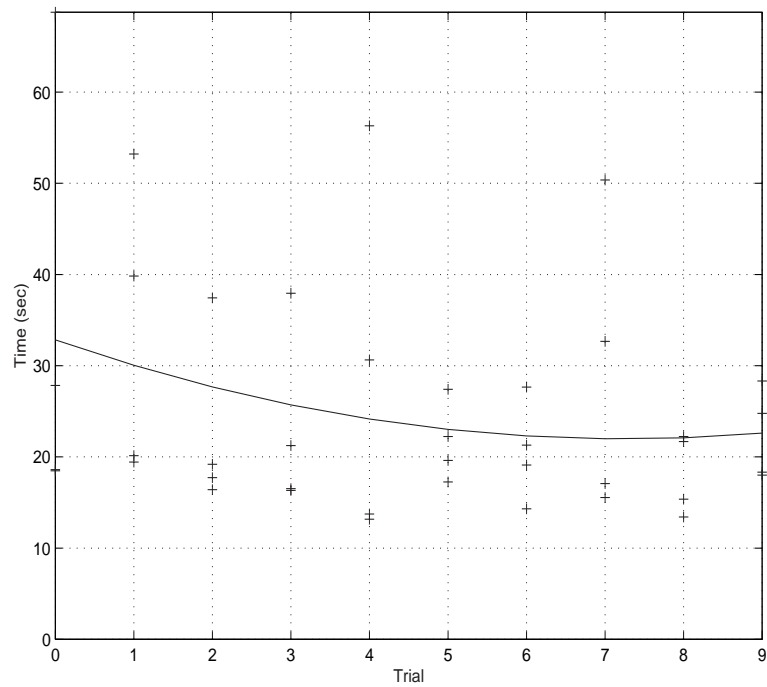
Figure 6.8: 2nd order regression plot for completion time, modes 3 and 4. Since the observed $F = 0.0397$ is smaller than the critical value $F(0.05; 28, 10) = 2.70$ the fit is accepted.

As expected, figures 6.7 and 6.8, which show the plots for time to completion, both show a general trend of improvement as operator experience increases. In addition, figure 6.8 (time to completion with haptic) shows a considerably higher rate of improvement than 6.7 which suggests that the addition of haptic feedback has increased the rate at which operators become familiar and competent with the system.

Unlike the time to completion data, the maximum z axis force data does not show a simple result. The plot for the mode without haptic feedback, 6.5, shows that the operators got worse at limiting the force before starting to improve by the fourth trial. The haptic plot of maximum z axis force, 6.6, shows a steady but slight improvement over most of the 10 trials with a slight levelling off in performance towards the end. It appears that as with time to completion, haptic feedback has introduced consistency to the force data and also the tendency for slight performance improvement with extra experience. In contrast, the plot of the results without haptic feedback shows a lack of consistency and no trend for improvement. Also, as shown in study A, maximum force values are generally much higher without haptic feedback, these results confirm this finding. It is believed that the lack of consistency and performance improvement trend can be attributed to the fact that when haptic feedback is not present, the operator has very little knowledge of the force that they are applying at the manipulator gripper.

Figures 6.5 and 6.6 both show a relatively large number of outliers that at first appear to suggest that there may be a problem with the data collection system or that the operator performance is highly erratic. On further examination, the outliers can be attributed to the nature of the peg insertion task which is highly non-linear. If the operator succeeds in inserting the peg without making an error by missing the hole then a very small maximum force is logged. However, if the operator makes a mistake and misses the hole, it is possible for a very large force to be generated in a very small time. Hence, this is why the data points for the maximum recorded force appear to be collected towards both the top and the bottom of the plot.

In general, the addition of haptic feedback appears to have induced a higher rate of learning and system familiarization within the operators. This effect is more pronounced in the time to completion data.

6.5 Grinding Task

6.5.1 Design

As with the previous task, the grinding experimentation was split into two studies, namely A and B. Study A focused on highlighting the performance gains offered by haptic communication, while study B aimed to highlight the effect of haptic communication on operator learning and familiarisation.

Each operator was required to cut through a bus bar shaped piece of steel, which measured 35mm by 5mm in cross section. Prior to each test, the manipulator was driven so that the grinder was in position above the area to be cut. Figure 6.9 shows a photo of the steel bar that was cut during the grinding experiments. The end of the bar overhung the edge of a steel table. The overhang was cut during the experiment, and then the bar was moved along so that a new overhang was created.
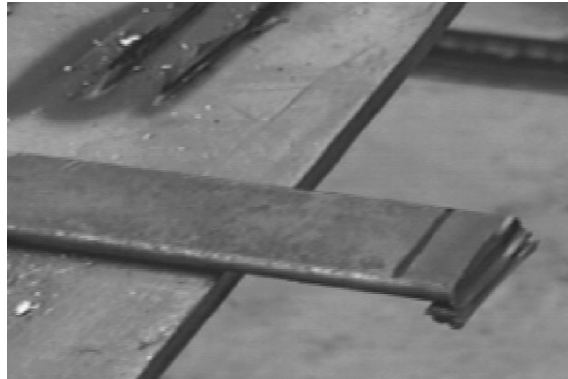
Figure 6.9: The steel bar that was cut during the grinding experiments

The task and the goal were explained to each operator in the same manner. Each operator was instructed to cut through the steel bar as fast as possible, but without stalling the tool or causing damage due to excessive force. In addition, the haptic feedback was also explained to the operators who used the haptic modes of operation.

The operators were given instructions according to whether they were using the haptic mode or not. Instructions for the non-haptic mode were as follows.

- The joystick twist axis controls the plunge velocity of the tool into the workpiece

- You are required to cut through the bar as fast as possible without exerting excessive force via the tool that could cause it to stall or to be damaged

126

- The forces and torques that you exert using the manipulator and the time it takes for you to complete the task will be recorded

Instructions for the haptic mode were exactly the same as shown in the previous list with the following additions.

- You will be provided with force feedback on the twist axis and torque feedback due to the tool on the left-to-right axis of the joystick. The torque feedback is presented as a vibration that becomes more severe as the torque on the tool increases

During the test, the operator only had control over the motion in the tool z-axis, thus only plunging motion was possible, and the tool could not be moved sideways or rotated. The z-axis velocity scale was set to 1%, which limited the maximum axis velocity to approximately 1.28mm/sec. The haptic feedback during grinding comprised of the slave end effector z-axis force displayed on the haptic joystick z-axis, and the slave end effector x-axis torque displayed on the haptic joystick x-axis.

The maximum plunge velocity of 1.28mm/sec and the thickness of the material to be cut (5mm) limited the minimum task completion time to approximately 4 seconds. However, it was not possible to perform the task in such a short time. In practice, it was noted that the fastest possible completion time was approximately 10 to 15 seconds.

Decommissioning work often involves cutting large structures into small enough pieces to fit into steel drums. Many hundreds of metres of steel piping and conduit trunking must be cut into approximately three foot long sections or smaller. Thus the bus bar shaped piece of steel was chosen for its similarity to both pipes and conduit trunking.

6.5.2 Study A

6.5.2.1 Hypothesis

Given the four modes of operation, the following two sets of hypothesis are proposed. The first set concerns haptic feedback:

- H_{H0}: Haptic feedback does not improve operator performance
- H_{H1}: Haptic feedback does improve operator performance.

The second set concerns visual feedback:

- H_{V0}: Increased visual feedback does not improve operator performance

- H_{V1}: Increased visual feedback does improve operator performance.

6.5.2.2 Participants

Six operators performed the task using teleoperation modes 1 and 2, whilst another six operators performed the tasks using modes 3 and 4.

A reminder of the modes of teleoperation follows:

- Mode 1: 1 Camera, no haptic

- Mode 2: 2 Cameras, no haptic

- Mode 3: 1 Camera, with haptic

- Mode 4: 2 Cameras, with haptic.

The operator profiles were the same as for the peg insertion experiments. None of the operators were trained in teleoperation. The primary operator vocation was engineering, exceptions to this were sales engineers and administration staff. Eleven of the operators were male, all of the operators were aged between 25 and 50.

6.5.2.3 Results

The following sections show the results of the experiments and also the statistical calculations that were performed to test for significance. As was stated previously, significance due to haptic feedback was tested using the Mann-Whitney U Test and significance due to visual feedback was tested using the Wilcoxon T Test for Dependent Samples.

6.5.2.4 Comparison of the maximum z axis force recorded for groups 1 and 3

Mann-Whitney U Test to test for significance where $\alpha = 0.05$. Table 6.16 shows the results for this experiment.

- H_{H0}: Haptic feedback does not improve operator performance.

- H_{H1}: Haptic feedback does improve operator performance.

No haptic, 1 camera. (N)	Rank R_1	Haptic, 1 camera. (N)	Rank R_2
29	5	30	6
6	1	34	7
39	10.5	22	4
39	10.5	36	8
19	3	39	10.5
39	10.5	18	2
$n_1 = 6$	$\Sigma R_1 = 40.5$	$n_2 = 6$	$\Sigma R_2 = 37.5$
$mean = 28.5$		$mean = 29.833$	

Table 6.16: Comparison of the maximum z axis force recorded for groups 1 and 3

Perform the computational check:

$$40.5 + 37.5 = \frac{(6+6)(6+6+1)}{2} \tag{6.37}$$

Calculate the test statistic:

$$U(6,6) = Smallest\ of \left[\begin{array}{c} (6)(6) + \dfrac{6(6+1)}{2} - 40.5 \\[2mm] (6)(6) + \dfrac{6(6+1)}{2} - 37.5 \end{array} \right] = 16.5 \tag{6.38}$$

$$U_{0.05/2;6,6} = 7 \tag{6.39}$$

Since the test statistic $U(6,6) = 16.5$ is not less then the critical value $U_{0.05/2;6,6} = 7$, H_{H0} is accepted.

6.5.2.5 Comparison of the maximum z axis force recorded for groups 2 and 4

Mann-Whitney U Test to test for significance where $\alpha = 0.05$. Table 6.17 shows the results for this experiment.

- H_{H0}: Haptic feedback does not improve operator performance.

- H_{H1}: Haptic feedback does improve operator performance.

Perform the computational check:

$$43.5 + 34.5 = \frac{(6+6)(6+6+1)}{2} \tag{6.40}$$

No haptic, 2 camera. (N)	Rank R_1	Haptic, 2 camera. (N)	Rank R_2
40	11	28	4
23	2	30	6.5
32	9	30	6.5
26	3	30	6.5
30	6.5	17	1
46	12	38	10
$n_1 = 6$	$\Sigma R_1 = 43.5$	$n_2 = 6$	$\Sigma R_2 = 34.5$
$mean = 32.833$		$mean = 28.833$	

Table 6.17: Comparison of the maximum z axis force recorded for groups 2 and 4

Calculate the test statistic:

$$U(6,6) = Smallest\ of \left[\begin{array}{c} (6)(6) + \dfrac{6(6+1)}{2} - 43.5 \\ \\ (6)(6) + \dfrac{6(6+1)}{2} - 34.5 \end{array} \right] = 13.5 \qquad (6.41)$$

$$U_{0.05/2;6,6} = 7 \qquad (6.42)$$

Since the test statistic $U(6,6) = 13.5$ is not less then the critical value $U_{0.05/2;6,6} = 7$, H_{H0} is accepted.

6.5.2.6 Comparison of the mean z axis force recorded for groups 1 and 3

Mann-Whitney U Test to test for significance where $\alpha = 0.05$. Table 6.18 shows the results for this experiment.

- H_{H0}: Haptic feedback does not improve operator performance.

- H_{H1}: Haptic feedback does improve operator performance.

Perform the computational check:

$$37 + 41 = \frac{(6+6)(6+6+1)}{2} \qquad (6.43)$$

Calculate the test statistic:

No haptic, 1 camera. (N)	Rank R_1	Haptic, 1 camera. (N)	Rank R_2
10.21	8	9.074	5
3.48	2	16.913	11
9.557	7	5.251	3
12.767	9	18.901	12
0.02	1	7.846	4
15.355	10	9.503	6
$n_1 = 6$	$\Sigma R_1 = 37$	$n_2 = 6$	$\Sigma R_2 = 41$
$mean = 7.405$		$mean = 11.248$	

Table 6.18: Comparison of the mean z axis force recorded for groups 1 and 3

$$U(6,6) = Smallest\ of \left[\begin{array}{c} (6)(6) + \dfrac{6(6+1)}{2} - 37 \\ (6)(6) + \dfrac{6(6+1)}{2} - 41 \end{array} \right] = 16 \qquad (6.44)$$

$$U_{0.05/2;6,6} = 7 \qquad (6.45)$$

Since the test statistic $U(6,6) = 16$ is not less then the critical value $U_{0.05/2;6,6} = 7$, H_{H0} is accepted.

6.5.2.7 Comparison of the mean z axis force recorded for groups 2 and 4

Mann-Whitney U Test to test for significance where $\alpha = 0.05$. Table 6.19 shows the results for this experiment.

- H_{H0}: Haptic feedback does not improve operator performance.

- H_{H1}: Haptic feedback does improve operator performance.

Perform the computational check:

$$37 + 14 = \frac{(6+6)(6+6+1)}{2} \qquad (6.46)$$

Calculate the test statistic:

No haptic, 2 camera. (N)	Rank R_1	Haptic, 2 camera. (N)	Rank R_2
5.853	6	5.34	5
1.24	1	7.722	9
5.963	7	4.59	3
6.082	8	12.034	10
5.006	4	2.641	2
15.314	11	19.013	12
$n_1 = 6$	$\Sigma R_1 = 37$	$n_2 = 6$	$\Sigma R_2 = 14$
$mean = 6.576$		$mean = 8.558$	

Table 6.19: Comparison of the mean z axis force recorded for groups 2 and 4

$$U(6,6) = Smallest\ of \left[\begin{array}{c} (6)(6) + \dfrac{6(6+1)}{2} - 37 \\[2ex] (6)(6) + \dfrac{6(6+1)}{2} - 14 \end{array} \right] = 16 \qquad (6.47)$$

$$U_{0.05/2;6,6} = 7 \qquad (6.48)$$

Since the test statistic $U(6,6) = 16$ is not less then the critical value $U_{0.05/2;6,6} = 7$, H_{H0} is accepted.

6.5.2.8 Comparison of maximum tool torque recorded for groups 1 and 3

Mann-Whitney U Test to test for significance where $\alpha = 0.05$. Table 6.20 shows the results for this experiment.

- H_{H0}: Haptic feedback does not improve operator performance.

- H_{H1}: Haptic feedback does improve operator performance.

Perform the computational check:

$$38 + 40 = \frac{(6+6)(6+6+1)}{2} \qquad (6.49)$$

Calculate the test statistic:

No haptic, 1 camera. (Nm)	Rank R_1	Haptic, 1 camera. (Nm)	Rank R_2
138	6	245	11
29	1	145	7
208	9	135	5
211	10	74	3
84	4	313	12
166	8	49	2
$n_1 = 6$	$\Sigma R_1 = 38$	$n_2 = 6$	$\Sigma R_2 = 40$
$mean = 139.333$		$mean = 160.167$	

Table 6.20: Comparison of maximum tool torque recorded for groups 1 and 3

$$U(6,6) = Smallest\ of \left[\begin{array}{c} (6)(6) + \dfrac{6(6+1)}{2} - 38 \\ \\ (6)(6) + \dfrac{6(6+1)}{2} - 40 \end{array} \right] = 17 \qquad (6.50)$$

$$U_{0.05/2;6,6} = 7 \qquad (6.51)$$

Since the test statistic $U(6,6) = 17$ is not less then the critical value $U_{0.05/2;6,6} = 7$, H_{H0} is accepted.

6.5.2.9 Comparison of maximum tool torque recorded for groups 2 and 4

Mann-Whitney U Test to test for significance where $\alpha = 0.05$. Table 6.21 shows the results for this experiment.

- H_{H0}: Haptic feedback does not improve operator performance.

- H_{H1}: Haptic feedback does improve operator performance.

Perform the computational check:

$$51 + 27 = \frac{(6+6)(6+6+1)}{2} \qquad (6.52)$$

Calculate the test statistic:

No haptic, 2 camera. (Nm)	Rank R_1	Haptic, 2 camera. (Nm)	Rank R_2
222	9	61	2
125	4	160	8
335	12	67	3
127	5	45	1
291	11	148	7
237	10	138	6
$n_1 = 6$	$\Sigma R_1 = 51$	$n_2 = 6$	$\Sigma R_2 = 27$
$mean = 222.833$		$mean = 103.167$	

Table 6.21: Comparison of maximum tool torque recorded for groups 2 and 4

$$U(6,6) = Smallest\ of \left[\begin{array}{c} (6)(6) + \dfrac{6(6+1)}{2} - 51 \\[4mm] (6)(6) + \dfrac{6(6+1)}{2} - 27 \end{array} \right] = 6 \qquad (6.53)$$

$$U_{0.05/2;6,6} = 7 \qquad (6.54)$$

Since the test statistic $U(6,6) = 6$ is less then the critical value $U_{0.05/2;6,6} = 7$, H_{H0} is rejected and thus H_{H1} is accepted.

6.5.2.10 Comparison of the mean tool torque recorded for groups 1 and 3

Mann-Whitney U Test to test for significance where $\alpha = 0.05$. Table 6.22 shows the results for this experiment.

- H_{H0}: Haptic feedback does not improve operator performance.

- H_{H1}: Haptic feedback does improve operator performance.

Perform the computational check:

$$36 + 42 = \frac{(6+6)(6+6+1)}{2} \qquad (6.55)$$

Calculate the test statistic:

No haptic, 1 camera. (Nm)	Rank R_1	Haptic, 1 camera. (Nm)	Rank R_2
4.681	1	23.573	8
3.803	2	28.609	9
13.865	4	18.109	7
50.506	11	15.07	5
16.176	6	9.901	3
59.206	12	31.698	10
$n_1 = 6$	$\Sigma R_1 = 36$	$n_2 = 6$	$\Sigma R_2 = 42$
$mean = 24.706$		$mean = 21.16$	

Table 6.22: Comparison of the mean tool torque recorded for groups 1 and 3

$$U(6,6) = Smallest\ of \left[\begin{array}{c} (6)(6) + \dfrac{6(6+1)}{2} - 36 \\[2mm] (6)(6) + \dfrac{6(6+1)}{2} - 42 \end{array} \right] = 15 \qquad (6.56)$$

$$U_{0.05/2;6,6} = 7 \qquad (6.57)$$

Since the test statistic $U(6,6) = 15$ is not less then the critical value $U_{0.05/2;6,6} = 7$, H_{H0} is accepted.

6.5.2.11 Comparison of the mean tool torque recorded for groups 2 and 4

Mann-Whitney U Test to test for significance where $\alpha = 0.05$. Table 6.23 shows the results for this experiment.

- H_{H0}: Haptic feedback does not improve operator performance.

- H_{H1}: Haptic feedback does improve operator performance.

Perform the computational check:

$$45 + 33 = \frac{(6+6)(6+6+1)}{2} \qquad (6.58)$$

Calculate the test statistic:

No haptic, 2 camera. (Nm)	Rank R_1	Haptic, 2 camera. (Nm)	Rank R_2
4.359	3	14.477	5
14.846	6	21.691	7
55.763	11	3.893	2
11.387	4	2.653	1
41.155	9	32.454	8
74.541	12	49.011	10
$n_1 = 6$	$\Sigma R_1 = 45$	$n_2 = 6$	$\Sigma R_2 = 33$
$mean = 33.675$		$mean = 19.812$	

Table 6.23: Comparison of the mean tool torque recorded for groups 2 and 4

$$U(6,6) = Smallest \ of \begin{bmatrix} (6)(6) + \dfrac{6(6+1)}{2} - 45 \\[2mm] (6)(6) + \dfrac{6(6+1)}{2} - 33 \end{bmatrix} = 12 \qquad (6.59)$$

$$U_{0.05/2;6,6} = 7 \qquad (6.60)$$

Since the test statistic $U(6,6) = 12$ is not less then the critical value $U_{0.05/2;6,6} = 7$, H_{H0} is accepted.

6.5.2.12   Comparison of the task completion time for groups 1 and 3

Mann-Whitney U Test to test for significance where $\alpha = 0.05$. Table 6.24 shows the results for this experiment.

- H_{H0}: Haptic feedback does not improve operator performance.

- H_{H1}: Haptic feedback does improve operator performance.

No haptic, 1 camera. (sec)	Rank R_1	Haptic, 1 camera. (sec)	Rank R_2
118.86	7	156.84	11
299.94	12	87.12	5
65.55	4	145.47	10
120.06	8	124.44	9
105.12	6	34.41	2
18.63	1	43.29	3
$n_1 = 6$	$\Sigma R_1 = 38$	$n_2 = 6$	$\Sigma R_2 = 40$
$mean = 121.36$		$mean = 98.595$	

Table 6.24: Comparison of the task completion time for groups 1 and 3

Perform the computational check:

$$38 + 40 = \frac{(6+6)(6+6+1)}{2} \tag{6.61}$$

Calculate the test statistic:

$$U(6,6) = Smallest\ of \left[\begin{array}{c} (6)(6) + \dfrac{6(6+1)}{2} - 38 \\[2mm] (6)(6) + \dfrac{6(6+1)}{2} - 40 \end{array} \right] = 17 \tag{6.62}$$

$$U_{0.05/2;6,6} = 7 \tag{6.63}$$

6.5.2.13   Comparison of the task completion time recorded for groups 2 and 4

Mann-Whitney U Test to test for significance where $\alpha = 0.05$. Table 6.25 shows the results for this experiment.

- H_{H0}: Haptic feedback does not improve operator performance.

No haptic, 2 camera. (sec)	Rank R_1	Haptic, 2 camera. (sec)	Rank R_2
83.61	7	75.63	6
212.49	12	54.24	4
30.57	2	93.39	8
142.74	11	126.87	10
62.25	5	107.76	9
26.82	1	35.82	3
$n_1 = 6$	$\Sigma R_1 = 38$	$n_2 = 6$	$\Sigma R_2 = 40$
$mean = 93.08$		$mean = 82.285$	

Table 6.25: Comparison of the task completion time recorded for groups 2 and 4

- H_{H1}: Haptic feedback does improve operator performance.

Perform the computational check:

$$38 + 40 = \frac{(6+6)(6+6+1)}{2} \tag{6.64}$$

Calculate the test statistic:

$$U(6,6) = Smallest\ of \left[\begin{array}{c} (6)(6) + \dfrac{6(6+1)}{2} - 38 \\ \\ (6)(6) + \dfrac{6(6+1)}{2} - 40 \end{array} \right] = 17 \tag{6.65}$$

$$U_{0.05/2;6,6} = 7 \tag{6.66}$$

Since the test statistic $U(6,6) = 17$ is not less then the critical value $U_{0.05/2;6,6} = 7$, H_{H0} is accepted.

6.5.2.14 Comparison of the maximum z axis force recorded for groups 1 and 2

Wilcoxon T Test to test for significance where $\alpha = 0.05$. Table 6.26 shows the results and calculations for this experiment.

- H_{V0}: Increased visual feedback does not improve operator performance.

- H_{V1}: Increased visual feedback does improve operator performance.

Perform the computational check:

Pair Id	No haptic, 1 camera. (N) X_1	No haptic, 2 camera. (N) X_2	Diff	Rank of difference ignoring polarity	Rank associated with +ve difference R_+	Rank associated with -ve difference R_-
1	29	40	11	3.5	3.5	
2	6	23	17	6	6	
3	39	32	-7	1.5		1.5
4	39	26	-13	5		5
5	16	30	11	3.5	3.5	
6	39	46	7	1.5	1.5	
	mean = 28.5	mean = 32.833			ΣR_+ = 14.5	ΣR_- = 6.5

Table 6.26: Comparison of the maximum z axis force recorded for groups 1 and 2

$$14.5 + \left|6.5\right| = \frac{6(6+1)}{2} \tag{6.67}$$

Calculate the test statistic:

$$T(6) = Smallest\ of \begin{bmatrix} 14.5 \\ |6.5| \end{bmatrix} = 6.5 \tag{6.68}$$

$$T_{0.05,6} = 2 \tag{6.69}$$

Since the test statistic $T(6) = 6.5$ is not less then the critical value $T_{0.05,6} = 2$, H_{V0} is accepted.

6.5.2.15 Comparison of the maximum z axis force recorded for groups 3 and 4

Wilcoxon T Test to test for significance where $\alpha = 0.05$. Table 6.27 shows the results and calculations for this experiment.

- H_{V0}: Increased visual feedback does not improve operator performance.

- H_{V1}: Increased visual feedback does improve operator performance.

Pair Id	No haptic, 1 camera. (N) X_1	No haptic, 2 camera. (N) X_2	Diff	Rank of difference ignoring polarity	Rank associated with +ve difference R_+	Rank associated with -ve difference R_-
1	30	28	-2	1		1
2	34	30	-4	2		2
3	22	30	8	4	4	
4	36	30	-6	3		3
5	39	17	-22	6		6
6	18	38	20	5	5	
	mean = 29.833	mean = 28.833			$\Sigma R_+ = 9$	$\Sigma R_- = 12$

Table 6.27: Comparison of the maximum z axis force recorded for groups 3 and 4

Perform the computational check:

$$9 + \left| 12 \right| = \frac{6(6+1)}{2} \tag{6.70}$$

Calculate the test statistic:

$$T(6) = Smallest\ of \begin{bmatrix} 9 \\ |12| \end{bmatrix} = 9 \tag{6.71}$$

$$T_{0.05,6} = 2 \tag{6.72}$$

Since the test statistic $T(6) = 9$ is not less then the critical value $T_{0.05,6} = 2$, H_{V0} is accepted.

6.5.2.16 Comparison of the mean z axis force recorded for groups 1 and 2

Wilcoxon T Test to test for significance where $\alpha = 0.05$. Table 6.28 shows the results and calculations for this experiment.

- H_{V0}: Increased visual feedback does not improve operator performance.

- H_{V1}: Increased visual feedback does improve operator performance.

Pair Id	No haptic, 1 camera. (N) X_1	No haptic, 2 camera. (N) X_2	Diff	Rank of difference ignoring polarity	Rank associated with +ve difference R_+	Rank associated with -ve difference R_-
1	10.21	5.853	-4.357	3		3
2	3.478	1.24	4.718	4	4	
3	9.557	5.963	-3.954	2		2
4	12.767	6.082	-6.686	6		6
5	0.02	5.006	4.986	5	5	
6	15.355	15.314	-0.04	1		1
	mean = 7.405	mean = 6.576			$\Sigma R_+ = 9$	$\Sigma R_- = 12$

Table 6.28: Comparison of the mean z axis force recorded for groups 1 and 2

Perform the computational check:

$$9 + \left|12\right| = \frac{6(6+1)}{2} \tag{6.73}$$

Calculate the test statistic:

$$T(6) = Smallest\ of \begin{bmatrix} 9 \\ |12| \end{bmatrix} = 9 \tag{6.74}$$

$$T_{0.05,6} = 2 \tag{6.75}$$

Since the test statistic $T(6) = 9$ is not less then the critical value $T_{0.05,6} = 2$, H_{V0} is accepted.

6.5.2.17 Comparison of the mean z axis force recorded for groups 3 and 4

Wilcoxon T Test to test for significance where $\alpha = 0.05$. Table 6.29 shows the results and calculations for this experiment.

- H_{V0}: Increased visual feedback does not improve operator performance.

- H_{V1}: Increased visual feedback does improve operator performance.

Pair Id	Haptic, 1 camera. (N) X_1	Haptic, 2 camera. (N) X_2	Diff	Rank of difference ignoring polarity	Rank associated with +ve difference R_+	Rank associated with -ve difference R_-
1	9.074	5.34	-3.734	2		2
2	16.913	7.722	-9.191	5		5
3	5.251	4.59	-0.661	1		1
4	18.901	12.034	-6.858	4		4
5	7.846	2.641	-5.205	3		3
6	9.503	19.013	9.51	6	6	
	mean = 11.248	*mean* = 8.558			$\Sigma R_+ = 6$	$\Sigma R_- = 15$

Table 6.29: Comparison of the mean z axis force recorded for groups 3 and 4

Perform the computational check:

$$6 + \left| 15 \right| = \frac{6(6+1)}{2} \tag{6.76}$$

Calculate the test statistic:

$$T(6) = Smallest\ of \begin{bmatrix} 6 \\ |15| \end{bmatrix} = 6 \tag{6.77}$$

$$T_{0.05,6} = 2 \tag{6.78}$$

Since the test statistic $T(6) = 6$ is not less then the critical value $T_{0.05,6} = 2$, H_{V0} is accepted.

6.5.2.18 Comparison of the maximum tool torque recorded for groups 1 and 2

Wilcoxon T Test to test for significance where $\alpha = 0.05$. Table 6.30 shows the results and calculations for this experiment.

- H_{V0}: Increased visual feedback does not improve operator performance.

- H_{V1}: Increased visual feedback does improve operator performance.

Pair Id	No haptic, 1 camera. (Nm) X_1	No haptic, 2 camera. (Nm) X_2	Diff	Rank of difference ignoring polarity	Rank associated with +ve difference R_+	Rank associated with -ve difference R_-
1	138	222	-84	2.5		2.5
2	29	125	-96	4		4
3	208	335	-127	5		5
4	211	127	84	2.5	2.5	
5	84	291	-207	6		6
6	166	237	-71	1		1
	$mean = $ 139.333	$mean = $ 222.833			$\Sigma R_+ = $ 2.5	$\Sigma R_- = $ 18.5

Table 6.30: Comparison of the maximum tool torque recorded for groups 1 and 2

143

Perform the computational check:

$$2.5 + \left| 18.5 \right| = \frac{6(6+1)}{2} \tag{6.79}$$

Calculate the test statistic:

$$T(6) = Smallest\ of \begin{bmatrix} 2.5 \\ |18.5| \end{bmatrix} = 2.5 \tag{6.80}$$

$$T_{0.05,6} = 2 \tag{6.81}$$

Since the test statistic $T(6) = 2.5$ is not less then the critical value $T_{0.05,6} = 2$, H_{V0} is accepted.

6.5.2.19 Comparison of the maximum tool torque recorded for groups 3 and 4

Wilcoxon T Test to test for significance where $\alpha = 0.05$. Table 6.31 shows the results and calculations for this experiment.

- H_{V0}: Increased visual feedback does not improve operator performance.

- H_{V1}: Increased visual feedback does improve operator performance.

Perform the computational check:

$$16 + \left| 5 \right| = \frac{6(6+1)}{2} \tag{6.82}$$

Calculate the test statistic:

$$T(6) = Smallest\ of \begin{bmatrix} 16 \\ |5| \end{bmatrix} = 5 \tag{6.83}$$

$$T_{0.05,6} = 2 \tag{6.84}$$

Since the test statistic $T(6) = 5$ is not less then the critical value $T_{0.05,6} = 2$, H_{V0} is accepted.

Pair Id	Haptic, 1 camera. (Nm) X_1	Haptic, 2 camera. (Nm) X_2	Diff	Rank of difference ignoring polarity	Rank associated with +ve difference R_+	Rank associated with -ve difference R_-
1	245	61	184	6	6	
2	145	160	-15	1		1
3	135	67	68	3	3	
4	74	45	29	2	2	
5	313	148	165	5	5	
6	49	138	-89	4		4
	mean =	mean =			$\Sigma R_+ = 16$	$\Sigma R_- = 5$

Table 6.31: Comparison of the maximum tool torque recorded for groups 3 and 4

6.5.2.20 Comparison of the mean tool torque recorded for groups 1 and 2

Wilcoxon T Test to test for significance where $\alpha = 0.05$. Table 6.32 shows the results and calculations for this experiment.

- H_{V0}: Increased visual feedback does not improve operator performance.

- H_{V1}: Increased visual feedback does improve operator performance.

Perform the computational check:

$$6 + \left|15\right| = \frac{6(6+1)}{2} \tag{6.85}$$

Calculate the test statistic:

$$T(6) = Smallest\ of \begin{bmatrix} 6 \\ |15| \end{bmatrix} = 6 \tag{6.86}$$

Pair Id	No haptic, 1 camera. (Nm) X_1	No haptic, 2 camera. (Nm) X_2	Diff	Rank of difference ignoring polarity	Rank associated with +ve difference R_+	Rank associated with -ve difference R_-
1	4.681	4.359	0.321	1	1	
2	3.803	14.846	-11.042	2		2
3	13.865	55.763	-41.898	6		6
4	50.506	11.387	39.118	5	5	
5	16.176	41.155	-24.979	4		4
6	59.206	74.541	-15.335	3		3
	$mean = 24.706$	$mean = 33.675$			$\Sigma R_+ = 6$	$\Sigma R_- = 15$

Table 6.32: Comparison of the mean tool torque recorded for groups 1 and 2

$$T_{0.05,6} = 2 \tag{6.87}$$

Since the test statistic $T(6) = 6$ is not less then the critical value $T_{0.05,6} = 2$, H_{V0} is accepted.

6.5.2.21 Comparison of the mean tool torque recorded for groups 3 and 4

Wilcoxon T Test to test for significance where $\alpha = 0.05$. Table 6.33 shows the results and calculations for this experiment.

- H_{V0}: Increased visual feedback does not improve operator performance.

- H_{V1}: Increased visual feedback does improve operator performance.

Pair Id	Haptic, 1 camera. (Nm) X_1	Haptic, 2 camera. (Nm) X_2	Diff	Rank of difference ignoring polarity	Rank associated with +ve difference R_+	Rank associated with -ve difference R_-
1	23.573	14.477	9.097	2	2	
2	28.609	21.691	6.917	1	1	
3	18.109	3.893	14.216	3	3	
4	15.07	-2.653	17.723	5	5	
5	9.901	32.454	-22.553	6		6
6	31.698	49.011	-17.313	4		4
	mean = 21.16	mean = 19.812			$\Sigma R_+ = 11$	$\Sigma R_- = 10$

Table 6.33: Comparison of the mean tool torque recorded for groups 3 and 4

Perform the computational check:

$$11 + \left| 10 \right| = \frac{6(6+1)}{2} \tag{6.88}$$

Calculate the test statistic:

$$T(6) = Smallest\ of \begin{bmatrix} 11 \\ \left|10\right| \end{bmatrix} = 10 \tag{6.89}$$

$$T_{0.05,6} = 2 \tag{6.90}$$

Since the test statistic $T(6) = 10$ is not less then the critical value $T_{0.05,6} = 2$, H_{V0} is accepted.

6.5.2.22 Comparison of the task completion time for groups 1 and 2

Wilcoxon T Test to test for significance where $\alpha = 0.05$. Table 6.34 shows the results and calculations for this experiment.

- H_{V0}: Increased visual feedback does not improve operator performance.

- H_{V1}: Increased visual feedback does improve operator performance.

Perform the computational check:

$$18 + \left| 3 \right| = \frac{6(6+1)}{2} \tag{6.91}$$

Calculate the test statistic:

$$T(6) = Smallest\ of \begin{bmatrix} 18 \\ \left|3\right| \end{bmatrix} = 3 \tag{6.92}$$

$$T_{0.05,6} = 2 \tag{6.93}$$

Since the test statistic $T(6) = 3$ is not less then the critical value $T_{0.05,6} = 2$, H_{V0} is accepted.

Pair Id	No haptic, 1 camera. (sec) X_1	No haptic, 2 camera. (sec) X_2	Diff	Rank of difference ignoring polarity	Rank associated with +ve difference R_+	Rank associated with -ve difference R_-
1	118.86	83.61	35.25	4	4	
2	299.94	212.49	87.45	6	6	
3	65.55	30.57	34.98	3	3	
4	120.06	142.74	-22.68	2		2
5	105.12	62.25	42.87	5	5	
6	18.63	26.82	-8.19	1		1
	$mean = 121.36$	$mean = 93.08$			$\Sigma R_+ = 18$	$\Sigma R_- = 3$

Table 6.34: Comparison of the task completion time for groups 1 and 2

6.5.2.23 Comparison of the task completion time for groups 3 and 4

Wilcoxon T Test to test for significance where $\alpha = 0.05$. Table 6.35 shows the results and calculations for this experiment.

- H_{V0}: Increased visual feedback does not improve operator performance.

- H_{V1}: Increased visual feedback does improve operator performance.

Pair Id	Haptic, 1 camera. (sec) X_1	Haptic, 2 camera. (sec) X_2	Diff	Rank of difference ignoring polarity	Rank associated with +ve difference R_+	Rank associated with -ve difference R_-
1	156.84	75.63	81.21	6	6	
2	87.12	54.24	32.88	3	3	
3	145.47	93.39	52.08	4	4	
4	124.44	126.87	-2.43	1		1
5	34.41	107.76	-73.35	5		5
6	43.29	35.82	7.47	2	2	
	$mean = 98.595$	$mean = 82.285$			$\Sigma R_+ = 15$	$\Sigma R_- = 6$

Table 6.35: Comparison of the task completion time for groups 3 and 4

Perform the computational check:

$$15 + \left| 6 \right| = \frac{6(6+1)}{2} \tag{6.94}$$

Calculate the test statistic:

$$T(6) = Smallest\ of \begin{bmatrix} 15 \\ |6| \end{bmatrix} = 6 \tag{6.95}$$

$$T_{0.05,6} = 2 \tag{6.96}$$

Since the test statistic $T(6) = 6$ is not less then the critical value $T_{0.05,6} = 2$, H_{V0} is accepted.

6.5.2.24 Discussion

The grinding task differs from the peg insertion task in several ways, the most noticeable of which is the fact that contact is not necessary to complete the peg insertion task, whereas grinding actually requires contact for task completion. Thus, to perform the peg insertion task, the operator need only know when a contact has occurred, but for grinding, the operator needs to know the magnitude of the applied force. This is then used to control the rate of the cutting. Unlike the peg insertion task, smaller values of forces in the results does not necessarily suggest better performance. Clearly the operator has to make contact with the material that is to be cut. This makes the force data more difficult to interpret than in the peg insertion task.

The previous results sections showed the results data and the statistical calculations that were performed to test for significance. The results of the statistical analysis is shown in the following tables, alongside the section number that contains the calculation of the result.

			Mode 2	Mode 3	Mode 4
			Non-Haptic	Haptic	Haptic
			2 Cameras	1 Camera	2 Cameras
Mode 1	Non-Haptic	1 Camera	Not Significant (6.5.2.14)	Not Significant (6.5.2.4)	no data
Mode 2	Non-Haptic	2 Cameras	no data	no data	Not Significant (6.5.2.5)
Mode 3	Haptic	1 Camera	no data	no data	Not Significant (6.5.2.15)

Table 6.36: Statistical significance within the maximum force in z-axis data

			Mode 2	Mode 3	Mode 4
			Non-Haptic	Haptic	Haptic
			2 Cameras	1 Camera	2 Cameras
Mode 1	Non-Haptic	1 Camera	Not Significant (6.5.2.16)	Not Significant (6.5.2.6)	no data
Mode 2	Non-Haptic	2 Cameras	no data	no data	Not Significant (6.5.2.7)
Mode 3	Haptic	1 Camera	no data	no data	Not Significant (6.5.2.17)

Table 6.37: Statistical significance within the mean force in z-axis data

			Mode 2	Mode 3	Mode 4
			Non-Haptic	Haptic	Haptic
			2 Cameras	1 Camera	2 Cameras
Mode 1	Non-Haptic	1 Camera	Not Significant (6.5.2.18)	Borderline $p < 0.05$ (6.5.2.8)	no data
Mode 2	Non-Haptic	2 Cameras	no data	no data	Significant $p < 0.05$ (6.5.2.9)
Mode 3	Haptic	1 Camera	no data	no data	Not Significant (6.5.2.19)

Table 6.38: Statistical significance within the maximum tool torque data

			Mode 2	Mode 3	Mode 4
			Non-Haptic	Haptic	Haptic
			2 Cameras	1 Camera	2 Cameras
Mode 1	Non-Haptic	1 Camera	Not Significant (6.5.2.20)	Not Significant (6.5.2.10)	no data
Mode 2	Non-Haptic	2 Cameras	no data	no data	Not Significant (6.5.2.11)
Mode 3	Haptic	1 Camera	no data	no data	Not Significant (6.5.2.21)

Table 6.39: Statistical significance within the mean tool torque data

			Mode 2	Mode 3	Mode 4
			Non-Haptic	Haptic	Haptic
			2 Cameras	1 Camera	2 Cameras
Mode 1	Non-Haptic	1 Camera	Not Significant (6.5.2.22)	Not Significant (6.5.2.12)	no data
Mode 2	Non-Haptic	2 Cameras	no data	no data	Not Significant (6.5.2.13)
Mode 3	Haptic	1 Camera	no data	no data	Not Significant (6.5.2.23)

Table 6.40: Statistical significance within the time for completion data

The results for the grinding task show no performance improvement due to adding the additional visual feedback that a second camera provides. Also, in general, the addition of haptic feedback did not provide any significant operator performance improvement, with the exception of maximum tool torque. Table 6.38 shows that haptic feedback made a significant reduction to the maximum recorded value of tool torque when the operator was using 2 cameras, and a borderline significant reduction when using a single camera. Clearly, a reduction in the maximum level of tool torque, with no significant increase in time to completion is highly beneficial. Very high levels of torque at the grinding wheel can result in motor stall or possibly even damage to the grinder wheel or motor.

The performance improvements shown by the reduction in maximum tool torque and the lack of improvement in reduction of force suggest that the haptic sensation used to present tool torque was superior to the sensation used to present force, i.e. the torque sensation was effective whilst the force sensation was not.

Great effort was taken to ensure that the visual, auditory and haptic feedback was controlled and consistent across both operators and tasks. However, for the grinding task, there was one major element of the visual feedback that could not be controlled or eliminated. This was the sparks that are emitted from the grinding wheel and the material during cutting. It is expected that these sparks

are responsible for eliminating performance improvements in force limitation due to haptic feedback. Since haptic feedback reduced the levels of maximum force for the peg insertion task, one would expect the same result for the grinding task, but this is not the case. The sparks emitted during cutting provide the operator with highly prominent visual cues as to the rate of the cutting operation. This is different to the peg insertion tasks where no similar visual cue exists, i.e. forces, are visually manifested in a very subtle manner. The sparks are suspected to be the reason why the grinding experiment results appear to be considerably different to the peg insertion results. It is suspected that the extra visual feedback created by the grinder caused the operators to ignore the haptic force feedback in favour of the visual feedback.

As noted by Smith (Smith, 1998), when both visual cues and haptic cues are present, operators tend to follow the visual cue. Much research has focussed on multi-modal sensory perception, and in particular perception when stimuli are conflicting. The "modality appropriateness" hypothesis (Welch & Warren, 1980) proposes that the sense that is most appropriate and reliable for a particular context is the one that dominates perception. A common example is known as the "ventriloquist effect", which is a common effect that can occur when one is watching a television or cinema screen. The actor's voices appear to come from their mouths even though the sounds can be coming from a very different location in reality. In general, it is accepted that vision is the dominant sense, particularly when the perception is that stimuli are conflicting (Rock & Victor, 1964). In the case of the grinding task, it is clear to see that the haptic force feedback and the visual effect caused by the sparks are in no way correlated. As noted by Campbell (Campbell *et al.*, 1999) and McGee (McGee, 2000), when a user is provided with contradicting multimodal feedback, the user tends to ignore one of the feedback channels and thus performance improvements are generally not seen.

It is interesting to note that although the haptic force feedback sensation was ignored, the haptic torque feedback sensation was not. This could be an indication that the force levels used in the force feedback sensation were not great enough to have the desired effect of communicating to the operator that the force level was becoming too great and should be reduced.

6.5.3 Study B

6.5.3.1 Hypothesis

As with the peg insertion task it is hypothesized that operator performance would increase as experience increases. It would also be expected that the learning rate (rate of performance improvement) would be higher for haptic modes of teleoperation.

6.5.3.2 Participants

The grinding task was performed by two operators. Each operator performed the task ten times for each mode of teleoperation. As with the peg insertion study, both operators were male engineers who had no previous training in teleoperation but were familiar with what teleoperation entails. Both operators were aged between 25 and 50.

6.5.3.3 Statistical Analysis

Least squares regression analysis was performed on the results data in order to test for performance improvements that arise with increased operator experience. MatLab was used to fit a 2nd order least squares linear regression to the maximum z axis force data, maximum tool torque data and the time to completion data. Analysis of variance (ANOVA) with alpha set to 0.05 was used to verify that the chosen model matches the data(Weisberg, 1985). This procedure is documented in appendix H.

6.5.3.4 Results

Figures 6.10 through to 6.15 show the regression plots for time to completion, maximum tool torque and maximum z axis force for both haptic and non-haptic teleoperation modes.
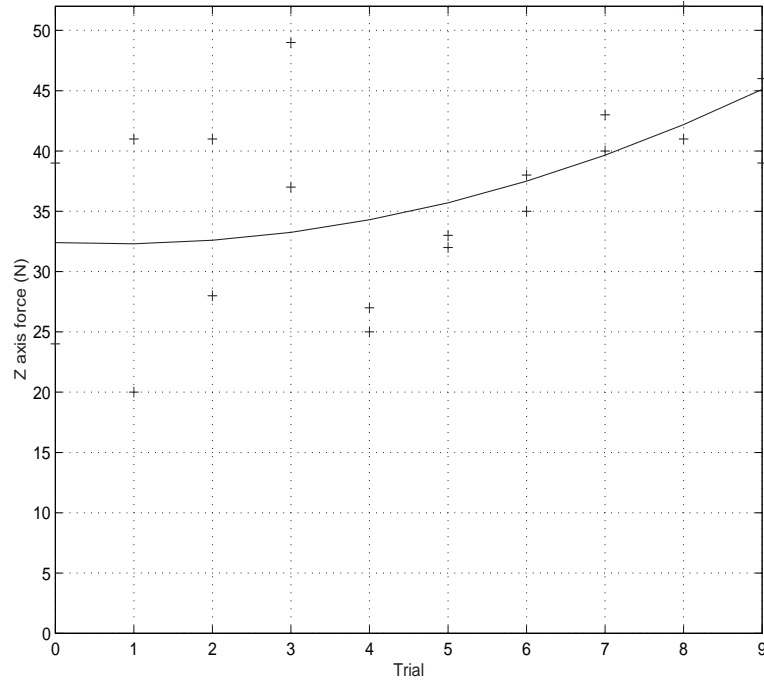
Figure 6.10: 2nd order regression plot for maximum z axis force, modes 1 and 2. Since the observed $F = 0.9812$ is smaller than the critical value $F(0.05; 8, 10) = 3.07$ the fit is accepted.
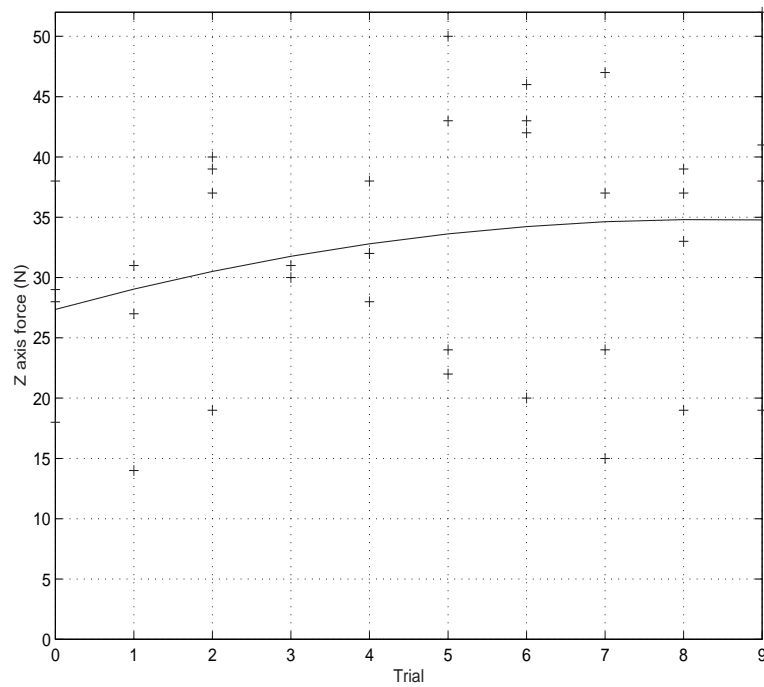
Figure 6.11: 2nd order regression plot for maximum z axis force, modes 3 and 4. Since the observed $F = 0.0334$ is smaller than the critical value $F(0.05; 28, 10) = 2.70$ the fit is accepted.
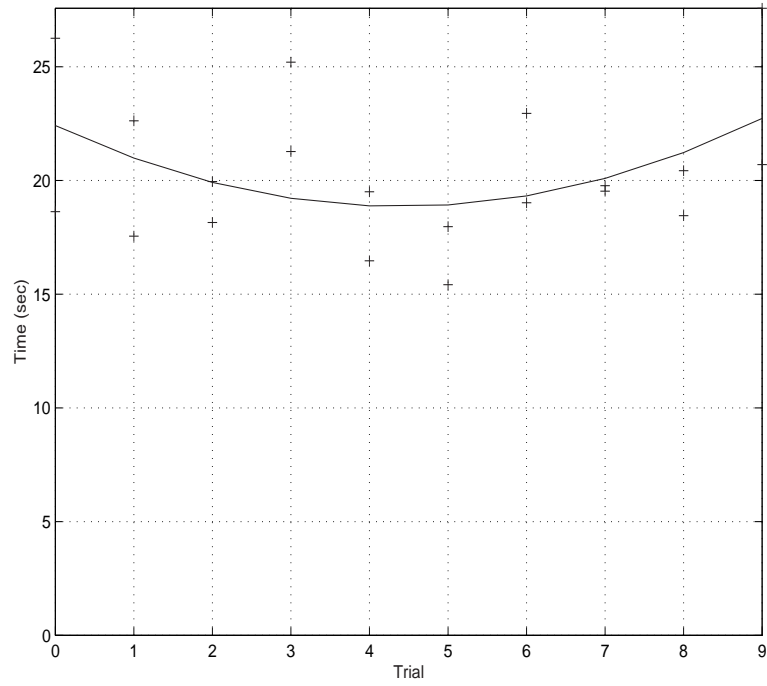
Figure 6.12: 2nd order regression plot for completion time, modes 1 and 2. Since the observed $F = 1.3355$ is smaller than the critical value $F(0.05; 8, 10) = 3.07$ the fit is accepted.
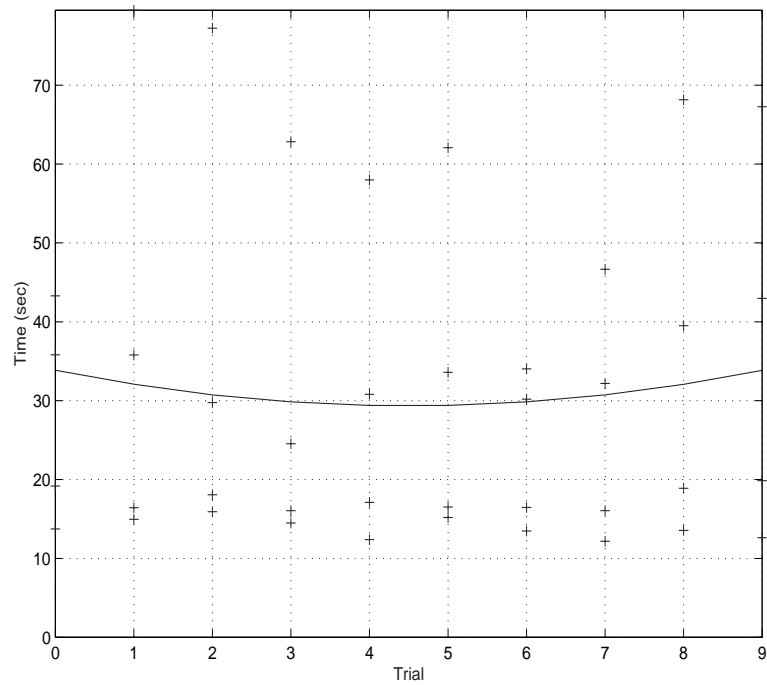
Figure 6.13: 2nd order regression plot for completion time, modes 3 and 4. Since the observed $F = 0.0171$ is smaller than the critical value $F(0.05; 28, 10) = 2.70$ the fit is accepted.
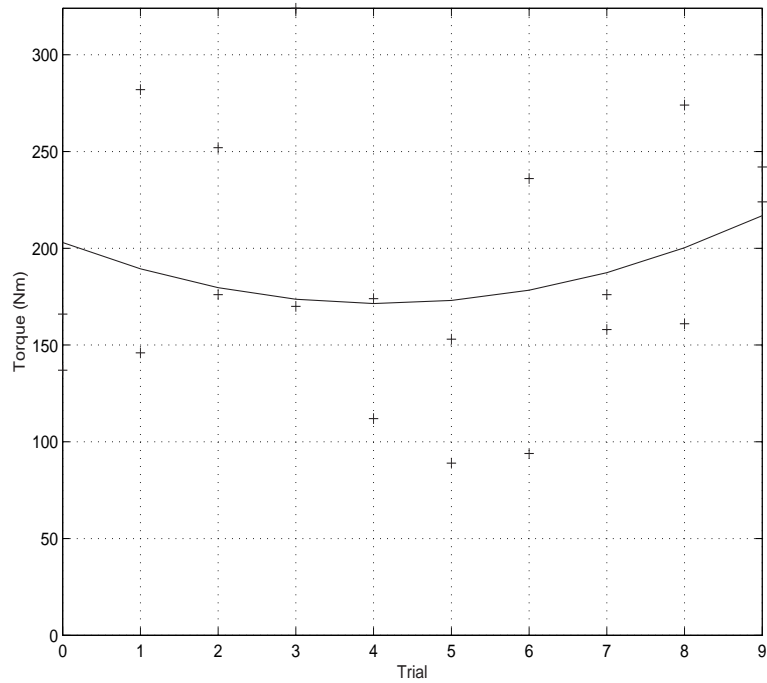
Figure 6.14: 2nd order regression plot for maximum tool torque, modes 1 and 2. Since the observed $F = 0.9044$ is smaller than the critical value $F(0.05; 8, 10) = 3.07$ the fit is accepted.
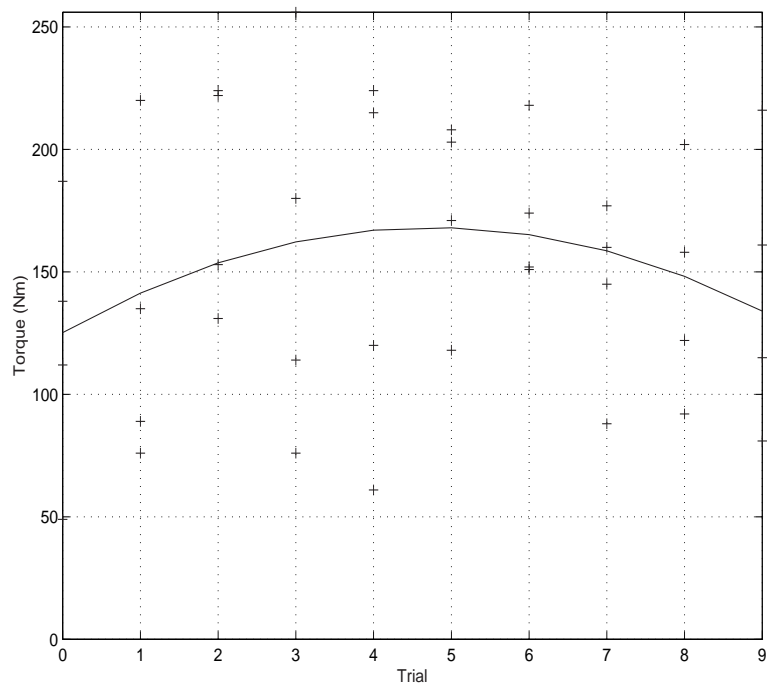
Figure 6.15: 2nd order regression plot for maximum tool torque, modes 3 and 4. Since the observed $F = 0.0525$ is smaller than the critical value $F(0.05; 28, 10) = 2.70$ the fit is accepted.

Figure 6.10 shows the plot for maximum z axis force without haptic feedback. This plot shows an almost steady increase in the level of force as experience increases. This is attributed to operator confidence. As the operator becomes more confident with the system, more force is applied. Since there is no haptic feedback, the operator has very little knowledge of the level of force that is being applied, and therefore, in time this could lead to damage of the tool. Figure 6.11 shows the plot for maximum z axis force with haptic feedback. Unlike figure 6.10, this plot shows that there is a trend towards stability. Initially, it seems that there is a familiarization stage where the operator is more cautious. Around the 6th trial, the plot starts to level off. This indicates that the operator has found what is thought to be an optimal level of grinding force.

It should be noted that the level of force without haptic feedback is generally higher than with haptic feedback. Also, as mentioned, the levels of maximum force recorded without haptic feedback are increasing with increased operator experience (confidence). Both these points indicate an increased possibility of damage to either the manipulator or the grinder.

Figure 6.12 shows the time for completion data without haptic feedback. The plot shows improvement to a performance peak at around the fourth and fifth trial followed by a regression in performance to the last trial. This is very similar to the plot for time to completion with haptic feedback, 6.13. Figure 6.13 also shows improvement to the fourth and fifth trial followed by a regression in performance through to the last trial. It is interesting to note that time to completion is not correlated to maximum z axis force, thus it is possible to record a reasonable time to completion without recording very high maximum values of z axis force which could possibly cause damage. In cases of extremely high z axis force, it is possible that a motor stall could be caused. Clearly this situation would have a detrimental effect on the completion time of the task.

Both plots of time to completion show the best time for completion to be between 12 and 15 seconds. Whereas the slowest completion time for the haptic plot is 80 seconds whilst the slowest completion time without haptic is 28 seconds, i.e. much faster. It appears that haptic feedback has had an adverse effect on the time to completion. This confirms the findings of Draper (Draper *et al.*, 1999) who noted that haptic force reflection can cause an increase in task completion time. The increase in task completion time could be seen as the cost of extra safety, or possibly attributed to operator confusion due to conflicting visual and haptic feedback. Study A of the grinding task discussed the possibility that a perceived contradiction between the visual feedback and haptic feedback could

have a detrimental effect on performance or possibly cancel out the effect of haptic feedback.

As with the plots of time to completion, the plots of maximum tool torque, 6.14 and 6.15, do not show a steady trend for improvement as experience increases. However, it is interesting to note that the plot for maximum tool torque shows increasing values of torque over the latter half of the plot which roughly matches the increasing maximum values of force that are seen towards the end of the plot of maximum force, 6.10. This appears to be further evidence that without haptic feedback, increasing operator confidence and experience causes both the levels of maximum force and torque to increase. As previously mentioned, this could lead to stalling of the grinder motor or possibly even damage.

In the analysis of the results of study A, it was noted that other researchers have found that perceived contradictions in feedback often lead to poorer performance or negate the positive effects of one particular sensory feedback channel such has haptic feedback (Smith, 1998), (Campbell *et al.*, 1999), (McGee, 2000). The conclusions of study A appear to be confirmed by the results of study B which show that haptic feedback did not cause a significant trend for improvement (with additional operator experience) within each test metric. Without further research that is beyond the scope of this project, it is not possible to make any further conclusions on the use of haptic feedback for the grinding task. In order to prove without doubt that the reason for a lack of performance improvements is due to operator sensory confusion or sensory prejudice, the grinding task would have to be repeated with elimination of the grinding sparks. This could possibly be performed by using a material that does not emit vast quantities sparks when it is cut or alternatively the visual feedback could be generated via simulation software such as Deneb Telegrip (Deneb Robotics Inc., 2003). Note that in the latter suggestion, the real Schilling manipulator would be used to drive the simulation since it would still be needed in order to perform the real task and to generate the real force/torque data.

6.6 Drilling Task

6.6.1 Design

As with the previous two tasks, the drilling experimentation was split into two studies, namely A and B. Study A focused on highlighting the performance gains offered by haptic communication, while study B aimed to highlight the effect of

haptic communication on operator learning and familiarisation.

Each operator was required to drill through a block of aluminium that measured 35mm in thickness. Prior to each experiment, the manipulator was driven so that the drill was in position above the aluminium block. Figure 6.16 shows a photo of the aluminium block.

Figure 6.16: The aluminium block that was drilled during the drill experiments

The instructions that were given to the operators were very similar to the grinding task. The task and the goal were explained to each operator in the same manner. Each operator was instructed to drill through the material as fast as possible, but without stalling the tool or causing damage due to excessive force. In addition, the haptic feedback was also explained to the operators who used the haptic modes of operation.

As with the grinding and peg insertion tasks, the operators were given instructions according to whether they were using the haptic mode or not. Instructions for the non-haptic mode were as follows.

- The joystick twist axis controls the plunge velocity of the tool into the workpiece

- You are required to drill through the material as fast as possible without exerting excessive force via the tool that could cause it to stall or to be damaged

- The forces and torques that you exert using the manipulator and the time it takes for you to complete the task will be recorded

Instructions for the haptic mode were exactly the same as shown in the previous list with the following additions.

- You will be provided with force feedback on the twist axis and torque feedback due to the tool on the left-to-right axis of the joystick. The torque feedback is presented as a vibration that becomes more severe as the torque on the tool increases

During the experiment, the operator only had control over the motion in the tool z-axis, thus, as with grinding, only plunging motion was possible. The z-axis velocity scale was set to 1%, which limited the maximum axis velocity to approximately 1.28mm/sec. The haptic feedback during drilling comprised of the slave end effector z-axis force displayed on the master z-axis, and the slave end effector z-axis torque displayed on the master x-axis.

The fastest possible completion time is estimated to be in the region of 150 to 200 seconds. Clearly, end effector velocity does not impose a limit on the task completion time since in free space the manipulator end effector would only take approximately 27 seconds to move 35mm (the thickness of the aluminium block) at the maximum rate of 1.28mm/sec.

Aluminium was chosen so that drill bit wear would not affect the results over the course of the tests.

6.6.2 Study A

6.6.2.1 Hypothesis

Given the four modes of operation, the following two sets of hypotheses are proposed. The first set concerns haptic feedback:

- H_{H0}: Haptic feedback does not improve operator performance

- H_{H1}: Haptic feedback does improve operator performance.

The second set concerns visual feedback:

- H_{V0}: Increased visual feedback does not improve operator performance

- H_{V1}: Increased visual feedback does improve operator performance.

6.6.2.2 Participants

Six operators performed the task using teleoperation modes 1 and 2, whilst another six operators performed the tasks using modes 3 and 4.

A reminder of the modes of teleoperation follows:

- Mode 1: 1 Camera, no haptic

- Mode 2: 2 Cameras, no haptic

- Mode 3: 1 Camera, with haptic

- Mode 4: 2 Cameras, with haptic.

The operator profiles were the same as for the previous experiments. None of the operators were trained in teleoperation. The primary operator vocation was engineering, exceptions to this were sales engineers and administration staff. Eleven of the operators were male, all of the operators were aged between 25 and 50.

6.6.2.3 Results

The following sections show the results of the experiments and also the statistical calculations that were performed to test for significance. As was stated previously, significance due to haptic feedback was tested using the Mann-Whitney U Test and significance due to visual feedback was tested using the Wilcoxon T Test for Dependent Samples.

6.6.2.4 Comparison of the maximum z axis force recorded for groups 1 and 3

Mann-Whitney U Test to test for significance where $\alpha = 0.05$. Table 6.41 shows the results for this experiment.

- H_{H0}: Haptic feedback does not improve operator performance.

- H_{H1}: Haptic feedback does improve operator performance.

Perform the computational check:

$$48 + 30 = \frac{(6+6)(6+6+1)}{2} \tag{6.97}$$

Calculate the test statistic:

$$U(6,6) = Smallest\ of \left[\begin{array}{c} (6)(6) + \dfrac{6(6+1)}{2} - 48 \\[2mm] (6)(6) + \dfrac{6(6+1)}{2} - 30 \end{array} \right] = 9 \tag{6.98}$$

No haptic, 1 camera. (N)	Rank R_1	Haptic, 1 camera. (N)	Rank R_2
132	9	35	1
133	10	129	4
129	4	130	7
130	7	144	12
130	7	129	4
141	11	109	2
$n_1 = 6$	$\Sigma R_1 = 48$	$n_2 = 6$	$\Sigma R_2 = 30$
$mean = 132.5$		$mean = 112.667$	

Table 6.41: Comparison of the maximum z axis force recorded for groups 1 and 3

$$U_{0.05/2;6,6} = 7 \tag{6.99}$$

Since the test statistic $U(6,6) = 9$ is not less then the critical value $U_{0.05/2;6,6} = 7$, H_{H0} is accepted.

6.6.2.5 Comparison of the maximum z axis force recorded for groups 2 and 4

Mann-Whitney U Test to test for significance where $\alpha = 0.05$. Table 6.42 shows the results for this experiment.

- H_{H0}: Haptic feedback does not improve operator performance.

- H_{H1}: Haptic feedback does improve operator performance.

No haptic, 2 camera. (N)	Rank R_1	Haptic, 2 camera. (N)	Rank R_2
137	10	54	1
130	5.5	150	12
130	5.5	130	5.5
141	11	131	8
130	5.5	128	3
132	9	124	2
$n_1 = 6$	$\Sigma R_1 = 46.5$	$n_2 = 6$	$\Sigma R_2 = 31.5$
$mean = 133.333$		$mean = 119.5$	

Table 6.42: Comparison of the maximum z axis force recorded for groups 2 and 4

Perform the computational check:

$$46.5 + 31.5 = \frac{(6+6)(6+6+1)}{2} \tag{6.100}$$

Calculate the test statistic:

$$U(6,6) = Smallest\ of\ \begin{bmatrix} (6)(6) + \dfrac{6(6+1)}{2} - 46.5 \\[2ex] (6)(6) + \dfrac{6(6+1)}{2} - 31.5 \end{bmatrix} = 10.5 \tag{6.101}$$

$$U_{0.05/2;6,6} = 7 \tag{6.102}$$

Since the test statistic $U(6,6) = 10.5$ is not less then the critical value $U_{0.05/2;6,6} = 7$, H_{H0} is accepted.

6.6.2.6 Comparison of the mean z axis force recorded for groups 1 and 3

Mann-Whitney U Test to test for significance where $\alpha = 0.05$. Table 6.43 shows the results for this experiment.

- H_{H0}: Haptic feedback does not improve operator performance.

- H_{H1}: Haptic feedback does improve operator performance.

No haptic, 1 camera. (N)	Rank R_1	Haptic, 1 camera. (N)	Rank R_2
116.753	5	18.436	1
120.843	12	117.117	7
118.565	8	116.833	6
119.871	10	100.653	3
118.853	9	109.603	4
120.387	11	52.552	2
$n_1 = 6$	$\Sigma R_1 = 55$	$n_2 = 6$	$\Sigma R_2 = 23$
$mean = 119.212$		$mean = 85.866$	

Table 6.43: Comparison of the mean z axis force recorded for groups 1 and 3

Perform the computational check:

$$55 + 23 = \frac{(6+6)(6+6+1)}{2} \tag{6.103}$$

Calculate the test statistic:

$$U(6,6) = Smallest\ of \begin{bmatrix} (6)(6) + \dfrac{6(6+1)}{2} - 55 \\ (6)(6) + \dfrac{6(6+1)}{2} - 23 \end{bmatrix} = 2 \qquad (6.104)$$

$$U_{0.05/2;6,6} = 7 \qquad (6.105)$$

Since the test statistic $U(6,6) = 2$ is less then the critical value $U_{0.05/2;6,6} = 7$, H_{H0} is rejected and thus H_{H1} is accepted.

6.6.2.7 Comparison of the mean z axis force recorded for groups 2 and 4

Mann-Whitney U Test to test for significance where $\alpha = 0.05$. Table 6.44 shows the results for this experiment.

- H_{H0}: Haptic feedback does not improve operator performance.

- H_{H1}: Haptic feedback does improve operator performance.

No haptic, 2 camera. (N)	Rank R_1	Haptic, 2 camera. (N)	Rank R_2
119.687	9	35.086	1
117.317	7	120.475	10
112.91	5	115.794	6
120.695	11	98.407	4
119.547	8	87.053	3
122.066	12	62.525	2
$n_1 = 6$	$\Sigma R_1 = 52$	$n_2 = 6$	$\Sigma R_2 = 26$
$mean = 118.704$		$mean = 86.557$	

Table 6.44: Comparison of the mean z axis force recorded for groups 2 and 4

Perform the computational check:

$$52 + 26 = \frac{(6+6)(6+6+1)}{2} \qquad (6.106)$$

Calculate the test statistic:

$$U(6,6) = Smallest\ of \begin{bmatrix} (6)(6) + \dfrac{6(6+1)}{2} - 52 \\[2mm] (6)(6) + \dfrac{6(6+1)}{2} - 26 \end{bmatrix} = 5 \qquad (6.107)$$

$$U_{0.05/2;6,6} = 7 \qquad (6.108)$$

Since the test statistic $U(6,6) = 5$ is less then the critical value $U_{0.05/2;6,6} = 7$, H_{H0} is rejected and thus H_{H1} is accepted.

6.6.2.8 Comparison of the maximum tool torque recorded for groups 1 and 3

Mann-Whitney U Test to test for significance where $\alpha = 0.05$. Table 6.45 shows the results for this experiment.

- H_{H0}: Haptic feedback does not improve operator performance.

- H_{H1}: Haptic feedback does improve operator performance.

No haptic, 1 camera. (Nm)	Rank R_1	Haptic, 1 camera. (Nm)	Rank R_2
51	3	64	8
54	5	55	6
63	7	122	12
75	11	49	2
66	10	65	9
39	1	53	4
$n_1 = 6$	$\Sigma R_1 = 37$	$n_2 = 6$	$\Sigma R_2 = 41$
$mean = 58$		$mean = 68$	

Table 6.45: Comparison of the maximum tool torque recorded for groups 1 and 3

Perform the computational check:

$$37 + 41 = \frac{(6+6)(6+6+1)}{2} \qquad (6.109)$$

Calculate the test statistic:

168

$$U(6,6) = Smallest \ of \left[\begin{array}{c} (6)(6) + \dfrac{6(6+1)}{2} - 37 \\ (6)(6) + \dfrac{6(6+1)}{2} - 41 \end{array} \right] = 16 \qquad (6.110)$$

$$U_{0.05/2;6,6} = 7 \qquad (6.111)$$

Since the test statistic $U(6,6) = 16$ is not less then the critical value $U_{0.05/2;6,6} = 7$, H_{H0} is accepted.

6.6.2.9 Comparison of the maximum tool torque recorded for groups 2 and 4

Mann-Whitney U Test to test for significance where $\alpha = 0.05$. Table 6.46 shows the results for this experiment.

- H_{H0}: Haptic feedback does not improve operator performance.

- H_{H1}: Haptic feedback does improve operator performance.

No haptic, 2 camera. (Nm)	Rank R_1	Haptic, 2 camera. (Nm)	Rank R_2
86	12	27	2
53	5.5	74	11
53	5.5	47	4
69	10	63	8
44	3	65	9
56	7	3	1
$n_1 = 6$	$\Sigma R_1 = 43$	$n_2 = 6$	$\Sigma R_2 = 35$
$mean = 60.167$		$mean = 46.5$	

Table 6.46: Comparison of the maximum tool torque recorded for groups 2 and 4

Perform the computational check:

$$43 + 35 = \frac{(6+6)(6+6+1)}{2} \qquad (6.112)$$

Calculate the test statistic:

$$U(6,6) = Smallest\ of \begin{bmatrix} (6)(6) + \dfrac{6(6+1)}{2} - 43 \\[2mm] (6)(6) + \dfrac{6(6+1)}{2} - 35 \end{bmatrix} = 14 \qquad (6.113)$$

$$U_{0.05/2;6,6} = 7 \qquad (6.114)$$

Since the test statistic $U(6,6) = 14$ is not less then the critical value $U_{0.05/2;6,6} = 7$, H_{H0} is accepted.

6.6.2.10 Comparison of the mean tool torque recorded for groups 1 and 3

Mann-Whitney U Test to test for significance where $\alpha = 0.05$. Table 6.47 shows the results for this experiment.

- H_{H0}: Haptic feedback does not improve operator performance.

- H_{H1}: Haptic feedback does improve operator performance.

No haptic, 1 camera. (Nm)	Rank R_1	Haptic, 1 camera. (Nm)	Rank R_2
26.605	4	34.233	7.5
27.336	5	28.796	6
37.699	10	42.615	11
48.868	12	5.541	1
34.233	7.5	36.908	9
14.228	2	23.743	3
$n_1 = 6$	$\Sigma R_1 = 40.5$	$n_2 = 6$	$\Sigma R_2 = 37.5$
$mean = 31.495$		$mean = 28.639$	

Table 6.47: Comparison of the mean tool torque recorded for groups 1 and 3

Perform the computational check:

$$40.5 + 37.5 = \frac{(6+6)(6+6+1)}{2} \qquad (6.115)$$

Calculate the test statistic:

$$U(6,6) = Smallest\ of \begin{bmatrix} (6)(6) + \dfrac{6(6+1)}{2} - 40.5 \\[2ex] (6)(6) + \dfrac{6(6+1)}{2} - 37.5 \end{bmatrix} = 16.5 \qquad (6.116)$$

$$U_{0.05/2;6,6} = 7 \qquad (6.117)$$

Since the test statistic $U(6,6) = 16.5$ is not less then the critical value $U_{0.05/2;6,6} = 7$, H_{H0} is accepted.

6.6.2.11 Comparison of the mean tool torque recorded for groups 2 and 4

Mann-Whitney U Test to test for significance where $\alpha = 0.05$. Table 6.48 shows the results for this experiment.

- H_{H0}: Haptic feedback does not improve operator performance.

- H_{H1}: Haptic feedback does improve operator performance.

No haptic, 2 camera. (Nm)	Rank R_1	Haptic, 2 camera. (Nm)	Rank R_2
59.273	12	5.829	1
26.414	5	42.499	11
33.704	8	18.675	4
33.299	7	28.308	6
10.876	2	38.363	10
35.542	9	15.572	3
$n_1 = 6$	$\Sigma R_1 = 43$	$n_2 = 6$	$\Sigma R_2 = 35$
$mean = 33.185$		$mean = 19.684$	

Table 6.48: Comparison of the mean tool torque recorded for groups 2 and 4

Perform the computational check:

$$43 + 35 = \frac{(6+6)(6+6+1)}{2} \qquad (6.118)$$

Calculate the test statistic:

$$U(6,6) = Smallest~of \begin{bmatrix} (6)(6) + \dfrac{6(6+1)}{2} - 43 \\[2mm] (6)(6) + \dfrac{6(6+1)}{2} - 35 \end{bmatrix} = 14 \qquad (6.119)$$

$$U_{0.05/2;6,6} = 7 \qquad (6.120)$$

Since the test statistic $U(6,6) = 14$ is not less then the critical value $U_{0.05/2;6,6} = 7$, H_{H0} is accepted.

6.6.2.12 Comparison of the time to completion recorded for groups 1 and 3

Mann-Whitney U Test to test for significance where $\alpha = 0.05$. Table 6.49 shows the results for this experiment.

- H_{H0}: Haptic feedback does not improve operator performance.

- H_{H1}: Haptic feedback does improve operator performance.

No haptic, 1 camera. (sec)	Rank R_1	Haptic, 1 camera. (sec)	Rank R_2
286.71	8	285.30	7
287.99	9	278.4	5
283.74	6	257.07	3
295.35	11	276.27	4
291.33	10	238.68	2
235.56	1	296.01	12
$n_1 = 6$	$\Sigma R_1 = 45$	$n_2 = 6$	$\Sigma R_2 = 33$
$mean = 280.11$		$mean = 271.955$	

Table 6.49: Comparison of the time to completion recorded for groups 1 and 3

Perform the computational check:

$$45 + 33 = \frac{(6+6)(6+6+1)}{2} \qquad (6.121)$$

Calculate the test statistic:

$$U(6,6) = Smallest\ of \begin{bmatrix} (6)(6) + \dfrac{6(6+1)}{2} - 45 \\[3mm] (6)(6) + \dfrac{6(6+1)}{2} - 33 \end{bmatrix} = 12 \qquad (6.122)$$

$$U_{0.05/2;6,6} = 7 \qquad (6.123)$$

Since the test statistic $U(6,6) = 12$ is not less then the critical value $U_{0.05/2;6,6} = 7$, H_{H0} is accepted.

6.6.2.13 Comparison of the time to completion recorded for groups 2 and 4

Mann-Whitney U Test to test for significance where $\alpha = 0.05$. Table 6.50 shows the results for this experiment.

- H_{H0}: Haptic feedback does not improve operator performance.

- H_{H1}: Haptic feedback does improve operator performance.

No haptic, 2 camera. (sec)	Rank R_1	Haptic, 2 camera. (sec)	Rank R_2
280.02	2	286.91	5
287.7	7	283.11	4
293.01	10	287.37	6
289.65	8	279.60	1
299.31	12	299.04	11
282.00	3	292.38	9
$n_1 = 6$	$\Sigma R_1 = 42$	$n_2 = 6$	$\Sigma R_2 = 36$
$mean = 288.615$		$mean = 288.07$	

Table 6.50: Comparison of the time to completion recorded for groups 2 and 4

Perform the computational check:

$$42 + 36 = \frac{(6+6)(6+6+1)}{2} \qquad (6.124)$$

Calculate the test statistic:

$$U(6,6) = Smallest\ of \begin{bmatrix} (6)(6) + \dfrac{6(6+1)}{2} - 42 \\[2ex] (6)(6) + \dfrac{6(6+1)}{2} - 36 \end{bmatrix} = 15 \qquad (6.125)$$

$$U_{0.05/2;6,6} = 7 \qquad (6.126)$$

Since the test statistic $U(6,6) = 15$ is not less then the critical value $U_{0.05/2;6,6} = 7$, H_{H0} is accepted.

6.6.2.14 Comparison of the maximum z axis force recorded for groups 1 and 2

Wilcoxon T Test to test for significance where $\alpha = 0.05$. Table 6.51 shows the results and calculations for this experiment.

- H_{V0}: Increased visual feedback does not improve operator performance.

- H_{V1}: Increased visual feedback does improve operator performance.

Pair Id	No haptic, 1 camera. (N) X_1	No haptic, 2 camera. (N) X_2	Diff	Rank of difference ignoring polarity	Rank associated with +ve difference R_+	Rank associated with -ve difference R_-
1	132	137	5	4	4	
2	133	130	-3	3		3
3	129	130	1	2	2	
4	130	141	11	6	6	
5	130	130	0	1	1	
6	141	132	-9	5		5
	mean = 132.5	mean = 133.333			$\Sigma R_+ = 13$	$\Sigma R_- = 8$

Table 6.51: Comparison of the maximum z axis force recorded for groups 1 and 2

Perform the computational check:

$$13 + \left|8\right| = \frac{6(6+1)}{2} \tag{6.127}$$

Calculate the test statistic:

$$T(6) = Smallest\ of \begin{bmatrix} 13 \\ |8| \end{bmatrix} = 8 \tag{6.128}$$

$$T_{0.05,6} = 2 \tag{6.129}$$

Since the test statistic $T(6) = 8$ is not less then the critical value $T_{0.05,6} = 2$, H_{V0} is accepted.

6.6.2.15 Comparison of the maximum z axis force recorded for groups 3 and 4

Wilcoxon T Test to test for significance where $\alpha = 0.05$. Table 6.52 shows the results and calculations for this experiment.

- H_{V0}: Increased visual feedback does not improve operator performance.

- H_{V1}: Increased visual feedback does improve operator performance.

Pair Id	Haptic, 1 camera. (N) X_1	Haptic, 2 camera. (N) X_2	Diff	Rank of difference ignoring polarity	Rank associated with +ve difference R_+	Rank associated with -ve difference R_-
1	35	54	19	5	5	
2	129	150	21	6	6	
3	130	130	0	1	1	
4	144	131	-13	3		3
5	129	128	-1	2		2
6	109	124	15	4	4	
	$mean =$ 112.667	$mean =$ 119.5			$\Sigma R_+ = 16$	$\Sigma R_- = 5$

Table 6.52: Comparison of the maximum z axis force recorded for groups 3 and 4

Perform the computational check:

$$16 + \left| 5 \right| = \frac{6(6+1)}{2} \tag{6.130}$$

Calculate the test statistic:

$$T(6) = Smallest\ of \begin{bmatrix} 16 \\ |5| \end{bmatrix} = 5 \tag{6.131}$$

$$T_{0.05,6} = 2 \tag{6.132}$$

Since the test statistic $T(6) = 5$ is not less then the critical value $T_{0.05,6} = 2$, H_{V0} is accepted.

6.6.2.16 Comparison of the mean z axis force recorded for groups 1 and 2

Wilcoxon T Test to test for significance where $\alpha = 0.05$. Table 6.53 shows the results and calculations for this experiment.

- H_{V0}: Increased visual feedback does not improve operator performance.

- H_{V1}: Increased visual feedback does improve operator performance.

Pair Id	No haptic, 1 camera. (N) X_1	No haptic, 2 camera. (N) X_2	Diff	Rank of difference ignoring polarity	Rank associated with +ve difference R_+	Rank associated with -ve difference R_-
1	116.753	119.687	2.934	4	4	
2	120.843	117.317	-3.526	5		5
3	118.565	112.91	-5.655	6		6
4	119.871	120.695	0.824	2	2	
5	118.853	119.547	0.694	1	1	
6	120.387	122.066	1.679	3	3	
	mean = 119.212	mean = 118.704			$\Sigma R_+ = 10$	$\Sigma R_- = 11$

Table 6.53: Comparison of the mean z axis force recorded for groups 1 and 2

Perform the computational check:

$$10 + \left|11\right| = \frac{6(6+1)}{2} \tag{6.133}$$

Calculate the test statistic:

$$T(6) = Smallest \; of \; \begin{bmatrix} 10 \\ \left|11\right| \end{bmatrix} = 10 \tag{6.134}$$

$$T_{0.05,6} = 2 \tag{6.135}$$

Since the test statistic $T(6) = 10$ is not less then the critical value $T_{0.05,6} = 2$, H_{V0} is accepted.

6.6.2.17 Comparison of the mean z axis force recorded for groups 3 and 4

Wilcoxon T Test to test for significance where $\alpha = 0.05$. Table 6.54 shows the results and calculations for this experiment.

- H_{V0}: Increased visual feedback does not improve operator performance.

- H_{V1}: Increased visual feedback does improve operator performance.

Perform the computational check:

$$12 + \left|9\right| = \frac{6(6+1)}{2} \tag{6.136}$$

Calculate the test statistic:

$$T(6) = Smallest \; of \; \begin{bmatrix} 12 \\ \left|9\right| \end{bmatrix} = 9 \tag{6.137}$$

$$T_{0.05,6} = 2 \tag{6.138}$$

Since the test statistic $T(6) = 9$ is not less then the critical value $T_{0.05,6} = 2$, H_{V0} is accepted.

Pair Id	Haptic, 1 camera. (N) X_1	Haptic, 2 camera. (N) X_2	Diff	Rank of difference ignoring polarity	Rank associated with +ve difference R_+	Rank associated with -ve difference R_-
1	18.436	35.086	16.65	5	5	
2	117.117	120.475	3.358	3	3	
3	116.833	115.794	-1.039	1		1
4	100.653	98.407	-2.246	2		2
5	109.603	87.053	-22.551	6		6
6	52.552	62.525	9.973	4	4	
	$mean = 85.866$	$mean = 86.557$			$\Sigma R_+ = 12$	$\Sigma R_- = 9$

Table 6.54: Comparison of the mean z axis force recorded for groups 3 and 4

6.6.2.18 Comparison of the maximum tool torque recorded for groups 1 and 2

Wilcoxon T Test to test for significance where $\alpha = 0.05$. Table 6.55 shows the results and calculations for this experiment.

- H_{V0}: Increased visual feedback does not improve operator performance.

- H_{V1}: Increased visual feedback does improve operator performance.

Perform the computational check:

$$11 + \left|10\right| = \frac{6(6+1)}{2} \tag{6.139}$$

Calculate the test statistic:

$$T(6) = Smallest\ of \begin{bmatrix} 11 \\ |10| \end{bmatrix} = 10 \tag{6.140}$$

Pair Id	No haptic, 1 camera. (Nm) X_1	No haptic, 2 camera. (Nm) X_2	Diff	Rank of difference ignoring polarity	Rank associated with +ve difference R_+	Rank associated with -ve difference R_-
1	51	86	-35	6		6
2	54	53	1	1	1	
3	63	53	10	3	3	
4	75	69	6	2	2	
5	66	44	22	5	5	
6	39	56	-17	4		4
	mean = 58	*mean* = 60.167			$\Sigma R_+ = 11$	$\Sigma R_- = 10$

Table 6.55: Comparison of the maximum tool torque recorded for groups 1 and 2

$$T_{0.05,6} = 2 \tag{6.141}$$

Since the test statistic $T(6) = 10$ is not less then the critical value $T_{0.05,6} = 2$, H_{V0} is accepted.

6.6.2.19 Comparison of the maximum tool torque recorded for groups 3 and 4

Wilcoxon T Test to test for significance where $\alpha = 0.05$. Table 6.56 shows the results and calculations for this experiment.

- H_{V0}: Increased visual feedback does not improve operator performance.

- H_{V1}: Increased visual feedback does improve operator performance.

Perform the computational check:

$$16 + \left| 5 \right| = \frac{6(6+1)}{2} \tag{6.142}$$

180

Pair Id	Haptic, 1 camera. (Nm) X_1	Haptic, 2 camera. (Nm) X_2	Diff	Rank of difference ignoring polarity	Rank associated with +ve difference R_+	Rank associated with -ve difference R_-
1	64	27	37	4	4	
2	55	74	-19	3		3
3	122	47	75	6	6	
4	49	63	-14	2		2
5	65	65	0	1	1	
6	53	3	50	5	5	
	mean = 68	mean = 46.5			$\Sigma R_+ = 16$	$\Sigma R_- = 5$

Table 6.56: Comparison of the maximum tool torque recorded for groups 3 and 4

Calculate the test statistic:

$$T(6) = Smallest\ of \begin{bmatrix} 16 \\ |5| \end{bmatrix} = 5 \tag{6.143}$$

$$T_{0.05,6} = 2 \tag{6.144}$$

Since the test statistic $T(6) = 5$ is not less then the critical value $T_{0.05,6} = 2$, H_{V0} is accepted.

6.6.2.20 Comparison of the mean tool torque recorded for groups 1 and 2

Wilcoxon T Test to test for significance where $\alpha = 0.05$. Table 6.57 shows the results and calculations for this experiment.

- H_{V0}: Increased visual feedback does not improve operator performance.

- H_{V1}: Increased visual feedback does improve operator performance.

Pair Id	No haptic, 1 camera. (Nm) X_1	No haptic, 2 camera. (Nm) X_2	Diff	Rank of difference ignoring polarity	Rank associated with +ve difference R_+	Rank associated with -ve difference R_-
1	26.605	59.273	-32.668	6		6
2	27.336	26.414	0.922	1	1	
3	37.699	33.704	3.995	2	2	
4	48.868	33.299	15.569	3	3	
5	34.233	10.876	23.356	5	5	
6	14.228	35.542	-21.314	4		4
	mean = 31.495	*mean* = 33.185			$\Sigma R_+ = 11$	$\Sigma R_- = 10$

Table 6.57: Comparison of the mean tool torque recorded for groups 1 and 2

Perform the computational check:

$$11 + \left|10\right| = \frac{6(6+1)}{2} \tag{6.145}$$

Calculate the test statistic:

$$T(6) = Smallest\ of \begin{bmatrix} 11 \\ \left|10\right| \end{bmatrix} = 10 \tag{6.146}$$

$$T_{0.05,6} = 2 \tag{6.147}$$

Since the test statistic $T(6) = 10$ is not less then the critical value $T_{0.05,6} = 2$, H_{V0} is accepted.

6.6.2.21 Comparison of the mean tool torque recorded for groups 3 and 4

Wilcoxon T Test to test for significance where $\alpha = 0.05$. Table 6.58 shows the results and calculations for this experiment.

- H_{V0}: Increased visual feedback does not improve operator performance.

- H_{V1}: Increased visual feedback does improve operator performance.

Pair Id	Haptic, 1 camera. (Nm) X_1	Haptic, 2 camera. (Nm) X_2	Diff	Rank of difference ignoring polarity	Rank associated with +ve difference R_+	Rank associated with -ve difference R_-
1	34.233	5.829	28.404	5	5	
2	28.796	42.499	-13.703	2		2
3	42.615	18.675	23.941	4	4	
4	5.541	28.308	-22.767	3		3
5	36.908	38.363	-1.454	1		1
6	23.743	-15.572	39.315	6	6	
	mean = 28.639	*mean* = 19.684			$\Sigma R_+ = 15$	$\Sigma R_- = 6$

Table 6.58: Comparison of the mean tool torque recorded for groups 3 and 4

Perform the computational check:

$$15 + \left| 6 \right| = \frac{6(6+1)}{2} \tag{6.148}$$

Calculate the test statistic:

$$T(6) = Smallest\ of \begin{bmatrix} 15 \\ |6| \end{bmatrix} = 6 \tag{6.149}$$

$$T_{0.05,6} = 2 \tag{6.150}$$

Since the test statistic $T(6) = 6$ is not less then the critical value $T_{0.05,6} = 2$, H_{V0} is accepted.

6.6.2.22 Comparison of the time to completion recorded for groups 1 and 2

Wilcoxon T Test to test for significance where $\alpha = 0.05$. Table 6.59 shows the results and calculations for this experiment.

- H_{V0}: Increased visual feedback does not improve operator performance.

- H_{V1}: Increased visual feedback does improve operator performance.

Pair Id	No haptic, 1 camera. (sec) X_1	No haptic, 2 camera. (sec) X_2	Diff	Rank of difference ignoring polarity	Rank associated with +ve difference R_+	Rank associated with -ve difference R_-
1	286.71	280.02	6.69	3	3	
2	287.99	287.7	0.29	1	1	
3	283.74	293.01	-9.27	5		5
4	295.35	289.65	5.7	2	2	
5	291.33	299.31	-7.98	4		4
6	235.56	282.00	-46.44	6		6
	$mean = 280.11$	$mean = 288.615$			$\Sigma R_+ = 6$	$\Sigma R_- = 15$

Table 6.59: Comparison of the time to completion recorded for groups 1 and 2

Perform the computational check:

$$6 + \left| 15 \right| = \frac{6(6+1)}{2} \tag{6.151}$$

184

Calculate the test statistic:

$$T(6) = Smallest \; of \begin{bmatrix} 6 \\ |15| \end{bmatrix} = 6 \tag{6.152}$$

$$T_{0.05,6} = 2 \tag{6.153}$$

Since the test statistic $T(6) = 6$ is not less then the critical value $T_{0.05,6} = 2$, H_{V0} is accepted.

6.6.2.23 Comparison of the time to completion recorded for groups 3 and 4

Wilcoxon T Test to test for significance where $\alpha = 0.05$. Table 6.60 shows the results and calculations for this experiment.

- H_{V0}: Increased visual feedback does not improve operator performance.

- H_{V1}: Increased visual feedback does improve operator performance.

Pair Id	Haptic, 1 camera. (sec) X_1	Haptic, 2 camera. (sec) X_2	Diff	Rank of difference ignoring polarity	Rank associated with +ve difference R_+	Rank associated with -ve difference R_-
1	285.30	286.91	-1.61	1		1
2	278.4	283.11	-4.71	4		4
3	257.07	287.37	-30.3	5		5
4	276.27	279.60	-3.33	2		2
5	238.68	299.04	-60.36	6		6
6	296.01	292.38	3.63	3	3	
	mean = 271.96	mean = 288.07			$\Sigma R_+ = 3$	$\Sigma R_- = 18$

Table 6.60: Comparison of the time to completion recorded for groups 3 and 4

Perform the computational check:

$$3 + \left| 18 \right| = \frac{6(6+1)}{2} \tag{6.154}$$

Calculate the test statistic:

$$T(6) = Smallest\ of \begin{bmatrix} 3 \\ |18| \end{bmatrix} = 3 \tag{6.155}$$

$$T_{0.05,6} = 2 \tag{6.156}$$

Since the test statistic $T(6) = 3$ is not less then the critical value $T_{0.05,6} = 2$, H_{V0} is accepted.

6.6.2.24 Discussion

The drilling task is similar to the grinding task due to the fact that the operator needs to know the magnitude of the applied forces in order to be able to perform the task accurately. This is contrary to the peg insertion situation where the operator need only know when an impulse/contact occurs. Thus, in the assessment of the drilling results, smaller force values do not necessarily suggest better performance.

The previous results sections showed the results data and the statistical calculations that were performed to test for significance. The results of the statistical analysis is shown in the following tables, alongside the section number that contains the calculation of the result.

			Mode 2	Mode 3	Mode 4
			Non-Haptic	Haptic	Haptic
			2 Cameras	1 Camera	2 Cameras
Mode 1	Non-Haptic	1 Camera	Not Significant (6.6.2.14)	Not Significant (6.6.2.4)	no data
Mode 2	Non-Haptic	2 Cameras	no data	no data	Not Significant (6.6.2.5)
Mode 3	Haptic	1 Camera	no data	no data	Not Significant (6.6.2.15)

Table 6.61: Statistical significance within the maximum force in z-axis data

			Mode 2	Mode 3	Mode 4
			Non-Haptic	Haptic	Haptic
			2 Cameras	1 Camera	2 Cameras
Mode 1	Non-Haptic	1 Camera	Not Significant (6.6.2.16)	Significant $p < 0.05$ (6.6.2.6)	no data
Mode 2	Non-Haptic	2 Cameras	no data	no data	Significant $p < 0.05$ (6.6.2.7)
Mode 3	Haptic	1 Camera	no data	no data	Not Significant (6.6.2.17)

Table 6.62: Statistical significance within the mean force in z-axis data

			Mode 2	Mode 3	Mode 4
			Non-Haptic	Haptic	Haptic
			2 Cameras	1 Camera	2 Cameras
Mode 1	Non-Haptic	1 Camera	Not Significant (6.6.2.18)	Not Significant (6.6.2.8)	no data
Mode 2	Non-Haptic	2 Cameras	no data	no data	Not Significant (6.6.2.9)
Mode 3	Haptic	1 Camera	no data	no data	Not Significant (6.6.2.19)

Table 6.63: Statistical significance within the maximum tool torque data

			Mode 2	Mode 3	Mode 4
			Non-Haptic	Haptic	Haptic
			2 Cameras	1 Camera	2 Cameras
Mode 1	Non-Haptic	1 Camera	Not Significant (6.6.2.20)	Not Significant (6.6.2.10)	no data
Mode 2	Non-Haptic	2 Cameras	no data	no data	Not Significant (6.6.2.11)
Mode 3	Haptic	1 Camera	no data	no data	Not Significant (6.6.2.21)

Table 6.64: Statistical significance within the mean tool torque data

			Mode 2	Mode 3	Mode 4
			Non-Haptic	Haptic	Haptic
			2 Cameras	1 Camera	2 Cameras
Mode 1	Non-Haptic	1 Camera	Not Significant (6.6.2.22)	Not Significant (6.6.2.12)	no data
Mode 2	Non-Haptic	2 Cameras	no data	no data	Not Significant (6.6.2.13)
Mode 3	Haptic	1 Camera	no data	no data	Not Significant (6.6.2.23)

Table 6.65: Statistical significance within the time for completion data

The results tables show a difference with respect to both the grinding and peg insertion results. Haptic feedback made a significant difference to the mean force applied in the axis of the drill bit with both 1 and 2 camera modes of operation. In contradiction to this, the maximum force level was not altered significantly. In no case did the addition of extra visual feedback create any significant difference in the data. Unlike the peg insertion task, one would not expect that a second camera would create a difference in the performance of the drilling task, and the results show this to be true. Clearly depth of vision is of little importance for tasks such as drilling and grinding. It is expected that tasks that require large amounts of precise motion in three degrees of freedom benefit from additional visual feedback. Similarly, tasks that require large amounts of contact between the manipulator and environment benefit from haptic feedback. These two points clearly do not occur in all cases.

6.6.3 Study B

6.6.3.1 Hypothesis

As with the previous tasks it is hypothesized that operator performance would increase as experience increases. It would also be expected that the learning rate

(rate of performance improvement) would be higher for haptic modes of teleoperation.

6.6.3.2 Participants

The drilling task was performed by two operators. The first operator performed the task ten times for each mode of teleoperation. Due to severe time constraints applied due to using the Schilling manipulator for the research and also the nature of the results from study A, the second operator performed the task ten times with modes 1 (no haptic, one camera) and 3 (haptic, one camera) only. Since study A of the drilling task shows that there were no differences in performance between one and two camera operation, the effect of the second operator only performing modes 1 and 3 is seen as just reducing the results sample size.

As with the peg insertion and grinding studies, both operators were male engineers who had no previous training in teleoperation but were familiar with what teleoperation entails. Both operators were aged between 25 and 50.

6.6.3.3 Statistical Analysis

Least squares regression analysis was performed on the results data in order to test for performance improvements that arise with increased operator experience. MatLab was used to fit a 2nd order least squares linear regression to the maximum z axis force data, maximum tool torque data and the time to completion data. Analysis of variance (ANOVA) with alpha set to 0.05 was used to verify that the chosen model matches the data(Weisberg, 1985). This procedure is documented in appendix H.

6.6.3.4 Results

Figures 6.17 through to 6.22 show regression plots for time to completion, maximum tool torque and maximum z axis force for both haptic and non-haptic modes of teleoperation.

Figure 6.17: 2nd order regression plot for maximum z axis force, modes 1 and 2. Since the observed $F = 0.7727$ is smaller than the critical value $F(0.05; 8, 10) = 3.07$ the fit is accepted.
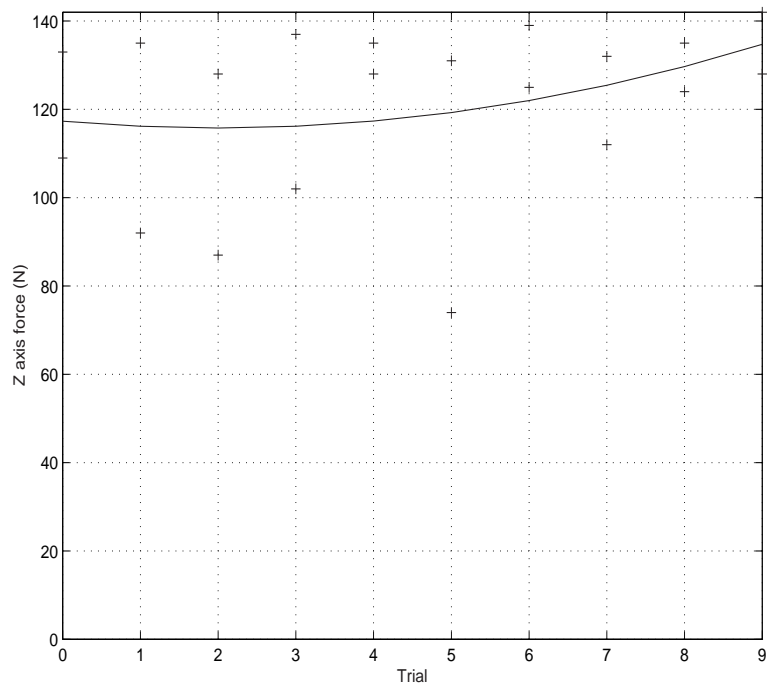
Figure 6.18: 2nd order regression plot for maximum z axis force, modes 3 and 4. Since the observed $F = 0.4053$ is smaller than the critical value $F(0.05; 8, 10) = 3.07$ the fit is accepted.

191
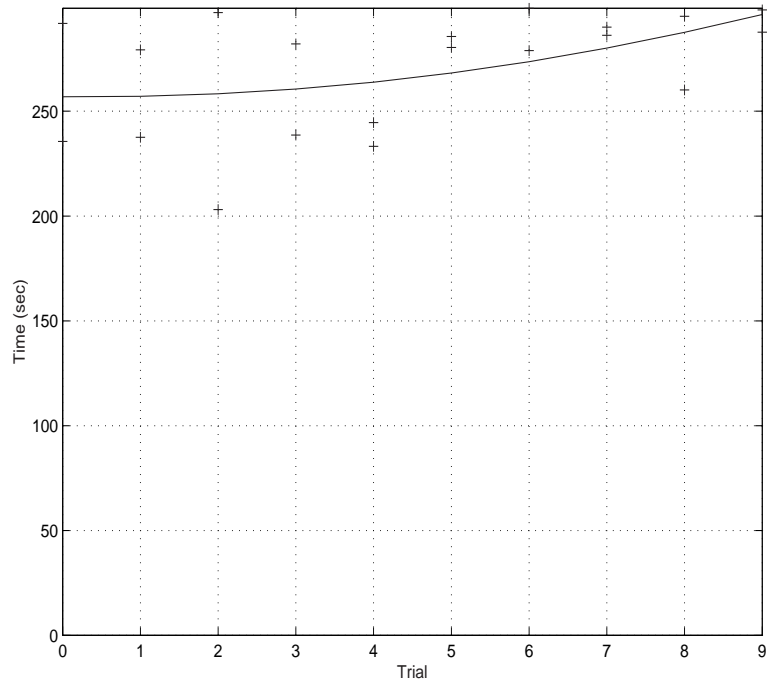
Figure 6.19: 2nd order regression plot for completion time, modes 1 and 2. Since the observed $F = 0.07$ is smaller than the critical value $F(0.05; 8, 10) = 3.07$ the fit is accepted.

Figure 6.20: 2nd order regression plot for completion time, modes 3 and 4. Since the observed $F = 0.1989$ is smaller than the critical value $F(0.05; 8, 10) = 3.07$ the fit is accepted.
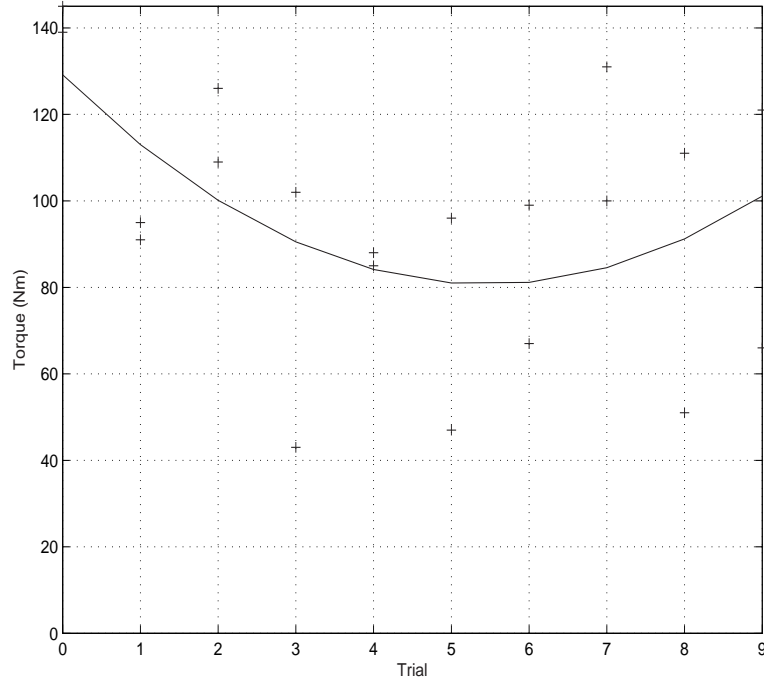
Figure 6.21: 2nd order regression plot for maximum tool torque, modes 1 and 2. Since the observed $F = 1.2829$ is smaller than the critical value $F(0.05; 8, 10) = 3.07$ the fit is accepted.
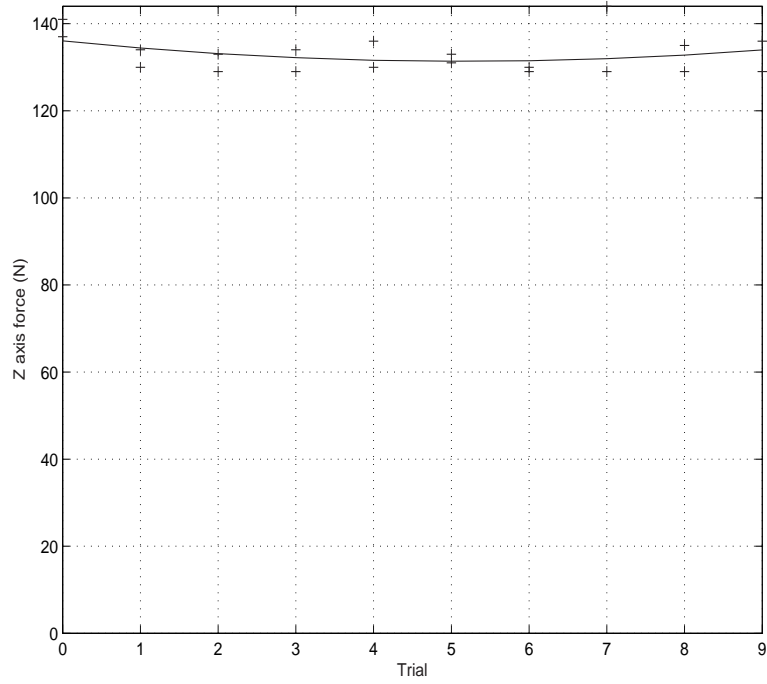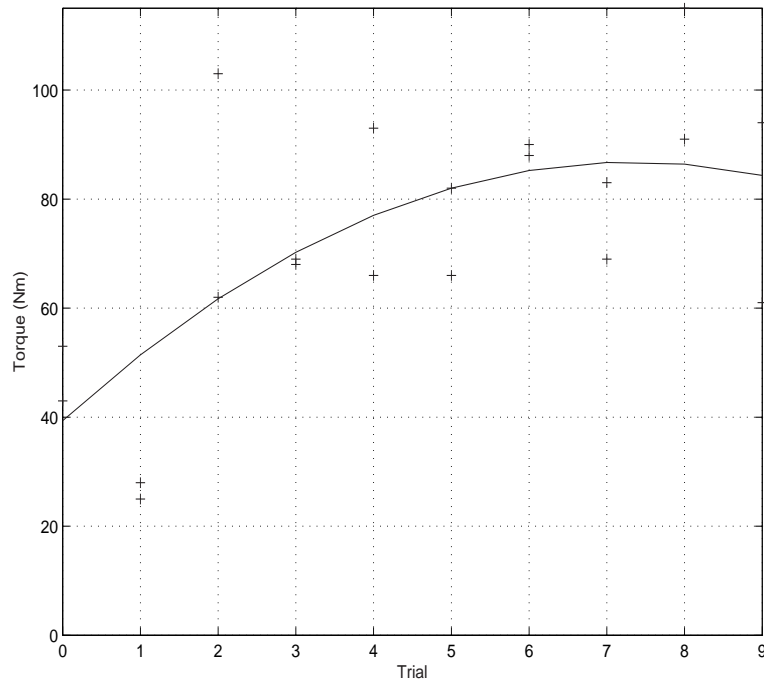

Figure 6.22: 2nd order regression plot for maximum tool torque, modes 3 and 4. Since the observed $F = 2.2228$ is smaller than the critical value $F(0.05; 8, 10) = 3.07$ the fit is accepted.

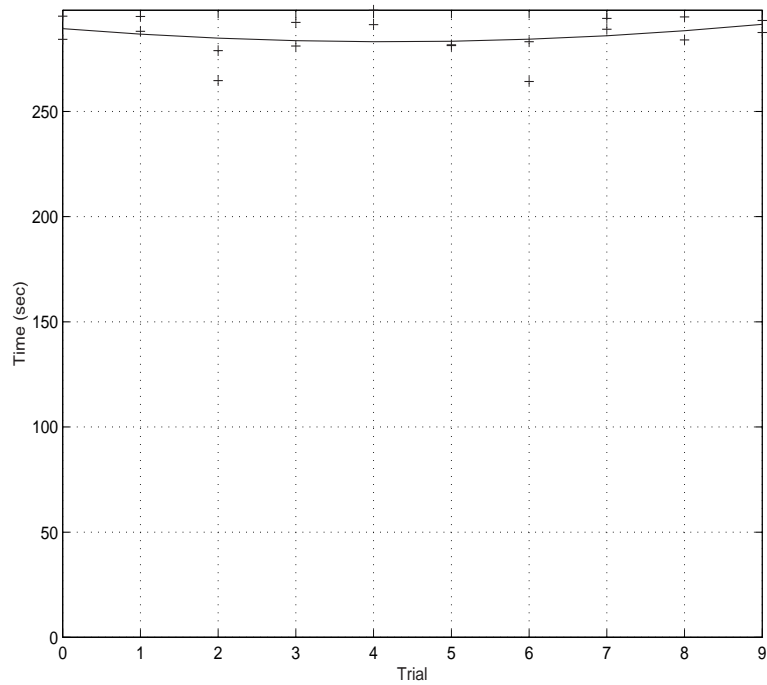Contrary to the hypothesis, the regression plots do not suggest that operator performance improves with increased task experience. The plots of maximum z axis force and time to completion both show relatively steady plots for both haptic and visual only modes of teleoperation. Despite the similarity of the maximum z axis force and time to completion plots for both haptic and visual only, the plot for maximum tool torque showed a different result depending on haptic feedback. The plot for maximum tool torque without haptic shows an initial decrease in the levels of maximum torque and then an increase after the 6th trial. This differs from the plot of maximum torque for the haptic mode where the levels of maximum torque initially increase and then level off towards the end of the trials. Further research is needed in this area if the effects of haptic feedback on operator task learning are to be understood in more depth. Of the three tasks performed, only the peg insertion task has shown evidence of performance improvement with extra operator experience and an increased rate of learning due to haptic feedback. Unlike the peg insertion task, the grinding task showed that haptic feedback had a stabilizing effect on the performance of the operator which should help to eliminate manipulator and tool damage over time. The different results for each task has shown that the effect of haptic feedback and also operator performance is very task specific. Hence one possible area of future research could address task classification in order to provide an understanding of what tasks are similar and thus what type of teleoperation systems and haptic feedback are best suited to performing the task.

Chapter 7

Conclusions

Haptic communication and its effect on operator performance has been evaluated for several differing tasks using both a mobile vehicle and an industrial hydraulic manipulator. For each task, varying modes of teleoperation were developed to allow the comparison of performance with different forms of feedback.

One might expect that haptic feedback would always provide performance improvements. As with the conclusions of other researchers, this has shown to be untrue. (Draper *et al.*, 1999), (Smith, 1998), (Campbell *et al.*, 1999), (McGee, 2000)

Novel haptic teleoperation systems have been developed for both a simulated mobile vehicle and also a real industrial hydraulic manipulator. The mobile vehicle simulation system used Deneb Telegrip (Deneb Robotics Inc., 2003) to generate the visual simulation of a Cybermotion mobile vehicle and its environment. The Telegrip simulation (running on a Silicon Graphics machine) was updated via a serial link from a PC that was also responsible for generating the haptic sensation for the operator via an Immersion Impulse Engine 2000 (Immersion Corp., 2000) haptic interface. Two different novel haptic communication systems were evaluated using a series of operator/task experiments.

Unlike the mobile vehicle research, the research using the manipulator was conducted with real hardware. The Schilling manipulator was controlled via a UK Robotics ATC control system. The ATC system was responsible for interfacing to the manipulator's low level servo controls and providing Cartesian resolved motion. In order to provide three dimensional haptic feedback for the manipulator, a high quality three degree of freedom haptic interface was built specifically for the purposes of the manipulator experiments. Novel haptic communication sensations were then implemented for the three degree of freedom haptic interface in order to provide force and torque feedback for the manipulator tool.

Device characterization was performed on the three degree of freedom interface. The device characterization provided a good evaluation of the performance of the device, which was essential before the device could be used in the research. Prior to the development of the haptic interface, the required performance specification was set. The device characterization showed that the actual performance of the device met the requirements that had been set previously. In addition to ensuring that the new haptic interface was suitable for the research, the device characterization also provided a means of comparing the performance of the device with other haptic interfaces, of both research and commercial origins.

In conclusion, the haptic interface provided performance and robustness that was comparable to other high performance devices. This research has also shown the superiority of the chosen mechanical design over that of the "classical" joystick design that was shown in figure 4.14. A device was built using the "classical" joystick design mechanism, however it was found to be inferior to the chosen mechanism due to high levels of friction.

The mobile vehicle research provided interesting results from the comparisons of performance with the five different modes of operation. Haptic plus visual feedback was shown to decrease the number of collisions that occurred relative to visual feedback alone. However, haptic feedback with semi-autonomous collision avoidance offered no performance improvement over visual only feedback with semi-autonomous collision avoidance. From this one could conclude that there is no point in adding haptic feedback to a system if it has been shown to offer no advantage. However, as discussed previously, in a safety critical environment it may be useful in some circumstances for the operator to be able to override the collision avoidance system. Haptic feedback offers a solution to this where visual feedback cannot. It should also be noted that this work was carried out in simulation, hence the collision avoidance could be tuned for very high performance which may not be possible in a real environment using real sensors. Hence, haptic feedback may prove to offer performance improvements if the semi-autonomous teleoperation system was used to control a real mobile vehicle.

In real hazardous environment teleoperation systems, redundancy is often provided by backup systems that can be used in the event of a primary system failure. Haptic feedback of the vehicle's local environment provides a natural backup to a collision avoidance system. If the collision avoidance system fails or causes problems due to an unusual local environment such as a local minima, haptic feedback can then be used to provide collision avoidance until the problem with the primary system is resolved. Such redundancy would allow the collision avoidance system to

be kept relatively simple and thus hopefully very robust. The collision avoidance system could then be implemented to fail in a very safe manner (such as stopping the vehicle). In this situation, the operator could then take complete control of the vehicle using the haptic feedback system. Clearly, redundancy in the obstacle sensor system is still required since the data that it provides would be shared by both the haptic feedback system and the collision avoidance system.

In conclusion, two novel forms of haptic feedback for remotely operated mobile vehicles have been developed and tested under strict conditions. The environmental haptic feedback system was shown to offer performance improvements over visual feedback alone. In contradiction to this, the behavioural form of haptic feedback that was generated from the collision avoidance system was shown to offer no performance improvements. However, it is suspected that in a non-simulation situation an operator would find the extra feedback beneficial to performing the task.

Further novel forms of haptic feedback were developed for a Schilling hydraulic manipulator that was used to perform peg insertion, grinding and drilling tasks. For the peg insertion task, the haptic feedback focused on providing force feedback in three axes, whereas for the grinding and drilling tasks, contact force and tool torque were provided to the user as a haptic sensation.

The haptic sensation used to convey force information used a novel algorithm that was based on the system that was developed by Salcudean et al (Salcudean *et al.*, 1997). This algorithm proved to be a very intuitive means of providing force information on a velocity input device.

As documented in section 5.5 of chapter 5, a novel approach to providing tool torque feedback to the operator was developed. This involved generating a sinusoidal oscillation on one of the haptic interface's degrees of freedom. Modulation of the frequency and amplitude of the oscillation was used to convey different levels of torque to the operator. This approach to providing the torque information to the operator is clearly very different to haptic feedback systems where the torque at the manipulator tool is displayed to the user as a torque on the joystick axis that is responsible for controlling motion in the axis of the manipulator tool torque. This is an important point to note, since it highlights the fact that the joystick is used for haptic communication rather than direct force feedback.

From the experiments, an overall conclusion was drawn such that haptic feedback provides different performance characteristics depending on the task that is being performed and also on the nature of other forms of feedback, such as visual feedback. This should be an important consideration for future research within

the haptic community.

The results for study A of the peg insertion experiments show that haptic feedback significantly reduced the level of the maximum recorded insertion force, whereas extra visual feedback did not. In contradiction to this, haptic feedback did not provide any performance advantages to the mean force in the z-axis or task completion time. The results also showed that adding an extra camera when there was no haptic feedback did not produce significant improvements. However, adding an extra camera when haptic feedback was present did provide improvements to task completion time and mean force in the z-axis. This is possibly not the result that one would initially expect. One might expect that improving visual feedback would make the task easier for the operator and thus reduce insertion force and task completion times.

Of the three metrics, maximum insertion force is possibly the most important measure of operator performance for this task since if one can keep the maximum force levels low, then damage to tools, manipulator and environment can be eliminated. Based on this fact, haptic feedback provided significant performance improvements by reducing the peak insertion forces, whereas increasing visual feedback did not yield similar results.

It is speculated in section 6.4.2.16 of chapter 6 that, despite the depth of view that a second camera provides, the maximum levels of force are not improved since vision alone is not sufficient to quickly inform the operator that contact with the environment has occurred. Thus, when a slight misalignment between the peg and the hole occurred, a high level of force was applied before the operator had time to react to the fact that the manipulator had stopped moving. In addition, it is also speculated that if the contact with the environment occurred in the small amount of time that the operator was not looking at the manipulator while changing use of cameras, then the addition of a second camera could actually have an adverse effect on the performance of the operator.

In conclusion, it is clear that haptic feedback provided the operators of the peg insertion task with a means of minimizing contact forces, which was not possible with additional visual feedback alone. This is an important finding for the nuclear industry, due to the fact that haptic feedback was provided via a velocity input device rather than a position controlling master/slave system.

As expected, study B of the peg insertion task showed that there was a general trend of performance improvement as operator experience increased. In addition, the rate of improvement of time to completion was higher when haptic feedback was present, which suggests that the addition of haptic feedback has increased

the rate at which operators become familiar and competent with the use of the teleoperation system.

The general conclusion from the peg insertion study is that haptic feedback provided performance improvements where additional visual feedback could not. Clearly, peg insertion is not a task that is performed often within a nuclear decommissioning environment. Despite this, these findings are still important since the skills that are required for good performance of the peg insertion task are common to many remote manipulation tasks.

The results of study A of the grinding task are provided in section 6.5.2.3 of chapter 6. The results showed no performance improvement due to adding the additional visual feedback that a second camera provides. Also, in general, the addition of haptic feedback did not provide any significant operator performance improvement, with the exception of maximum tool torque which was significantly lower when haptic feedback was used. A reduction in the maximum level of tool torque, with no significant increase in time to completion, is considered to be a performance improvement since high levels of torque at the grinding wheel can result in motor stall or possibly even damage to the grinder wheel or motor.

It is speculated that the performance improvements shown by the reduction in maximum tool torque and the lack of improvement in reduction of force suggest that the haptic sensation used to present tool torque was superior to the sensation used to present force. i.e. the torque sensation was effective whilst the force sensation was not.

In the results analysis in section 6.5.2.3 of chapter 6, it is speculated that a perceived contradiction between the haptic feedback and visual feedback was responsible for eliminating the expected performance gains due to haptic feedback. It is believed that the operators erroneously used the size of the spark shower and brightness of the grinder wheel glow as an indication of the level of force that was being applied. Clearly, the visual effects of the grinding task are not correlated to the applied force, hence if the operator uses these prominent visual effects as an indication of the levels of force that are being applied, then he/she will not be able to accurately control and limit the force.

Research has shown that when both visual feedback and haptic feedback provide what is perceived to be the same information, operators are inclined to ignore haptic feedback in favour of the visual feedback (Smith, 1998). Also, other research has shown that when a user is provided with contradicting multimodal feedback, the user tends to ignore one of the feedback channels and thus performance improvements are generally not seen (Campbell *et al.*, 1999)(McGee, 2000).

Further research is necessary in order to make any further conclusions on the use of haptic feedback for the grinding task. Further research could possibly carry out the grinding experimentation in a manner so as to eliminate the shower of sparks. Doing so should allow conclusions to be drawn with respect to the effect of the highly prominent visual feedback due to the shower of sparks and the perceived contradiction in feedback that it produces.

In conclusion, it is believed that the haptic torque feedback was successful in providing performance improvements for the grinding task, whilst the haptic force feedback was not. Multi-modal feedback interaction is speculated as being the primary reason why performance improvements due to haptic force feedback were not seen. This should be an important consideration for future research in this field.

With respect to visual feedback, the conclusions from the drilling research are similar to the conclusions from the grinding research, since no performance improvements were found when the second camera was used. Depth of vision is clearly of little importance for tasks such as drilling and grinding.

In the drilling experimentation, haptic feedback made a significant reduction to the mean force applied in the axis of the drill bit. Despite this, the maximum force level results were not altered significantly. This could be due to the "snagging" action of drilling that can cause sudden motion in the axis of the drill bit which can cause high force and torque values to be recorded that are beyond the control of the operator, regardless of the feedback that is provided.

The varying results for each manipulator task has shown that the effect of haptic feedback and also operator performance is very task specific. Thus, one possible area of future research could address task classification in order to provide an understanding of what tasks are similar and thus what type of teleoperation systems and haptic feedback are best suited to performing the task. For example, haptic feedback may be shown to be of no use to certain task classes but highly beneficial to others.

In addition, it could be concluded that haptic feedback on a velocity control interface does provide performance improvements to tasks that are similar to the peg insertion task, however it does not offer significant performance improvements to power tool tasks such as grinding and drilling. Future research could investigate if haptic feedback on position control interfaces provides performance improvements for grinding and drilling tasks, i.e. it is possible that velocity control is not suitable to control of power tool operation tasks.

Future work is also possible in the area of haptic interface design. Although the

haptic interface that was developed for the manipulator research was shown to be comparable in performance to a high quality commercial device, there are possible areas of improvement that may allow for a broader range of haptic sensations and thus possibly improved haptic communication.

Increased resolution of the position sensing could be achieved by using optical encoders with more steps per revolution. The three degree of freedom haptic interface used encoders with 500 steps per revolution. These units could be replaced with encoders that have 1000 or more steps per revolution. The primary benefit of increasing the resolution of the position resolving would be that higher gains would be possible before instability occurred. This would enable a wider range of haptic sensations, particularly where high gains are required such as in the presentation of sensations such as walls or other hard objects. Such haptic sensations could be further improved by eliminating as much of the backlash/play in the transmission system as possible. High quality planetary gearheads were used between the motors and manipulandum of the haptic interface. Although the small amount of backlash in the gearheads was deemed not to have a noticeably adverse effect on the haptic sensation, it clearly will have an effect on the force bandwidth and maximum achievable stiffness of the manipulandum. Such backlash could be reduced by a high torque direct drive system or possibly with use of an opposing actuation system where two motor/gearhead assemblies are used on the same axis.

Another possible improvement would be to increase the maximum torque that can be generated on each of the axes of the interface. While the maximum levels of torque that were achievable by the interface were shown to be comparable to other similarly sized haptic interfaces, an improvement could possibly allow for a broader range of sensations. Clearly such an increase would require changes to the design of the interface mechanics in order to cope with the extra stresses.

In addition to haptic interface design improvements, future work could also focus on building upon the haptic communication algorithms that were developed and evaluated in this research. As previously concluded, novel haptic communication algorithms were developed for both the mobile and manipulator teleoperation systems. In conclusion upon the evaluation of these haptic communication systems, it was noted that the expected performance gains due to the addition of the haptic feedback were not always seen. Thus, a possible area of future work would be to develop and evaluate new haptic communication algorithms that could possibly offer performance improvements.

Research into the suitability of haptic interfaces for other teleoperation tasks would be a valuable focus for future work. Tasks such as the following could be

evaluated:

- Turning valves on and off in sub sea environments

- Turning bolts and screw fittings

- Cutting tasks

- Fixing push and twist and force fittings

- Crimping

- Soldering.

Conclusions on the mobile vehicle research noted that different results may be found if the experiments were performed with a real mobile vehicle rather than in simulation. Hence, future work could possibly repeat or extend the mobile vehicle experiments with a real mobile vehicle in a real environment. Such research could possibly reveal the effect of real proximity sensors on the generation of the haptic feedback and also draw conclusions on how haptic feedback can be used to complement autonomous collision avoidance systems.

Although experimentation with real hardware as opposed to simulated systems has the potential to offer a better insight into the area of research, there are often far more project overheads that have to be dealt with which can make tasks far more time consuming and detract from the focus of the research. This is especially the case with research that involves hazardous procedures. Due to the fact that the manipulator research was performed with a large hydraulic manipulator performing tasks using high power grinding and drilling tools, risk assessments were a requirement and all work was carried out under a permit to work system. This was a necessary project overhead, which, in addition to construction of clamps to hold experiment apparatus, experiment startup and stop procedures and general manipulator cell maintenance added considerable time to the procedure of conducting the manipulator experimentation. Extra time constraints were introduced by the fact that the manipulator was being used for commercial development in tandem with this research. This severely limited the total time available for research involving the manipulator, which limited the total number of experiments that were possible. Given more time, it would have been possible to perform study A and B of the peg, grinding and drilling tasks with a larger population. Doing so may enable a better understanding of the effect of haptic feedback on both performance and operator familiarization.

References

Adelstein, B. D. 1989. *A virtual environment system for the study of human arm tremor.* Ph.D. thesis, MIT.

Akamatsu, M., & MacKenzie, L. S. 1996. Movement characteristics using a mouse with tactile and force feedback. *International journal of human computer studies*, **45**, 483–493.

Akamatsu, M., & Sato, S. 1994. A multi-modal mouse with tactile and force feedback. *International journal of human computer studies*, **40**, 443–453.

Arkin, R. C. 1989. Motor schema-based mobile robot navigation. *International journal of robotics research*, **8**(4), 92–112.

Ayache, N., Cotin, S., & Delingette, H. 1997. Surgery simulation with visual and haptic feedback. *Pages 311–316 of: Robotics research, the 8th international symposium.*

Barnes, D. P. 1996. *Advanced robotics and intelligent machines.* IEE Control Engineering Series 51. Chap. 19, pages 295–314.

Barnes, D. P., & Counsell, M. S. 1998. *Haptic communication for telerobotic applications.* Presented at "Advanced Robotics: Beyond 2000. The 29th International Symposium on Robotics (ISR98)", Birmingham, UK.

Barnes, D. P., & Counsell, M. S. 1999. Haptic communication for remote mobile manipulator robot operations. *In: American nuclear society, 8th international topical meeting on robotics and remote systems (proc. on cdrom, session 15: Human machine interfaces, isbn 0-89448-647-0).*

Barnes, D. P., Ghanea-Hercock, R. A., Aylett, R. S., & Coddington, A. M. 1997. Many hands make light work? an investigation into behaviourally controlled co-operant autonomous mobile robots. *Pages 413–420 of: International conference on, autonomous agents.*

Basavaraj, U., & Duffy, J. 1993. End-effector motion capabilities of serial manipulators. *The international journal of robotics research*, **12**(2), 132–145.

Bergamasco, M., & Prisco, G. 1997. Design of an anthropomorphic haptic interface for the human arm. *In: Robotics research, the 8th international symposium.*

Bevan, N. R., Burrows, M. S., Pattinson, A., Bamforth, C., & Schilling, R. 1996. Integration of a manipulator system with a mobile vehicle to perform multiple tasks in a hazardous environment. *Pages 242–248 of: Remote techniques for hazardous environments.*

Brewster, S., Masters, M. M., Glendye, A., Kriz, N., & Reid, S. 1998. Haptic feedback in the training of veterinary students. *In: First international workshop on usability evaluation for virtual environments.*

Brokk AB. 2003 (Jan). http://www.brokk.com/.

Brooks, R. A. 1986. A robust layered control system for a mobile robot. *Robotics and automation*, **RA-2**, 14–23.

Brooks Jr., F. P., Ouh-Young, M., Batter, J. J., & Jerome, P. 1990. Project grope - haptic displays for scientific visualisation. *Computer graphics*, **24**(4), 177–185.

Brown, J. M. 1995. *A theoretical and experimental investigation into the factors affecting the z-width of a haptic display.* M.Phil. thesis, Northwestern University.

Burdea, G., Langrana, N., Roskos, E., Silver, D., & Zhuang, J. 1992. A portable dextrous master with force feedback. *Presence: Teleoperators and virtual environments*, **1**(1), 18–28.

Burdea, G., Richard, P., & Coiffet, P. 1996. Multi-modal virtual reality: Input/output devices, system integration and human factors. *International journal of human-computer interaction (IJHCI), special issue on human-virtual environment interaction*, **8**(1), 5–24.

Burdea, G., Deshpande, S., Popescu, V., Langrana, N., Gomez, D., DiPaola, D., & Kanter, M. 1997a. Computerised hand diagnostic/rehabilitation system using a force feedback glove. *In: Medicine meets virtual reality.*

Burdea, G., Deshpande, S., Liu, B., Langrana, N., & Gomez, D. 1997b. A virtual reality-based system for hand diagnosis and rehabilitation. *Presence: Teleoperators and virtual environments*, **6**(2), 229–240.

Burdea, G. C. 1996. *Virtual reality and robotics in medicine.* Based in part on the tutorial "Virtual Reality and Robotics in Medicine" presented at the 1996 Robotics and Automation Conference, Minneapolis, MN.

Burdea, G. C. 1997. Virtual reality and medicine: Technology and applications. *In: Industrial virtual reality.*

Buttolo, P., & Hannaford, B. 1995. Pen-based force display for precision manipulation in virtual environments. *Pages 217–224 of: Virtual reality annual international symposium.*

Caldwell, D. G., Favede, C., & Tsagarakis, N. 1998. Dextrous exploration of a virtual world for improved prototyping. *Pages 298–303 of: International conference on robotics and automation.*

Campbell, C. S., Khai, S., May, K. W., & Maglio, Paul. P. 1999. What you feel must be what you see: Adding tactile feedback to the trackpoint. *Pages 383–390 of: Human-computer interaction, INTERACT 99.*

Colgate, J. E., & Brown, J. M. 1994. Factors affecting the z-width of a haptic display. *Pages 3205–3210 of: International conference on robotics and automation.*

Colgate, J. E., & Schenkel, G. 1994. Passivity of a class of sampled-data systems: Application to haptic interfaces. *Pages 3236–3240 of: American control conference.*

Counsell, M. S., & Barnes, D. P. 1999. Haptic communication for manipulator tooling operations in hazardous environments. *Pages 222–233 of: Telemanipulator and telepresence technologies vi*, vol. 3840.

Craig, J. J. 1986. *Introduction to robotics, mechanics and control.* Addison-Wesley Publishing Company.

Crossan, A., Brewster, S., Reid, S., & Mellor, D. 2000. Multimodal feedback cues to aid veterinary training simulations. *Pages 45–49 of: 1st workshop on haptic human-computer interaction.*

Cybernet Systems. 2000 (Dec). http://www.cybernet.com/.

Daniel, R. W., & McAree, P. R. 1998. Fundamental limits of performance for force reflecting teleoperation. *The international journal of robotics research*, **17**(8), 811–830.

Daniel, R. W., Fischer, P. J., & Hunter, B. 1993. A high performance parallel input device. *Pages 272–281 of: Telemanipulator technology and space telerobotics*, vol. 2057.

Dede, C., Salzman, M., Loftin, R. B., Calhoun, C., Hoblit, J., & Regian, J. W. 1994. The design of artificial realities to improve learning newtonian mechanics. *Pages 34–41 of: East-west international conference on multimedia, hypermedia, and virtual reality.*

Deneb Robotics Inc. 2003 (Jan). http://www.deneb.com/.

Deo, A., & Walker, I. 1997. Minimum effort inverse kinematics for redundant manipulators. *IEEE transactions on robotics and automation*, **13**(5), 767–775.

Dinsmore, M., Langrana, N., Burdea, G., & Ladeji, J. 1997. Virtual reality training simulation for palpation of subsurface tumors. *Pages 54–60 of: Virtual reality annual international symposium (VRAIS 97).*

Draper, J. V., Wrisberg, C. A., Blair, L. M., & Omori, E. 1988. Measuring operator skill and teleoperator performance. *Pages 277–290 of: International symposium on teleoperation and control.*

Draper, J. V., Jarad, B. C., & Noakes, M. W. 1999. Manipulator performance evaluation using fitts' tapping task. *In: 8th topical meeting on robotics and remote systems.*

Ellis, R. E., Ismaeil, O. E., & Lipsett, M. G. 1996. Design and evaluation of a high-performance haptic interface. *Pages 321–327 of: Robotica*, vol. 4.

Fischer, P., Daniel, R., & Siva, K. V. 1992. Specification and design of input devices for teleoperation. *Pages 540–545 of: International conference on robotics and automation.*

Fitts, P. M. 1954. The information capacity of the human motor system in controlling the amplitude of movement. *Journal of experimental psychology*, **47**(6), 381–391.

Fitts, P. M., & Posner, M. I. 1973. *Human performance.* Basic Concepts in Psychology Series, Prentice/Hall International, Inc.

Flatau, C. R. 1965. Development of servo manipulators for high energy accelerator requirements. *Pages 29–35 of: 13th conf. on remote systems technology.*

Flatau, C. R. 1973. The manipulator as a means of extending our dextrous capabilities to larger and smaller scales. *Pages 47–50 of: 21st conference on remote systems technology.*

Flatau, C. R. 1977. Sm-229 - a new compact servo master-slave manipulator. *Pages 169–173 of: 25th conference on remote systems technology.*

Flatau, C. R., Vertut, J, Guilbaud, J, Jgermond, & Glachet, C. 1972. Ma22-a compact bilateral servo master-slave manipulator. *Pages 296–302 of: 20th conference on remote systems technology.*

Freund, E., & Pesara, J. 1998. High-bandwidth force and impedance control for industrial robots. *Robotica*, **16**, 57–87.

Glass, K., Colbaught, R, Lim, D., & Seraji, H. 1993. Real-time collision avoidance for redundant manipulators. *In: IEEE international conferance on robotics and automation.*

Goertz, R. 1964. Manipulator systems development at anl. *Pages 117–136 of: 12th conference on remote systems technology.*

Goertz, R. C. 1952. Fundamental of general-purpose remote manipulators. *Nucleonics*, Nov, 36–45.

Goertz, R. C. 1954. Electronically controlled manipulator. *Nucleonics*, Nov, 46–47.

Goertz, R. C., Blomgren, R. A., Grimson, J. H., Forster, G. A., Thompson, W. M., & Kline, W. H. 1961. The anl model 3 master-slave electric manipulator - it's design and use in a cave. *Pages 121–142 of: The 9th conference on hot labour equipment.*

Gosselin, C., & Angeles, J. 1991. A global performance index for the kinematic optimization of robotic manipulators. *ASME Journal of mechanical design*, **113**(3), 220–226.

Gottlieb, I. M. 1994. *Electric motors and control techniques.* TAB Books, a division of McGraw-Hill Inc.

Hamel, W. R., & Feldman, M. J. 1984. The advancement of remote systems technology: Past perspectives and future plans. *Pages 11–24 of: National topical meeting on robotics and remote handling in hostile environments.*

Hannaford, B., Wood, L., McAffee, D. A., & Zak, H. 1991. Performance evaluation of a six axis generalized force reflecting teleoperator. *IEEE transactions on systems, man, and cybernetics*, **21**(3), 620–633.

Haptic Technologies Inc. MouseCAT(TM). 2000 (Dec). http://www.haptech.com/.

Hill, J. W. 1977. Two measures of performance in a peg-in-hole manipulation task with force feedback. *Pages 301–309 of: 13th annual conference on manual control.*

Hockey, R. 1984. *Stress and fatigue in human performance.* John Wiley and Sons.

Hopper, D., Boddy, C., & Reilly, D. 1996. Advanced teleoperation testbed- a system you can see through. *Robotica*, **14**(4), 457–461.

Howe, R. D. 1992. A force-reflecting teleoperated hand system for the study of tactile sensing in precision manipulation. *Pages 1321–1326 of: International conference on robotics and automation.*

Howe, R. D., & Kontarinis, D. 1992. Task performance with a dextrous teleoperated hand system. *Pages 199–207 of: Telemanipulator technology*, vol. 1833.

Immersion Corp. 2000 (Dec). http://www.immerse.com/.

Jacobsen, S. C., Iverson, E. K., Davies, C. C., Potter, D. M., & McLain, T. W. 1989. Design of a multiple degree of freedom, force reflective hand master/slave with a high mobility wrist. *In: Third topical meeting on robotics and remote systems.*

Jones, L. A., & Hunter, I. W. 1990. Influence of the mechanical properties of a manipulandum on human operator dynamics. *Biological cybernetics*, **62**, 299–307.

Kenzo, T. 1996. *Electric motors and their controls.* Oxford Science Publications.

Khatib, O. 1986. Real-time obstacle avoidance for manipulators and mobile robots. *International journal of robotics research*, **5**(1), 90–98.

Khatib, O. 1987. A unified approach for motion and force control of robot manipulators: The operational space formulation. *IEEE journal of robotics and automation*, **RA-3**(1), 43–53.

Kim, W. S., Tendick, F., Ellis, S. R., & Stark, L. W. 1987. A comparison of position and rate control for telemanipulators with consideration of manipulator system dynamics. *IEEE journal of robotics and automation*, **RA-3**(5), 426–436.

Kirk, R. E. 1999. *Statistics, an introduction*. Harcourt Brace College Publishers.

Lawrence, P. D., Salcudean, S. E., Sepehri, N., Chan, D., Bachmann, S., Parker, N., Zhu, M., & Frenette, R. 1995. Coordinated and force-feedback control of hydraulic excavators. *Pages 181–194 of: Fourth international symposium on experimental robotics*.

Liu, A., & Chang, S. 1995. Force feedback in a stationary driving simulator. *Pages 1711–1716 of: Proceedings of the ieee international conference on systems, man and cybernetics*, vol. 2.

Liu, A., Tharp, G., Hirose, M., & Stark, L. 1991. Visual factors affecting human operator performance with a head-mounted display. *SAE society of automotive engineers*.

Liu, A., Tharp, G., French, L., Lai, S., & Stark, L. 1993. Some of what one needs to know about using head-mounted displays to improve teleoperator performance. *IEEE transactions on robotics and automation*, **9**, 638–648.

MacKenzie, S. 1992. Fitts' law as a research and design tool in human-computer interaction. *Human-computer interaction*, **7**, 91–139.

Maekawa, H., & Hollerbach, J. M. 1998. Haptic display for object grasping and manipulation in virtual environment. *Pages 2566–2573 of: IEEE international conference on robotics and automation*.

Massie, T. H., & Salisbury, J. K. 1994. The phantom haptic interface: A device for probing virtual objects. *Pages 295–302 of: International mechanical engineering expositions and congress*.

Massimino, M. J., & Sheriden, T. B. 1994. Teleoperator performance with varying force and visual feedback. *Human factors*, **36**(1), 145–157.

McGee, M. R. 1999. A haptically enhanced scrollbar: Force-feedback as a means of reducing the problems associated with scrolling. *In: First phantom users research symposium.*

McGee, M. R. 2000. The effective combinations of haptic and audio textural information. *Pages 33–38 of: Haptics in HCI workshop.*

McKinnon, M., & King, M. 1988. Manual control of telemanipulators. *Pages 263–276 of: International symposium on teleoperation and control.*

Microsoft SideWinder Force Feedback Pro. 2002 (Dec). http://www.microsoft.com/.

Nahvi, A., Nelson, D. D., Hollerbach, J. M., & Johnson, D. E. 1998. Haptic manipulation of virtual mechanisms from mechanical cad designs. *Pages 375–380 of: International conference on robotics and automation.*

Nakamura, A., & Hanafusa, H. 1986. Inverse kinematics solutions with singularity robustness for robot manipulator control. *ASME journal of dynamic systems, measurement, and control*, **108**, 163–171.

Nakamura, K., Eto, K., Mori, Y., Matsumura, S., & Kusama, E. 1989. Power steering system with travelling condition judgement function. *SAE society of automotive engineers*, 1512–1518.

Nakamura, Y. 1991. *Advanced robotics redundancy and optimization.* Addison-Wesley Publishing Company, Inc.

Oakley, I. 1999. Comparing haptic effects in a gui. *In: First phantom users research symposium.*

Oakley, I., McGee, M. R., Brewster, S., & Grey, P. 2000. Putting the feel in 'look and feel'. *Pages 415–422 of: Chi 2000.* ACM Press, Addison-Wesley.

Ostoja-Starzewski, M., & Skibniewski, M. 1989. A master-slave manipulator for excavation and construction tasks. *Pages 333–337 of: Robotics and autonomous systems 4.*

Ouh-young, M., Beard, D. V., & Brooks Jr., F. P. 1989. Force display performs better than visual display in a simple 6-d docking task. *Pages 1462–1466 of: International conference on robotics and automation.*

Oxford-Dictionary. 1999. Oxford University Press. Page 648.

Paredis, C. 1993. Kinematic design of serial link manipulators from task specifications. *The international journal of robotics research*, **12**(2), 274–287.

Parker, N. R., Salcudean, S. E., & Lawrence, P. D. 1993. Application of force feedback to heavy duty hydraulic machines. *Pages 375–381 of: Robotics and automation conference.*

Repperger, D. W., Remis, S. J., & Merrill, G. 1990. Performance measures of teleoperation using an exoskeleton device. *Pages 552–557 of: International conference on robotics and automation.*

Rock, I., & Victor, J. 1964. Vision and touch: an experimentally created conflict between the two senses. *Science*, **143**, 594–596.

Ruspini, D., & Khatib, O. 1998. Dynamic models for haptic rendering systems. *Pages 523–532 of: Advances in robot kinematics, ark98.*

Ruspini, D., Kolarov, K., & Khatib, O. 1997a. The haptic display of complex graphical environments. *Pages 345–352 of: Computer graphics.*

Ruspini, D., Kolarov, K., & Khatib, O. 1997b. Haptic interaction in virtual environments. *Pages 128–133 of: International conference on intelligent robots and systems, IROS'97.*

Ryu, J., & Kim, H. 1999. Virtual environment for developing electronic power steering and steer-by-wire systerns. *Pages 1374–1379 of: Proceedings of the ieee/rsj international conference on intelligent robots and systems.*

Salcudean, S. E., Tafazoli, S., Hashtrudi-Zaad, K., & Lawrence, P. D. 1997. Evaluation of impedance and teleoperation control of a hydraulic mini-excavator. *Pages 187–198 of: Experimental robotics v: The fifth international symposium.*

Schmelz, F., Seherr-Thoss, H., & Aucktor, E. 1992. *Universal joints and drive-shafts, analysis, design, applications.* Springer Verlag.

Schumann, J. 1993. *On the use of discrete proprioceptive-tactile warning signals during manual control - the steering wheel as an active control device.* Ph.D. thesis, Universitat der Bundeswehr Mnchen.

Sensable Technologies. 2000 (Dec). http://www.sensable.com/.

Seraji, H., & Bon, B. 1999. Real-time collision avoidance for position-controlled manipulators. *IEEE transactions on robotics and automation*, **15**(4), 670–677.

Setlur, P., Dawson, D., Chen, J., & Wagner, J. 2002. A nonlinear tracking controller for a haptic interface steer-by-wire systems. *Pages 3112–3117 of: Proceedings of the 41st ieee conference on decision and control.*

Shinohara, Y., Usui, H., Saito, S., Kumagai, A., & Fujii, Y. 1984. Experimental remote handling systems. *Pages 117–121 of: National topical meeting on robotics and remote handling in hostile environments.*

Siva, K. V., Dumbreck, A. A., Fischer, P. J., & Abel, E. 1988. Development of a general purpose hand controller for advanced teleoperation. *Pages 277–290 of: International symposium on teleoperation and control.*

Smith, M. 1998. *Human factors in haptic interfaces.* An ACM Electronic Publication, http://www.acm.org/crossroads/xrds3-3/haptic.html.

Stredney, D., Sessanna, D., McDonald, J., Hemenze, L., & Rosenburg, L. 1996. A virtual simulation environment for learning epidural anaesthesia. *Medicine meets virtual reality iv: Health care in the information age*, 164–175.

Taylor, P. M., & Milella, F. 1997. A study of operator-induced instabilities in a tactual virtual environment. *Pages 1027–1032 of: The 8th international conference on advanced robotics, ICAR'97.*

UK Robotics Ltd. 2003 (Feb). (now RTS Advanced Robotics Ltd) http://www.rts-group.com/.

Vertut, J. 1964. Through-the-wall master-slave manipulator with indexing for forward and backward movement. *Pages 67–72 of: 12th conference on remote systems technology.*

Vertut, J., Marchal, P., Debrie, G., Petit, M., Francois, D., & Coiffet, P. 1976. The ma23 bilateral servomanipulator system. *Pages 175–187 of: 24th conference on remote systems technology.*

Virtual Technologies Inc. CyberGrasp(TM). 2000 (Dec). http://www.virtex.com/.

Wallersteiner, U., Sager, P., & Lawrence, P. 1988. A human factors evaluation of teleoperation hand controllers. *Pages 291–296 of: Proceedings of the international symposium on teleoperation and control.*

Weisberg, S. 1985. *Applied linear regression.* Wiley. Chap. 4, pages 89–91.

Welch, R. B., & Warren, D. H. 1980. Immediate perceptual response to intersensory discrepancy. *Psychological bulletin*, **88**(3), 638–667.

Whitney, D. 1969. Resolved motion rate control of manipulators and human prostheses. *IEEE transactions on man-machine systems*, **MMS-10**(2), 47–52.

Whitney, D. 1987. Historical perspective and state of the art in robot force control. *The international journal of robotic research*, **6**(1).

Wilhelmsen, K. C. 1997. Tele-robotic/autonomous control using controlshell. *In: 7th topical meeting on robotics and remote systems.*

Yerkes, R. M., & Dodson, J. D. 1908. The relation of strength of stimulus to rapidity of habit-formation. *Journal of comparative neurology and psychology*, **18**, 459–482.

Yu, W., Ramloll, R., & Brewster, S. 2000. Haptic graphs for blind computer users. *Pages 102–107 of: 1st workshop on haptic human-computer interaction.*

Zhu, M., & Salcudean, S. E. 1995. Achieving transparency for teleoperator systems under position and rate control. *Pages 7–12 of: International conference on intelligent robots and systems (IROS'95).*

Appendix A

Maxon product data

Product code	114472
Axial play	max. 0.47mm
Radial play 5mm from flange	0.28mm
Ave backlash no load per stage	less than 1.3 degrees
Num of stages	2
Mass inertia	$1.87 - 1.687 gcm^2$
Bearing at output	ball bearing
Reduction	28:1
Max continuous torque	2.25 Nm

Table A.1: Maxon 32mm Planetary Gearhead Technical Data

Product code	110511
Supply voltage	5V +- 10%
Output signal	TTL compatible
Num of channels	2 plus 1 index
Counts per turn	500
Phase shift nominal	90degrees e
Logical state width s	min. 45degrees e
Signal rise time	180ns
Signal fall time	40ns
Moment of inertia of code wheel	$0.6gcm^2$
Pin 1	Gnd
Pin 2	Channel I
Pin 3	Channel A
Pin 4	Vcc
Pin 5	Channel B

Table A.2: Maxon (HP) HEDS55 500 Step Digital Encoder Technical Data

Product code	118743
Power rating	10W
Nominal voltage	12V
No load speed	4860RPM
Stall torque	132mNm
Max. continuous current	1.26A
Max. continuous torque	29.61mNm
Max. power output at nominal voltage	16800mW
Max. efficiency	86.3%
Rotor inertia	$10.6gcm^2$

Table A.3: Maxon RE25 10W Technical Data

Appendix B

Altera JTAG port to PC parallel port buffer

ByteBlaster Parallel Port Download Cable Data Sheet

Figure 2 shows a schematic of the ByteBlaster download cable.

Figure 2. ByteBlaster Schematic

Note:
(1) All resistors are 33 Ω.

The 10-pin female plug connects to a 10-pin male header on the circuit board containing the target device(s). Figure 3 shows the dimensions of the female plug.
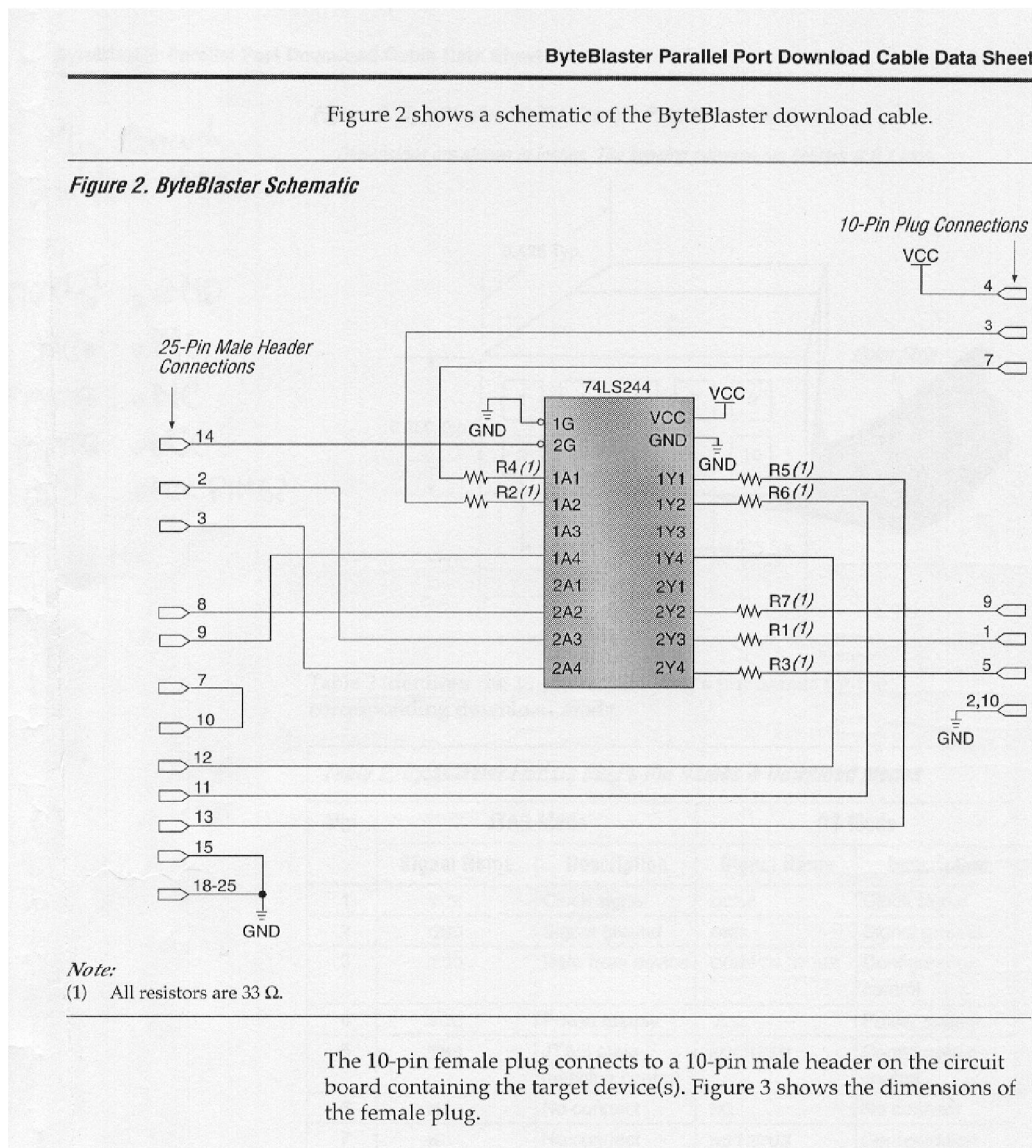
Appendix C

Schematic for the RS strain gauge. Taken from data sheet 232-5975

Basic circuit for printed circuit board **RS** stock no. 435-692 (gain approx. 1000)
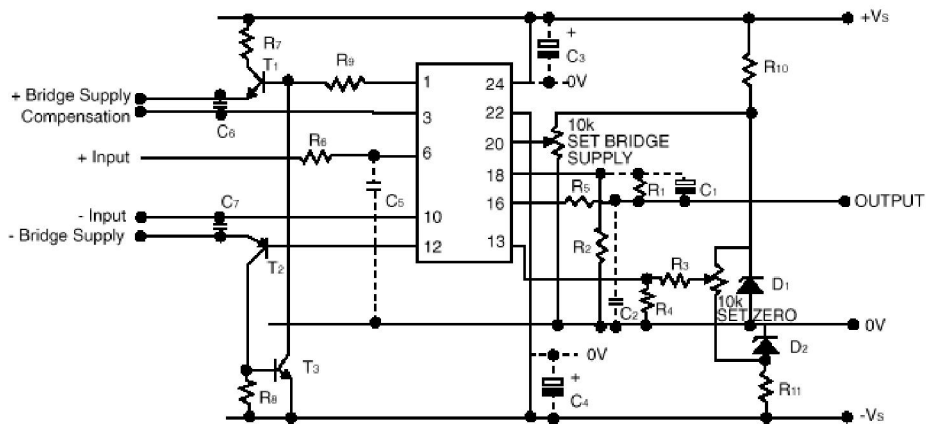
Appendix D

Single Degree of Freedom Prototype Haptic Joystick Development

This appendix documents the development of the prototype single degree of freedom haptic interface that was built as a proof of concept. This research lead to the development of the final three degrees of freedom haptic interface that was used in the manipulator research. The mechanical design of the prototype device was essentially a manipulandum attached to a source of actuation as shown in figure D.1.
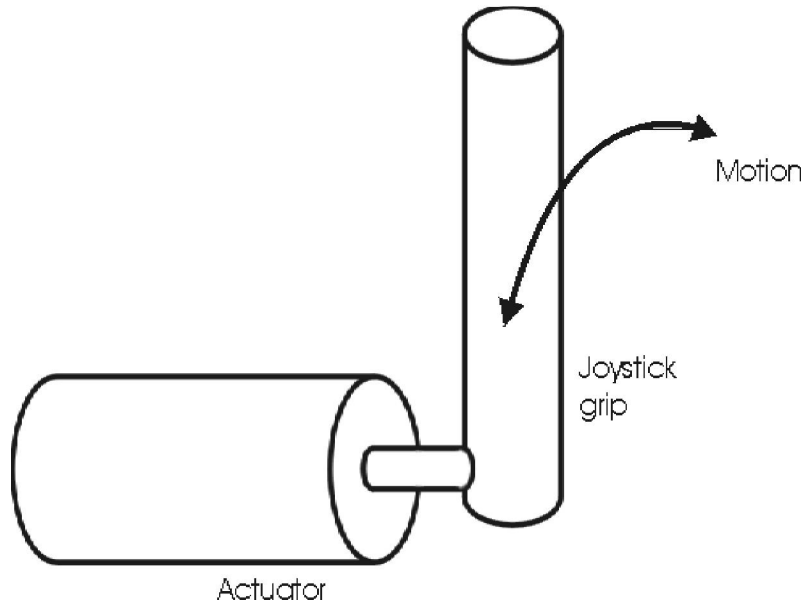
Figure D.1: Mechanical design of the prototype single degree of freedom haptic device

This appendix provides only a low level of information on the prototype interface development. In the interest of avoiding repetition most of the design decisions are not covered in this appendix since they are covered in great detail within section 4.2 of chapter 4.

D.1 Actuator Choice

Electrical actuation via a high quality DC motor was chosen for the source of actuation. The chosen motor was a 10 Watt Maxon RE25 device. Table D.1 shows the specification of the motor.

Product code	118743
Nominal voltage	12V
Max. continuous current	1.26A
Max. continuous torque	29.61mNm

Table D.1: Maxon RE25 10W Technical Data

D.2 Torque Transmission Factors

The choice of a torque transmission system for a haptic interface is considerably complex due to the number of opposing design factors that must be considered. These considerations are discussed in detail in section 4.2.3 of chapter 4. Several torque transmissions systems were evaluated for the prototype device. The chosen device was a Maxon 32mm Planetary Gearhead. This gearhead is designed for the chosen Maxon motor and hence simplifies the mechanical design of the device.

Table D.2 shows the specification of the gearhead.

Product code	114472
Reduction	28:1
Number of stages	2
Backlash	<2.6 degrees
Max continuous torque	2.25 Nm

Table D.2: Maxon 32mm Planetary Gearhead Technical Data

D.3 Motor Control

Torque control for DC motors can be achieved by two very different principles.

- Pulse Width Modulation

- Linear Amplification

Pulse Width Modulation (PWM) was chosen for the prototype device since it requires no digital to analogue conversion and is also generally more efficient than the linear amplifier approach. The PWM was generated with a Motorola 68HC11 microcontroller.

D.4 Pulse Width Modulation Generation

A Motorola 68HC11 microcontroller was chosen to provide the motor control. The 68HC11 device is a very popular 8 bit microcontroller that uses the enhanced

M6800/M6801 instruction set. The microcontroller controls the torque of the motor via the PWM signal and the direction of the motor via a H-bridge amplifier circuit.

D.5   Motorola 68HC11 software

Software for the 68HC11 is written in assembly language and then assembled on a PC. The program is then downloaded to the microcontroller via the serial communications interface. Initial prototype software was written that read a signed byte from one of the input ports on the device and then converted it to PWM. Different PWM modulation frequencies were tested to evaluate the highest frequency that could be felt as an oscillation via the hand and finger tips. PWM modulation frequencies in the range of 500Hz to 1KHz were found to be the highest frequencies that could cause palpable oscillations. The chosen modulation frequency was 8Khz. This was the maximum frequency that was achievable using the 68HC11 microcontroller.

D.6   Position Resolving

A 500 step Hewlett Packard encoder as shown in appendix A was chosen to perform the position resolving for the prototype device. This device couples directly to the chosen motor and thus allows for simple device construction.

D.7   Encoder Handling

Initially the encoder was handled by the microcontroller in software. The two channels from the encoder were connected to interrupt input pins on the microcontroller and the software incremented or decremented an internal counter. This worked at slow speeds, but despite optimising the interrupt service routines with respect to execution time, the microcontroller was not fast enough to deal with high speed rotations of the encoder which can produce cycle rates in excess of 30KHz. Thus, this approach was discarded in favour of a hardware encoder handler. This was developed comprising of discrete logic chips. Figure D.2 shows the schematic for the hardware encoder handler.
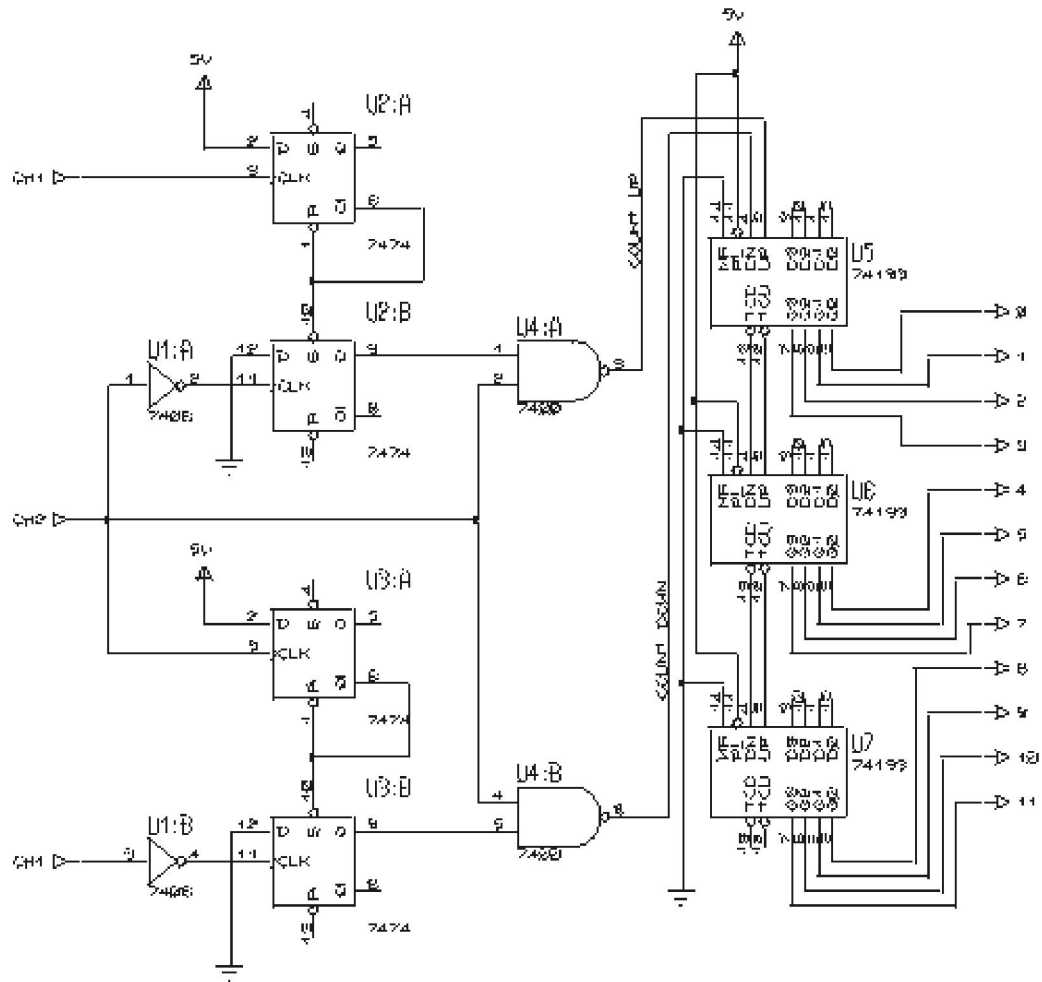
Figure D.2: Schematic showing prototype encoder handler hardware

D.8 PC Interface

The PC interface to the hardware is a critical part of the design since the PC is within the control loop of the haptic interface and must be able to perform control and communications in real time. Due to the high data rate requirements and the real time nature of the system, an RS232 serial interface would not be suitable. Hence an ISA bus interface was developed that allowed the PC to read the encoder position and control the torque of the motor at the required rate. The ISA card used the 8 bit ISA XT bus. The card was produced using discrete logic chips mounted on stripboard for speed of prototyping and low cost. In addition to the ISA bus interface hardware, the encoding handler as shown in figure D.2 was also mounted on the ISA card. Figure D.3 shows the prototype ISA card.
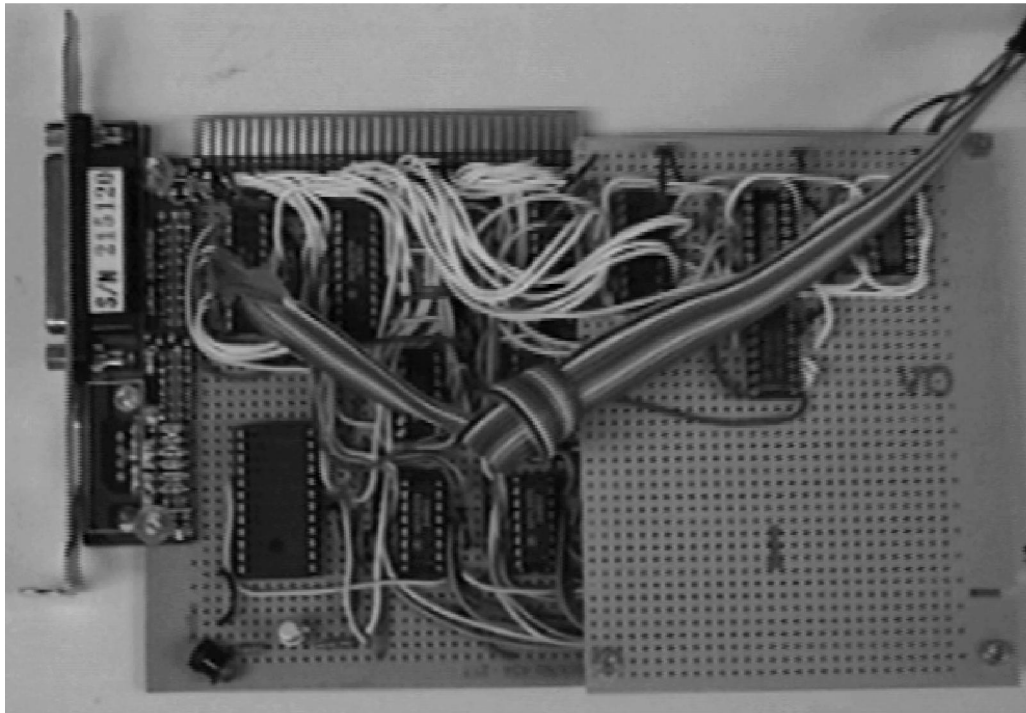

Figure D.3: The prototype ISA card

The PC writes the 8 bit force command to the 68HC11 and reads the high and low bytes of the 12 bit encoder position via the ISA interface card. Figure D.4 shows the architecture of the prototype haptic interface.
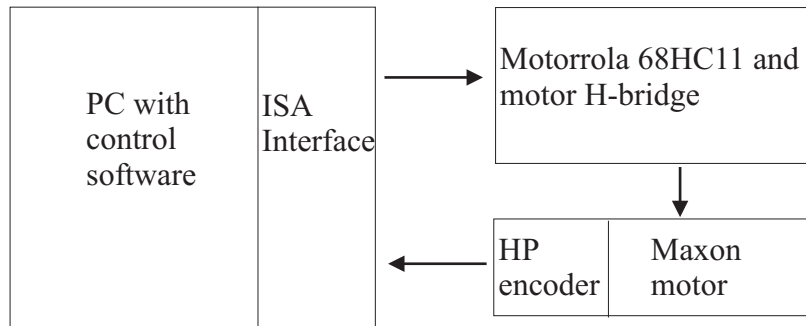
Figure D.4: The architecture of the prototype haptic interface

D.9   Final Device Specification

Table D.3 shows the actual specification of the prototype single degree of freedom haptic joystick whilst figure D.5 shows an image of the prototype haptic interface.

Max Cont. Force	8.3N at palm centre
Force Resolution	8 bit signed
Position Resolution	0.02571 Degrees
Joystick displacements	-53 to +53 Degrees
Sample and update rate	4 KHz

Table D.3: Specification of the prototype single degree of freedom haptic device

Figure D.5: The prototype haptic interface

D.10 Empirical Performance Testing

In order to augment the performance specification data provided in table D.3, software was developed that generated a wide range of haptic sensations. The software was then used in an empirical manner to assess the performance of the haptic interface and also to compare the haptic feedback that it generated relative to a high quality commercial haptic interface. Haptic sensations such as walls, springs, dampers and vibrations where implemented in addition to a simple game that allowed an operator to throw and catch a virtual ball with a virtual bat. Such a game is ideally suited to the prototype device since it only requires one degree of freedom that controls the vertical motion of the bat. The mathematical model of the ball in the environment was generated in a PC using Runge Kutta numerical integration. Environmental model parameters, such as ball mass, gravity (g), air friction coefficient and bat stiffness could be changed at run time to allow a broader range of sensations. Since the operator only had control of the vertical motion of the bat, the motion of the ball was not allowed to deviate from a position directly above the bat. The software was developed to utilise both the prototype 1 d.o.f. device and the Immersion Impulse Engine 2000. This allowed the performance of the prototype device to be compared with that of a high performance commercial device. Several different operators used both haptic interfaces to experience both the bat and ball game and also the well, spring, damper and vibration sensations. All of the operators agreed that differences in performance and haptic sensation between the two haptic interfaces were negligible. Section 4.2.3 of chapter 4 raised the issue of backlash within planetary gearboxes, and whether it affects the haptic sensations generated by the device. From the remarks of the operator's whilst using the demonstration software, it was concluded that the small amount of backlash did not significantly alter the haptic sensation.

Appendix E

Mann-Whitney U Test

The Mann-Whitney U test is used to test the hypothesis that two population distributions are the same. It assumes that participants are assigned at random or that samples are drawn at random from continuous populations. Since the test statistic is based on the ranks of observations rather than on numerical values the Mann-Whitney U test is suitable for data from education and the behavioural sciences research. The U test is often used as an assumption freer alternative to the two-sample t test for independent samples.

This test was originally developed in 1945 by Frank Wilcoxon and called the Wilcoxon rank-sum test. Various forms of the test have been developed by Festinger in 1946, Mann and Whitney in 1947 and White in 1952.

The computational procedure is split for large and small samples sizes. The procedure discussed here is for small sample sizes where both sample sizes are 20 or less. The first computational step is to rank order the scores. The two populations are treated as one and a rank is given to each score where the smallest score is assigned the rank of 1 and the next smallest 2 and so on until all of the scores have ranks. If two or more scores are exactly the same, they are given the mean of the ranks that are they would have occupied if they had not had an identical value to another score. For example, if two scores share the value 10 where the value 10 is the fourth largest score, the two scores would have taken the ranks of 4 and 5. Hence the identical scores of 10 are assigned the rank of 4.5 (this is the mean of 4 and 5).

Table E.1 shows the time taken in seconds for two groups of imaginary athletes to run a 100m sprint race. The experimental group used a novel training technique whilst the control group used a normal training technique. Participants where placed into the groups in a random fashion. We would like to know if the new training technique results in a different performance level and hence we would like

to know if there is a difference between the two group's results. The statistical hypothesis are as follows:

- H_0: The new training technique does not alter performance.

- H_1: The new training technique does alter performance.

In table E.1, n_1 and n_2 are the size of the two groups and ΣR_1 and ΣR_2 are the sums of the ranks. Equation E.1 shows the computational check that should be used prior to calculation of equation E.2. To be significant at a given level of α, the value of equation E.2 must be less than or equal to the critical value $U_{\alpha/2;n_1,n_2}$. Tables of the critical values of U are used to establish whether the result of the test is significant.

Equation E.3 shows the value of $U(8, 8)$ for the data in table E.1 to be 14. To be significant at the 0.05 level, the test statistic $U(8, 8)$ must be less than or equal to the critical value $U_{.05/2;8,8}$. Since the critical value, $U_{.05/2;8,8}$, is 15 (Kirk, 1999) we would reject H_0 and thus accept H_1.

$$\Sigma R_1 + \Sigma R_2 = \frac{(n_1 + n_2)(n_1 + n_2 + 1)}{2} \tag{E.1}$$

$$U(n_1, n_2) = Smallest\ of\ \left[\begin{array}{c} n_1 n_2 + \dfrac{n_1(n_1 + 1)}{2} - \Sigma R_1 \\[2ex] n_1 n_2 + \dfrac{n_2(n_2 + 1)}{2} - \Sigma R_2 \end{array} \right] \tag{E.2}$$

$$U(8, 8) = Smallest\ of\ \left[\begin{array}{c} (8)(8) + \dfrac{8(8 + 1)}{2} - 50 \\[2ex] (8)(8) + \dfrac{8(8 + 1)}{2} - 86 \end{array} \right] = 14 \tag{E.3}$$

Exp. Group (sec)	Rank, R_1	Control Group (sec)	Rank, R_2
11.12	6	11.59	11
10.99	2	11.69	12
11.10	5	11.90	15
12.20	16	11.49	10
10.57	1	11.03	3
11.04	4	11.70	13
11.41	9	11.89	14
11.25	7	11.27	8
$n_1 = 8$	$\Sigma R_1 = 50$	$n_2 = 8$	$\Sigma R_2 = 86$

Table E.1: Table of ranked results for the two groups of imaginary athletes

Appendix F

Wilcoxon T Test for Dependent Samples

The Wilcoxon T test for dependent samples is used to test if two population distributions are identical. The test is appropriate for dependent samples that can result from the following.

- Repeated measures on the same participant

- Participants matched on a variable that is known to be correlated with the dependant variable

- Identical twins

- Obtaining pairs of participants who are patched by mutual selection.

The Wilcoxon T test makes the assumption that the populations are continuous and that a random sample of paired elements has been obtained or that the paired elements have been randomly assigned to the conditions.

The computational procedure shown here for the Wilcoxon T statistic is to be used when the data contains no more than 50 pairs of scores.

Imagine that a group of new teenage drivers are to be have their driving reassessed 12 months after passing their test. The examiner marks the student with a percentage for both the initial driving test and the retest.

The following statistical hypotheses are proposed by the researcher.

- H_0: The population distributions for both assessments are identical.

- H_1: The population distributions for the reassessments is shifted above the initial assessments. Increased scores due to extra driving experience.

Table F.1 shows the scores obtained by the drivers in both tests. The first column shows the identity of the particular driver. X_1 and X_2 show the scores for the first test and retest respectively. The fourth column, named *Diff* is the difference between the scores of the two tests. The fifth column shows the ranks of the differences between the two scores, i.e. the ranks of the fourth column. The smallest difference is given the rank of 1 and the next smallest is given the rank of 2. This continues until all of the score differences have ranks. In the case that two or more score differences are identical, as with drivers 5 and 9 in table F.1, the assigned rank is the mean of the available ranks. In table F.1 drivers 5 and 9 share the ranks 2 and 3. Hence they are assigned the rank of 2.5 which is the mean of the available ranks (2 and 3). ΣR_+ and ΣR_- are the sums of the ranks associated with a positive score difference and the sums of the ranks associated with a negative score difference respectively.

Equation F.1 shows the computational check that should be used prior to calculation of equation F.2. Equation F.3 shows the calculation of the test statistic $T(10)$.

$$\Sigma R_+ + \left| \Sigma R_- \right| = \frac{n(n+1)}{2} \tag{F.1}$$

$$T(n) = Smallest\ of \begin{bmatrix} \Sigma R_+ \\ |\Sigma R_-| \end{bmatrix} \tag{F.2}$$

$$T(10) = Smallest\ of \begin{bmatrix} 43 \\ 12 \end{bmatrix} = 12 \tag{F.3}$$

To be significant at a given level of α the calculated test statistic $T(n)$ must be less than or equal to the critical value $T_{\alpha,n}$. Since $T(10) = 12$ is not less then the one tailed test critical value $T_{.05,10} = 10$(Kirk, 1999) we accept H_0 and conclude that driving performance did not improve during the first 12 months.

Id	$X_1(\%)$	$X_2(\%)$	Diff	Rank of Difference Ignoring Polarity	Rank Associated with +ve Difference R_+	Rank Associated with -ve Difference R_-
1	61	65	4	4	4	
2	80	75	-5	6		6
3	66	76	10	9	9	
4	70	75	5	6	6	
5	62	64	2	2.5	2.5	
6	63	85	22	10	10	
7	70	65	-5	6		6
8	81	82	1	1	1	
9	75	77	2	2.5	2.5	
10	68	76	8	8	8	
	mean = 69.6	mean = 74.0			$\Sigma R_+ = 43$	$\Sigma R_- = 12$

Table F.1: Table of data showing the driving assessments scores

Appendix G

Data File Format for the Haptic Experimentation

Data was recorded automatically by the software during the experiments. The data was recorded to files for both human reading and also input to Mathcad. The difference between the two files is very small. Effectively, the file intended for human reading is just a verbose version of the raw input file for Mathcad. Since the recording rate was so high (33Hz) a large amount of data was collected, below is a small clip from one experiment that shows the same data from both the verbose human readable file and the Mathcad data file. Both files show the same data, i.e. a line number followed by three force values and a time stamp in seconds.

The human readable data file.

001708 FORCES X -02 Y 000 Z 000 51.240000s
001709 FORCES X -03 Y 000 Z 000 51.270000s
001710 FORCES X -06 Y 000 Z 000 51.300000s
001711 FORCES X -13 Y 000 Z 000 51.330000s
001712 FORCES X -24 Y 000 Z 000 51.360000s
001713 FORCES X -43 Y 000 Z 001 51.390000s
001714 FORCES X -68 Y -01 Z 002 51.420000s
001715 FORCES X -87 Y -01 Z 003 51.450000s

The Mathcad readable data file.

001708 -02 000 000 51.240000
001709 -03 000 000 51.270000
001710 -06 000 000 51.300000
001711 -13 000 000 51.330000
001712 -24 000 000 51.360000

001713 -43 000 001 51.390000
001714 -68 -01 002 51.420000
001715 -87 -01 003 51.450000

Appendix H

Using ANOVA to test for lack of fit of a linear regression model

The test relies on analysis of varience or the F test to determine if there is a lack of fit (Weisberg, 1985). This test makes use of variations between cases with the same values on all of the predictors. Consider the example data shown in table H.1 where column X is the predictor. Table H.1 shows that the sum of squares of pure error is calculated from the sum of column 4 and the degrees of freedom of pure error is calculated from the sum of column 5. The F value is calculated using ANOVA as shown in tables H.2 and H.3. From table H.3, the observed value of F is 0.9045. This is considerably smaller than $F(0.05; 3, 8) = 4.07$ suggesting no lack of fit of the model to this data. This conclusion is confirmed by visual inspection of the regression plot.

$$SXY = \Sigma(x_i - \bar{x})(y_i - \bar{y}) \tag{H.1}$$

$$SXX = \Sigma(x_i - \bar{x})^2 \tag{H.2}$$

$$SYY = \Sigma(y_i - \bar{y})^2 \tag{H.3}$$

$$RSS = SYY - \frac{(SXY)^2}{SXX} \tag{H.4}$$

$$SS_{reg} = SYY - RSS \tag{H.5}$$

x	y	$\bar{y}$	$\Sigma(y_i - \bar{y})^2$	degrees of freedom
1	1.2			
1	1.1	1.15	0.005	1
2	2.3			
2	2.0	2.15	0.045	1
3	3.2			
3	3.5	3.35	0.045	1
4	4.1			
4	4.5	4.30	0.08	1
5	5.6			
5	5.9	5.75	0.045	1
	$n = 10$		$SS(p.e.) =$ 0.22	$d.f.(p.e.) = 5$

Table H.1: Imaginary data table showing sum of squares and degrees of freedom for pure error

$$d.o.f.(l.o.f.) = d.o.f.(residual) - d.o.f.(p.e.) \qquad \text{(H.6)}$$

$$SS(l.o.f.) = RSS - SS(p.e.) \qquad \text{(H.7)}$$

Source	d.o.f	SS	MS	F
regression	$d.o.f.(reg)$	$SSreg$	$SSreg/1$	
residual	$d.o.f.(res)$	RSS	$RSS/(n-2)$	
lack-of-fit	$d.o.f(l.o.f.)$	$SS(l.o.f.)$	$\dfrac{SS(l.o.f.)}{d.o.f(l.o.f.)}$	$\dfrac{MS(l.o.f.)}{MS(p.e.)}$
pure-error	$d.o.f(p.e.)$	$SS(p.e.)$	$\dfrac{SS(p.e.)}{d.o.f.(p.e.)}$	

Table H.2: The analysis of variance equations

Source	d.o.f	SS	MS	F
regression	1	25.7645	25.7645	
residual	8	0.3395	0.0424	
lack-of-fit	3	0.1195	0.0398	0.9045
pure-error	5	0.22	0.044	

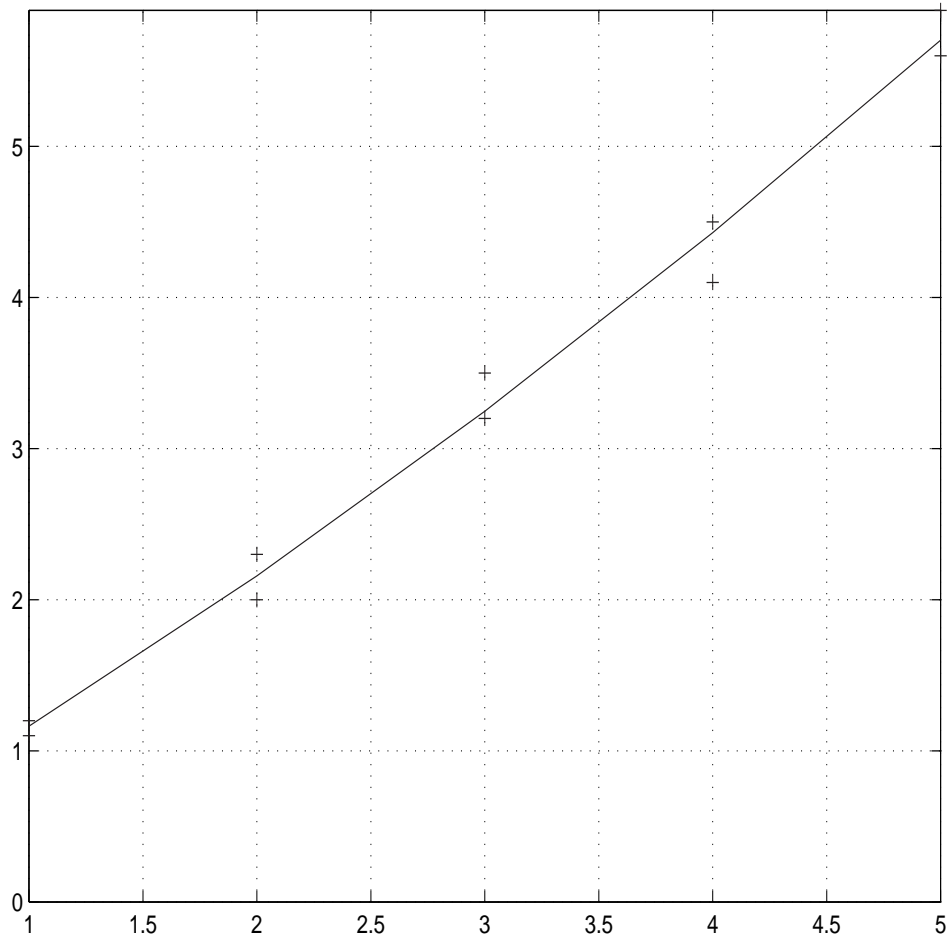Table H.3: The analysis of variance for this data

Figure H.1: 2nd order regression plot for the example data

Appendix I

Publications

I.1 Text

M. S. Counsell & D. P. Barnes, 1999. Haptic Communication for Manipulator Tooling Operations in Hazardous Environments. *Pages 222–233 of: Telemanipulator and Telepresence Technologies VI,* vol. 3840

D. P. Barnes & M. S. Counsell, 1999. Haptic Communication for Remote Mobile Manipulator Robot Operations. *In: American Nuclear Society, 8th International Topical Meeting on Robotics and Remote Systems (Proc. on CDROM, Session 15: Human Machine Interfaces, ISBN 0-89448-647-0)*

I.2 Bibtex

@inproceedings{D.P.BarnesM.S.Counsell1999,
author = {D. P. Barnes and M. S. Counsell},
title = "Haptic Communication for Remote Mobile Manipulator Robot Operations",
booktitle = {American Nuclear Society, 8th International Topical Meeting on Robotics and Remote Systems (Proc. on CDROM, Session 15: Human Machine Interfaces, ISBN 0-89448-647-0)},
year = {1999},
organisation = {American Nuclear Society},
}

@inproceedings{M.S.CounsellD.P.Barnes,
author = {M. S. Counsell and D. P. Barnes},

title = "Haptic Communication for Manipulator Tooling Operations in Hazardous Environments",
booktitle = {Telemanipulator and Telepresence Technologies VI},
year = {1999},
pages = {222–233},
volume = {3840},
organisation = {SPIE},
}